2016

The Study of the Regulon of OxyR in Escherichia coli and Porphyromonas gingivalis

Christopher K. Pham

The Study of the Regulon of OxyR in *Escherichia coli* and *Porphyromonas gingivalis*

A thesis submitted in partial fulfillment for the requirements for the degree of Masters of Science in Biochemistry at Virginia Commonwealth University.

By
Christopher Khoa Pham
Bachelor of Arts (Neuroscience), University of Southern California, Los Angeles, California
May 2013

Director: **JANINA P. LEWIS**, Ph.D., Associate Professor

The Philips Institute for Oral Health Research
School of Dentistry, Virginia Commonwealth University

Virginia Commonwealth University

Richmond, Virginia

May 2016

Acknowledgements

I would like to extend my deep appreciation and gratitude for my advisor and mentor, Dr. Janina P. Lewis. I would like to thank her for guiding me through my project and believing in my capabilities as a graduate research student. She has been kind and understanding mentor and I cannot express my gratitude enough for her guidance and accepting me as a student in her lab.

I would also like to thank my committee members, Dr. Andrei Ivanov and for his input and avice and Dr. William Barton for his input and advice as well as letting me use his laboratory equipment.

I would also like to extend my thanks and appreciation towards my fellow researchers at the Wood building and the Philips Institute. A special thanks to Dr. Todd Kitten for letting me use his vacant lab space to conduct my experiments and use of his lab equipment. Dr. John Burgner and his expertise on analytical ultracentrifugation which was critical for this project.

I am truly grateful for my fellow colleagues and friends in the Lewis lab. I cannot express my gratefulness to Ross Belvin, whose invaluable guidance and patience are invaluable to my project. A large part of my project would not be possible without his assistance. To the rest of the lab: Nicai Zollar, Kat Sinclair, Qin Gui, and Steve Kokorelis, getting to know and spend time with each and every one of you has made lab a very enjoyable and entertaining experience that I will never forget.

Lastly but not least, I would like to thank my parents, James Pham and Hao Ngueyn, and my sister Jessica Pham. I am forever indebted to them for believing in me and supporting me in this journey. They have been there every step of the way me for moral and emotional support. I can always count on them. I love you guys all very much. I would also like to thank my girlfriend, Nina Ong. You have been there for me through thick and thin. Meeting you has been the best thing to come out of my time here in Richmond.

Table of Contents

List of Tables

List of Figures

Abstract

THE STUDY OF THE REGULON OF OXYR IN *ESCHERICHIA COLI* AND *PORPHYROMONAS GINGIVALIS*

By: Christopher Khoa Pham

A thesis submitted in partial fulfillment of the requirements for the degree of Master of Science at Virginia Commonwealth University.

Virginia Commonwealth University, 2016

Major Director: Janina P. Lewis, Ph.D., Philips Institute for Oral Health Research

The facultative anaerobe, *Escherichia coli* and the obligate anaerobe, *Porphyromonas gingivalis* are two bacteria that reside in our body. Although they reside in separate environments, they are both subject to hydrogen peroxide stress and have mechanisms to regulate the stress. OxyR is the primary transcriptional regulator/sensor of oxidative stress response caused by hydrogen peroxide. OxyR in *P. gingivalis* is not well-characterized compared to OxyR in *E. coli.* We sought to characterize and compare the two forms of OxyR in order to gain a better understanding of the protein. We determined the oligomeric state of both proteins: primarily a tetramer for *E. coli* and primarily a tetramer for *P. gingivalis* OxyR.. We demonstrated DNA binding with *E. coli* OxyR, indicating purification of the functional form of *E. coli* OxyR.Through pulldown assays we discovered potential novel binding targets, *mobB* for *E. coli* OxyR and PG1209 for *P. gingivalis* OxyR. Many of the other targets corresponded to intergenic regions within genes, which may pertain to small RNAs or small proteins. These results show that OxyR in *E. coli* and *P. gingivalis* has novel function and properties indicating an expanded role in addition to the well-characterized oxidative stress response.

Chapter 1 - Background Significance

1.1 - Microbiome of the Human Body

The human body provides various environments suitable for a variety of microorganisms. The microorganisms that reside throughout the human body are classified as the microbiota of the human body (Turnbaugh et al., 2007). Different regions of the body serve as hosts to different types of flora. These environments can range anywhere from the outer surface of our skin, the oral cavity, and to even the gastrointestinal tract. While these environments are separate from one another and possess unique characteristics, microorganisms are not exclusive to just one of these environments. The bacteria or microbes are of special interest because of the types of relationship they have with the human body.

The bacteria that reside throughout the human body are generally part of normal human physiology and function. These are the normal flora and do not normally cause disease or complications. These are the commensal bacteria. They reap the benefits the human body provides—such as a suitable environment for growth as well as various nutrients. However, a number of seemingly harmless bacteria are actually opportunistic pathogens. They can become pathogenic when the immune system becomes compromised—allowing them to cause disease. Without the presence of the immune system to keep them at bay, these bacteria are able to cause harm. Another mechanism for normal flora to become pathogenic is if they manage to acquire virulence factors. Some bacteria are unable to cause harm because they lack virulence factors that would allow them to invade host cells. Acquiring virulence factors would

allow normal flora bacteria to invade normal cells and cause problems (Escobar-Páramo et al., 2004). Two important sites of the human body are the oral cavity and the gastrointestinal tract.

1.2 - Gut Microbiome

The human gastrointestinal tract is home to an estimated over 100 trilllion microorganisms in the intestines alone (Björkstén et al, 2001). Many human gut microorganisms are considered to be commensal bacteria. The human gut provides an adequate environment for various microorganisms to thrive due to our digestive system. The foods we eat and digest are a source of rich nutrients and energy for the gut flora (Guarner & Malagelada, 2003). The gut itself also functions as a physically protective environment or home for these organisms. By harnessing the nutrients our foods provide, the flora in turn generates various nutrients that benefit the human body. For example, gut flora produce both vitamin B and vitamin K which are needed for cell metabolism and protein synthesis respectively (Cummings & Macfarlane, 1997). Under healthy homeostatic conditions, their residency in the human gut helps prevent colonization of pathogenic bacteria. *Escherichia coli* is one of thousands of bacteria that reside in human gut as a commensal organism under normal healthy conditions. However, if conditions are altered that allow the commensal strains of *E. coli* to escape the gut, they are capable of causing peritonitis or infections elsewhere in the body.

1.3 - *Escherichia coli*

Escherichia coli is a rod-shaped, Gram-negative facultative anaerobe. It is one of the most extensively studied organisms and arguably the most studied microorganism. As an intensely studied organism, *E. coli* is the prime example of a model organism.

Model organisms are species that have undergone extensive studies to be used as a basis for comparison when studying other organisms. The rapid reproductive rate of *E. coli* allowed for extensive studies to be done further contributing to its status as a model organism for microorganisms.

E. coli exists in various microbiomes throughout the human body such as the skin flora and the gut flora. The GI tract is the primary home to *E. coli* in the human body. The gut *E. coli* are commensal strains and do not possess adequate virulence factors to cause problems such as diarrhea (Katouli, 2010). The pathogenic strains are the ones that carry virulence factors that enable them to cause disease. These primarily enter the human body via fecal-oral transmission through contaminated food or sub-par hygiene.

As a facultative anaerobe, *E. coli* is able to survive in both aerobic and anaerobic conditions. Under aerobic conditions, *E. coli* will utilize normal aerobic respiration. Under anaerobic conditions, *E. coli* is able to switch to anaerobic respiration or fermentation with the latter as a last resort in order to survive (Unden, Becker, Bongaerts, Schirawski, & Six, 1994).

1.4 - Oral Microbiome

The human oral cavity provides a very suitable environment for microorganisms such as bacteria to grow and thrive. There is an estimated over 700 different species of bacterium alone in the oral cavity (Aas, Paster, Stokes, Olsen, & Dewhirst, 2005). Within the oral cavity there are a number of different surfaces such as the lateral sides of the tongue, the subgingival plaque, etc. Each of these unique surfaces has its own coats of bacteria making up the bacterial biofilm. Some of the bacteria in the oral cavity

are exclusive to certain biofilms, but some can be found throughout most of the oral cavity. Many of the bacteria residing in the oral cavity are commensal, but there are strains implicated in diseases that range from just the oral cavity to systemic disease (Aas et al., 2005; Hasegawa et al., 2007). *Porphyromonas gingivalis* is one of these oral cavity bacteria implicated in diseases pertaining to the oral cavity and can lead to systemic disease.

1.5 - *Porphyromonas gingivalis*

Porphyromonas gingivalis is a Gram-negative, anaerobic, rod-shaped bacterium. It produces black colonies when plated on blood agar plates. It is one of the pathogens implicated in periodontal diseases like periodontitis. Like *E. coli,* it also exists in the human GI tract. However, it primarily resides in the human oral cavity. *P. gingivalis* is one of the primary agents known to cause periodontal disease (Loesche, Syed, Schmidt, & Morrison, 1985; Slots, 1986). Periodontal disease is primarily an inflammatory disease of the periodontium of the oral cavity. The inflammation leads to all sorts of complications—from aggregation of microbial plaque, bone loss, and formation of a periodontal pocket or gap (Newman, Takei, Klokkevold, & Carranza, 2002). These diseases are caused by the bacterial biofilm or dental plaque that form on teeth as a result of bacterial aggregation on various surfaces.

Although *P. gingivalis* is implicated in periodontal disease, it does not cause the disease on its own. *P. gingivalis* is believed to be a “keystone” pathogen in that a low amount of bacteria can cause localized or widespread inflammation through modification of the normal microbiota into a dysbiotic one (Hajishengallis, Darveau, & Curtis, 2012). Essentially a small amount of bacteria can corrupt the whole microbiota.

As a result, *P. gingivalis* also plays a role in systemic diseases such as cardiovascular disease and rheumatoid arthritis (Desvarieux et al., 2005; Ogrendik, Kokino, Ozdemir, Bird, & Hamlet, 2005) due to the inflammation it causes. Within the oral cavity, *P. gingivalis* localizes into specific areas such as the subgingival pockets and the periodontal pockets. In these pockets of the oral cavity, *P. gingivalis* secretes toxins to cause inflammation, which facilitates the progression of periodontitis, a disease characterized by inflammation which can lead to alveolar bone loss and other complications. The toxins released here cause damage to both the surrounding gum tissue and the teeth itself. As a result, neutrophils and other inflammatory response agents are activated in response to the inflammation caused by *P. gingivalis*. This can lead to an increase in cytokines, reactive oxygen species and other inflammatory responses (Graves & Cochran, 2003).

1.6 - Environmental Stress

While the human body provides optimal environments for these bacteria, it is not a free ticket to ride. These bacteria must learn to survive against various environmental stressors such as oxidative stress, nitrosative stress, and the immune system (McMahon, Xu, Moore, Blair, & McDowell, 2007). Bacteria can encounter these stressors on a daily basis and must exhibit adaptive or defensive mechanisms in order to survive within the human body. Under normal homeostatic conditions, the host immune system is more than capable of eradicating unwanted pathogens. A healthy immune system is capable of recognizing foreign invaders and eliminating them from the body before they are able to cause problems. At the same time, the normal flora of the body also serves as another source of protection against these microbes by taking

up residency which prevents colonization by pathogenic microorganisms (Edlund & Nord, 2000; Sekirov, Russell, Antunes, & Finlay, 2010; H. Wu & Wu, 2012). However, invasive bacteria such as *P. gingivalis* have the ability to invade host cells to hide and protect against the host immune system (Singh et al., 2011). Being inside a host cell makes it much harder for the immune system to locate and identify the target bacteria. There are many different adaptive mechanisms to wide variety of environmental stressors.

1.6.1 - Gene regulation and environmental stress

Microbes such as *E. coli* and *P. gingivalis* have evolved and developed specific mechanisms to combat environmental stress. Of the thousands of genes found in microbes, some of these genes and their gene products are dedicated to defense mechanisms against external stressors such as oxidative stress. These gene products are proteins that function as transcriptional factors or regulators. When these transcription factors are induced by stress factors, they induce transcription of genes in the genome in order to activate the transcription of these genes as part of the stress response (Latchman, 1997). These factors induce transcription by binding to a region upstream of these genes known as the promoter region. Binding to this region allows these factors to regulate the transcription and thus expression levels of these genes.Transcription factors can regulate multiple genes as part of a stress response. These stress responses allow the microbe to clear or protect against the environmental stressor and thus ensure survival.

1.7 - Oxidative Stress

Oxidative stress is one of the most common environmental stressors bacteria can constantly deal with on a daily basis. There are various sources of oxidative stress ranging from their own cellular metabolism to the host cell metabolism. Oxidative stress is toxic to both aerobic and anaerobic bacteria. Oxidative stress comes in the form of reactive oxygen species, which can occur naturally from the environment or as a byproduct of cellular metabolism (Christman, Morgan, Jacobson, & Ames, 1985; Fang, 2004). Hydrogen peroxide is one of the most common reactive oxygen species that results from normal cell metabolism (Fridovich, 1978).

1.7.1 - Aerobic respiration is a source of oxidative stress

One of the consequences of aerobic respiration is the production of harmful byproducts known as reactive oxygen species (ROS) such as hydrogen peroxide. Hydrogen peroxide is generated as a byproduct of aerobic metabolism. Through Fenton chemistry (Figure 1), hydrogen peroxide reacts with free intracellular Ferrous (Fe^{2+}) iron by oxidizing it and turning it into Ferric (Fe^{3+}) iron. This reaction generates the harmful hydroxyl radical ($^{\cdot}OH$). The hydroxyl radical is toxic to organisms because it is highly reactive and can cause intracellular damage—particularly to the organism's DNA (Imlay, Chin, & Linn, 1988; Mancini & Imlay, 2015; Seaver & Imlay, 2001; Varghese, Wu, Park, Imlay, & Imlay, 2007). Because hydrogen peroxide is capable of bypassing cell membranes, it affects virtually all microorganisms. As a result, many organisms possess defense mechanisms specifically to combat hydrogen peroxide stress.

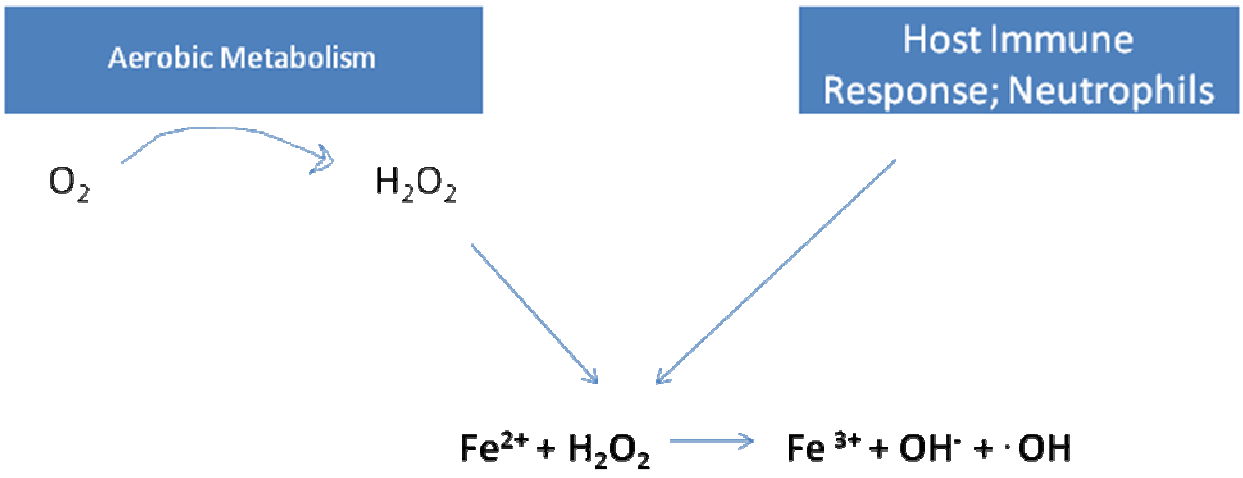

Figure 1: Overview of Hydrogen Peroxide Induced Oxidative Stress

Hydrogen peroxide from various sources can react with intracellular Ferrous iron to generate ferric iron and the toxic hydroxyl radical.

1.7.2 - Oxidative stress use against foreign invaders

Despite all the self-harm inflicted by reactive oxygen species if left unchecked, ROS can be used to combat foreign pathogens and infection (Fang, 2004). Reactive oxygen species react with thiols, which can lead to oxidative stress when the ROS are released as byproducts. However, there is an alternative use for these ROS. Reactive oxygen species can serve as signaling molecules to activate the transduction of various pathways leading to a reaction against foreign pathogens. Reactive oxygen species also function as a signaling molecule to activate phagocytes such as neutrophils as part of the immune response to kill off bacteria via phagocytosis (Fang, 2004; Graves & Cochran, 2003). Neutrophils can also kill off bacteria by generating hydrogen peroxide which is harmful to the bacteria (Weiss, Young, LoBuglio, Slivka, & Nimeh, 1981). In addition to activating phagocytes, the reaction of ROS with thiols can lead to antibacterial or antimicrobial challenges that the foreign pathogens and bacteria must face. Invasive bacteria like *P. gingivalis* have virulence factors that allow them to invade host cells in order to escape the host immune system (Lamont & Yilmaz, 2002). Invading a host cell essentially masks the bacteria against the immune response as well as providing a safe environment within the host to reproduce. This gives protection against phagocytes, but it does not provide protection against reactive oxygen species such as hydrogen peroxide, which can bypass cell membranes.

1.8 - *Escherichia coli* response to oxidative stress

As a facultative anaerobe, *E. coli* is exposed to various sources of oxidative stress. The bacterium itself will produce reactive oxygen species as a result of its own cellular metabolism. Free Ferrous iron is capable of producing reactive oxygen species

via oxidation from hydrogen peroxide through Fenton Chemistry. The host body environment is also source of reactive oxygen species due to the oxygen in the air as well as the host cell metabolism. The host immune system is also a source of reactive oxygen species to combat foreign pathogens. In order to protect against oxidative stressors such as hydrogen peroxide, aerobic organisms like *Escherichia coli* possess various methods to clear or break down hydrogen peroxide. One defense mechanisms of *E. coli* against oxidative stress, specifically hydrogen peroxide stress, is through the transcriptional regulator OxyR.

1.8.1 - OxyR in *Escherichia coli*

OxyR in *E.* coli is a transcriptional regulator that belongs to the LysR family of regulators (Zheng, Ming et al, 2001). When activated, OxyR will turn on a variety of genes in response to carry out various functions. The primary and most-studied activity of OxyR is its role in the oxidative stress response. OxyR is primarily activated via oxidation by hydrogen peroxide. Once activated, OxyR is known to turn on at least 30 different genes including *katG, grxA, ahpCF,* and *dps*. Many of the genes under regulation of OxyR are part of the oxidative stress response. These genes encode for the following proteins respectively: KatG (a catalase), GrxA (a glutathione reductase), AhpCF (two subunits since reclassified as a NADH peroxidase instead of an alkylhydroperoxide reductase), and Dps (DNA-binding protein). These genes each have their own role in the oxidative stress response as a defense mechanism against hydrogen peroxide. KatG codes for a catalase-peroxidase that functions as a scavenger at high concentrations of hydrogen peroxide. Once it encounters hydrogen peroxide,

KatG functions to reduce hydrogen peroxide to nullify oxidative stress. AhpCF has a similar role as a scavenger of endogenous hydrogen peroxide at lower concentrations.

When OxyR is in its active form, it binds to the promoter region of these genes it regulates (L. Tartaglia, Gimeno, Storz, & Ames, 1992; L. A. Tartaglia, Storz, & Ames, 1989). How and why OxyR binds to these sequences is not fully understood. There is very little sequence similarities between binding targets of OxyR other than a small consensus binding motif of ATAGnnnnCTAT (Kullik, Stevens, Toledano, & Storz, 1995). Despite the extensive studies and knowledge regarding *E. coli* OxyR and the oxidative stress response, the full extent of its activities outside of this response is not fully known.

The activity of OxyR depends on its oxidation state (Kullik, Toledano, Tartaglia, & Storz, 1995; L. A. Tartaglia, Storz, Brodsky, Lai, & Ames, 1990). When OxyR is oxidized, it is in its active form. In this active form, OxyR activates RNA polymerase in order to initiate transcription of these genes. Because hydrogen peroxide is an oxidizing agent, OxyR becomes activated in response to hydrogen peroxide and thus initiates transcription of the oxidative stress response genes. When OxyR is reduced, it becomes inactivated and ceases the transcription of these genes. There is a conformational change between the oxidized and reduced form of OxyR.

1.8.2 - The difference in structure of OxyR between active and inactive forms

Each monomer of OxyR contains 6 different cysteine residues. The Cys199 residues play a major role in the activation of OxyR (Kullik, Toledano et al., 1995). When exposed to hydrogen peroxide, OxyR is oxidized at the Cys199 residue. The oxidation results in the creation of a disulfide bond between Cys199 and Cys208 (Lee et

al., 2004). The oxidized form of OxyR is the activated form of OxyR in which it is able to turn on the transcription of genes such as those of the oxidative stress response. When OxyR binds to its target gene, it binds to both RNA polymerase and DNA, forming a transcription intiation complex. This complex gives additional stability in order to further stabilize the oxidized form of OxyR.

OxyR is inactivated by one of targets in the oxidative stress response—GrxA. GrxA is a glutathione reductase that is turned on by OxyR, but will also negatively regulate OxyR and turn it off. The byproduct of GrxA negatively regulates OxyR by reducing the two cysteine residues (Cys199 and Cys208), which breaks the disulfide bond, effectively reducing OxyR. The reduced form of OxyR is the inactivated state in which it no longer initiates transcription of the genes it regulates. In addition to reduction by GrxA, conformational changes also occur when OxyR releases itself from the transcription initiation complex after it has turned on a gene. When OxyR is released from the complex, the additional stability lent by binding with DNA and RNA polymerase is no longer present—giving favor to a reduced conformation. When OxyR is reduced at the Cys199 residue, there is a separation of approximately 17 Angstroms between Cys 199 and Cys 208. This distance is small, but still great enough so that a disulfide bond cannot be formed in the reduced forms. The combination of reduction by GrxA and the physical changes instilled by release of the transcription initiation complex favor the reduced form, which inactivates OxyR.

1.8.3 The redox switch of OxyR

Most of current literature regarding OxyR describes the mechanism of OxyR activation and inactivation relying on the redox state of two Cysteine residues—Cys199

and Cys208. It is believed that when these two Cysteines are oxidized, this results in the creation of a disulfide bridge between the two residues (Storz, Tartaglia, & Ames, 1990a; Svintradze, Peterson, Collazo-santiago, Lewis, & Wright, 2013; Zheng, Åslund, & Storz, 1998). The formation of this bridge activates OxyR and to regulate transcription of other genes. Reduction of these cysteines, often through the byproduct of GrxA, breaks the disulfide bridge, thus inactivating OxyR (Choi et al., 2001). This so-called redox switch is the means in OxyR activates the transcription of other genes and thus regulating the OxyR regulon in the oxidative stress response.

However, there is also data that does not argue with the formation of the disulfide bridge. It is reported that the distance between Cys199 and Cys208 is approximately 17 Angstroms (Choi et al., 2001; Kim et al., 2002). It is believed by some that this distance is too far to allow for disulfide bridge formation. The exact mechanism of this disulfide bond formation is not fully understood and requires speculation. During bridge formation, there are disulfide intermediates that can actually occur naturally and exist as stable intermediates (Kim et al., 2002). Because these intermediates form stably in wild-type *E. coli*, there is reason to believe there are other mechanisms of OxyR outside of the oxidative stress response. There was also previous work (data not shown) performed in this lab that also disagreed with the redox switch mechanism of OxyR. No matter what was tried, there was no evidence of the creation of a disulfide bridge (Oog, Kimet 2002; Lewis, Janina et al). The lack of evidence in bridge formation combined with stable reaction intermediates leads to the belief that OxyR may have other unknown roles aside from the typical oxidative stress response. The formation of disulfide intermediates may implicate unknown functions.

1.9 - The expanded role of OxyR in *Escherichia. coli*

Oxidative stress through hydrogen peroxide is a caused by reactions between the hydrogen peroxide molecules and ferrous iron. As a result, there is evidence and growing belief that implicates iron pathology as the driving force behind oxidative stress (Bresgen et al., 2010; Mancini & Imlay, 2015). *E. coli* OxyR has been shown to play a role in iron homeostasis as part of the oxidative stress response. When activated through oxidation, OxyR has been shown to induce the expression of Fur. Fur is a ferritin uptake regulator in that it regulates various iron-uptake mechanisms by acting as a repressor for iron-importer proteins (Varghese et al., 2007). By repressing these importers during influx of hydrogen peroxide stress, Fur regulates iron levels by limiting the activity of iron-importers to reduce the amount of intracellular ferrous iron. This minimizes the availability of ferrous iron for Fenton Chemistry. OxyR has also been shown to directly regulate *hemH*, a gene which encodes for HemH, a ferrochetalase, which plays a significant role in the biosynthetic pathway to generate heme. HemH is responsible for the final step in the generation of heme by inserting iron into protophoryin ix in order to generate heme (Mancini & Imlay, 2015; Varghese et al., 2007). During hydrogen peroxide stress, the levels of intracellular iron is nearly depleted by the activity of Dps, which sequesters intracellular iron in order to prevent Fenton chemistry. This limits the availability of iron for heme synthesis, which is problematic because heme is an important molecule for a variety of functions. At the same time, KatG, a catalase part of the regulon of OxyR that detoxifies hydrogen peroxide, requires heme for its activities. OxyR regulates the expression of *hemH* in order to maintain adequate levels of heme. OxyR has a role in iron homeostasis as an indirect response

to hydrogen peroxide stress as evident by the regulation of the expression of *fur* and particularly *hemH.*

The majority of studies conducted on OxyR in *E. coli* has been done under and focused on the aerobic aspect. These studies focused on the redox state of the protein because OxyR was shown to be activated when it becomes oxidized by hydrogen peroxide. However, *E. coli* is a facultative anerobe—meaning that it is capable of surviving and functioning through anaerobic metabolism.

OxyR purified under anaerobic conditions from *E. coli* grown under anaerobic conditions display functions relating to nitrosylation and nitrosative stress of OxyR (Kim et al., 2002; Seth, Hausladen, Wang, & Stamler, 2012). These studies indicate a distinctly different function and regulon from the standard oxidative stress response caused by hydrogen peroxide. It was shown that modification of these cysteine residues via nitrosylation can occur in *E. coli* OxyR (Kim et al., 2002). They engineered stable modifications on these cysteines via nitrosylation to show these thiol groups can form S-NO, S-OH, and S-SG bonds (Kim et al., 2002). These conformational changes were shown to occur both *in vitro* and *in vivo*. These modifications created both structural and conformational differences from OxyR under aerobic conditions. Recent studies indicate that OxyR has a regulatory role in endogenous S-nitrosylation during anaerobic respiration (Seth et al., 2012) when *E. coli* is grown under anaerobic conditions on nitrate. Much like the oxidative stress response, OxyR appears to play a role in the nitrosative stress response when under anaerobic respiration. These findings indicate that despite extensive studies conducted on the redox aspect of OxyR, perhaps there are other functions of OxyR that are currently unknown.

1.10 - OxyR in *Porphyromonas gingivalis*

As a resident in the oral cavity where oxygen constantly passes through, *P. gingivalis* can be subjected to reactive oxygen species on a consistent basis. The air we breathe is just one of the sources of oxidative stress that *P. gingivalis* can encounter. Because *P. gingivalis* causes inflammation in the oral cavity, the human body will activate the inflammatory response agents such as neutrophils (Graves & Cochran, 2003). As mentioned previously, reactive oxygen species can serve as signaling molecules for phagocytes such as neutrophils. As a result, *P. gingivalis* can come under duress from oxidative stress from both the environment of the oral cavity as well as the inflammatory response trying to fight it off. It is logical to assume *P. gingivalis* has adapted to these oxidative conditions and likely has defense mechanism to survive under such regular oxidative stressors.

As a homolog to OxyR found in *E. coli*, it is reasonable to believe OxyR in *P. gingivalis* has similar functions to the form in *E. coli*. As mentioned previously, OxyR in *E.coli* is responsible for regulating the oxidative stress response to hydrogen peroxide and will activate a variety of genes in response to hydrogen peroxide stress (Storz, Tartaglia, & Ames, 1990b; Tao, Makino, Yonei, Nakata, & Shinagawa, 1991). The OxyR homologues found in other bacteria such as *P. aeruginosa* and *S. typhimurium* share similar functions—inducing the expression of genes pertaining to hydrogen peroxide regulation. Many of the genes are the same or similar homologs across these different aerobic organisms. Despite being tucked away in the periodontal pockets, *P. gingivalis* can still be exposed to hydrogen peroxide produced by the immune response (neutrophils) or by other oral bacteria. However, the presence of hydrogen peroxide

does not result in increased expression of common OxyR-regulated genes such as *ahpCF* and *dps* in *P. gingivalis* compared to other bacteria.(Diaz et al., 2006). However, these genes appear to still be under OxyR regulation because mutant studies show that regular expression of these genes require fully-functional OxyR.

Current literature indicates that OxyR in *P. gingivalis* has additional roles outside of regulating the common OxyR-regulated genes (Henry, McKenzie, Robles, & Fletcher, 2012). *P. gingivalis* OxyR has been shown to regulate both *sod* and *fimA* under aerobic conditions. The aerotolerance of *P. gingivalis* has been shown as a function of *sod* through mutagenic studies (J. Wu, Lin, & Xie, 2008). Thus OxyR in *P. gingivalis* has a role in aerotolerance of *P. gingivalis* because it regulates the expression of *sod* evident by the increased gene expression of *sod*s. On the other hand, *fimA* encodes for one of the subunits for the major or long Fimbriae. *P gingivalis* has both major (long) and minor (short) fimbriae which are used for attachment or colonization to various surfaces such as the oral cavity (Amano, Nakagawa, Okahashi, & Hamada, 2004). Fimbriae are one of many virulence factors that *P. gingivalis* has in its arsenal. It is theorized that OxyR represses *fimA* during aerobic conditions in order to focus its energy on survival rather than unnecessary activities. Aside from these findings, the role and regulon of OxyR in *P. gingivalis* still remains a mystery.

1.11 - Comparison of OxyR in *Escherichia coli* and *Porphyromonas gingivalis*

The state and function of OxyR in *Escherichia coli* is determined by the redox state of two cysteine residues (Cys199 and Cys208). When oxidized, a disulfide bridge is formed and OxyR becomes activated to turn on other genes. When the products of GrxA reduces these two cysteines, OxyR is inactivated and no longer intiates

transcription of the genes it regulates. The redox state of OxyR in *E. coli* is accompanied by conformational changes in the structure of OxyR. Between the reduced and oxidized forms, there is an approximately 30^{o} rotation between the monomers in the dimer of OxyR (Choi et al, 2001). The reduction by GrxA causes a physical conformation change that disrupts and breaks the disulfide bond in OxyR in *Escherichia coli*, causing a structural difference between oxidized and reduced forms of OxyR.

However, these structural changes and rotations are not seen in OxyR in *Porphyromonas gingivalis*. There is no major change between oxidized and reduced forms of OxyR in *P. gingivalis*. Rather, both the oxidized and reduced forms of OxyR in *P. gingivalis* resemble the oxidized form of OxyR in *E. coli* (Svintradze et al., 2013). It was determined that OxyR in *P. gingivalis* contains a short insert at residue 215. It was believed this insert conferred additional structural stability resulting in similar oxidized and reduced forms in *P. gingivalis.* The conformational change between the two forms is not as significant compared to the changes seen in *E. coli* OxyR. Nevertheless, the similarity in structures in both organisms makes it reasonable to believe that OxyR has a similar role in both organisms.

When *E. coli* OxyR is exposed to hydrogen peroxide, OxyR is activated and induces expression of a number of genes belonging to the oxidative stress regulon. The OxyR-induced genes that have a role in the oxidative stress response include *katG, grxA¸ahpCF* and *dps.* However, when *P. gingivalis* is exposed to the same concentration of hydrogen peroxide, there was only a minor up-regulation of nine different genes. Of these genes, none of them were genes linked to the oxidative stress response. Instead, the typical OxyR-mediated genes were found to only require a

functional OxyR in *P. gingivalis* and appeared to be constitutively active (Diaz et al., 2006).

The oligomeric state of *E. coli* OxyR is currently believed to exist as a tetramer in solution (Choi et al., 2001; Kullik et al., 1995). However, other studies have reported it exists as a dimer in solution(L. Tartaglia et al., 1992). The oligomeric state of the protein has not been thoroughly investigated compared to the regulatory domain of OxyR. Despite extensive studies conducted on the regulatory domain of OxyR, there can still be other unknown functions or properties as evidenced by S-nitrosylation of OxyR under anaerobic respiration. Evidence supports the conformation of a tetramer in solution because *E. coli* OxyR was found to interact with DNA at four major grooves with the conesus binding motif of ATAGnnnnCTAT (Kullik et al., 1995; Toledano et al., 1994) which indicates a tetramer in solution. The C-terminal domain is believed to play a role in the oligomerization of the protein (Kullik et al., 1995).

On the other hand, the oligomeric state of full-length *P. gingivalis* OxyR is unknown. The truncuated form of the protein has been crystallized (Svintradze et al., 2013). The truncuated form is missing the N-terminal or DNA-binding domain. As a result, the conformation of the full-length protein is currently unknown. The conformations of the regulatory domain of reduced and oxidized forms of *P. gingivalis* OxyR are very similar to the oxidized form of *E. coli* OxyR (Svintradze et al., 2013) of which there is evidence suggesting it is a tetramer in solution.

Due to similarities in structure to *E. coli* OxyR which has been implied to exist as a tetramer, perhaps *P. gingivalis* OxyR also exists as a tetramer in solution.

Chapter 2 – Hypothesis and Aims

2.1 Hypothesis

If we are able to purify OxyR and show that is fully functional in both *Escherichia coli* and *Porphyromonas gingivalis,* we can determine both full-length oligomeric state of the protein as well as its regulon and make any comparisions between the two forms.

2.2 Aims

The main purpose of this project is to better characterize the function of OxyR in both *E. coli* and *P. gingivalis*. While its role in the oxidative stress response is well-documented, there is reason to believe OxyR has other regulatory mechanisms.

Aim 1: Determine the oligomerization states of OxyR in *E. coli* and *P. gingivalis*.
There are conflicting reports on the oligomerization state of OxyR. We believe *E. coli* OxyR exists as a tetramer in solution. The oligomeric state of full-length *P. gingivalis* OxyR is unknown. However, we believe *P.* gingivalis OxyR also exists as a tetramer in solution. By determining the oligomeric state of both forms of OxyR, we can better characterize the mechanisms of OxyR. Gel filtration and sedimentation velocity experiments will allow us to determine the states.

Aim 2: Examination of DNA binding and comparison of *E. coli* and *P. gingivailis* OxyR.
We sought to verify that we purified fully functional protein by demonstrating binding with known targets of OxyR. By knowing the oligomeric state of the OxyR produced by each purification method, we can also infer which form of the protein is the DNA-binding

form. We also wanted to compare the different purification methods to determine which which method is better to use for pulldown assays. We also wanted to determine and optimize the binding conditions for OxyR to use in the pulldown assays. Electromobility shift assays (EMSAs) will be performed for these studies.

Aim 3: Determine the OxyR regulon in vitro in *E. coli* and *P. gingivalis*.

We believe OxyR in *E. coli* regulates the expression of other unknown genes outside of the oxidative stress response. We believe OxyR in *P. gingivalis* is responsible for the expression of genes pertaining to survival in the event of oxidative stress. Performing an *in vitro* pulldown assay followed by genomic library sequencing will be conducted for these studies.

Chapter 3 – Materials and Methods

3.1 - Cloning and Expression of *Escherichia coli* OxyR

The sequence of *oxyR* was obtained using the Ecogene 3.0 database for *E. coli* (ecogene.org). Forward and reverse primers were generated for *oxyR* (IDT). The primers were used to PCR amplify *oxyR* from *E. coli* genomic DNA (Table 1). The primers were designed to contain specific restriction sites to use in restriction digestion. The forward primer was designed to have a restriction site for *BamH*1. The reverse primer was designed to have the restriction site for *Xho*1. A modified pET21d vector was used (provided by Darrell Peterson for the Lewis Lab) for cloning and expression of *oxyR* (Table 2). The m-pET21d vector contains a 6x His-Tag for protein purifications. The vector also contains a TEV cleavage site in order to cleave the His-Tag via TEV protease. The T7 region on the vector allows for induction via IPTG to overexpress the target protein, OxyR.

A double digestion was performed on the PCR amplified *oxyR* and the m-pET21d vector. The digestions were run on a 1% agarose gel and gel extracted (QIAGEN) after positive verification. The *oxyR* insert and vector were T4 DNA ligated (NEB) to generate m-pET21d-*oxyR* (Figure 2). The m-pET21d-*oxyR* was transformed into DH5-alpha cells. The transformed DH5-alpha-*oxyR* cells were screened for successful insertion of *oxyR* via restriction digest using BamH1 and Xho1. After confirmation of the insertion of *oxyR,* the vector was transformed into BL21(DE3) for expression.

A Halo-tagged OxyR strain was created previously in the Lewis lab. The OxyR gene was cloned into a pFC20K vector, (Table 2) which adds a Halo-tag to the protein in order to generate Halo-*oxyR*. The pFC20K vector contains a T7 site for

overexpression of protein via IPTG induction. The pFC20K-*oxyR* also contains a TEV cleavage site to remove the Halo tag from purified OxyR. The OxyR gene was PCR amplified and then successfully cloned and transformed into DH5-alpha competent cells. The cells were screened for successful insertion using Kanamycin for antibiotic screening. A successful clone was transformed into BL21(DE3) cells for expression.

3.2 - Cloning and Expression of Recombinant *Porphyromonas gingivalis* OxyR

P. ginigvalis OxyR was cloned into m-pET21d and pFC20K vectors for His-tag and Halo-tag purification tehchniques. The recombinant *P. gingivalis* OxyR strains were created previously in the Lewis lab using the similar methods described in Lewis, Yanamandra et al., 2012.

Table 1 - Primers used for cloning *E. coli* OxyR

Name	**Sequence**	**Description**
oxyR-Forward	CTT CCA GGG ATC CAT GAA TAT TCG TGA TC (BamH1)	Forward primer for *oxyR*
oxyR-Reverse	CAG CGC ACT CGA GTT AAA CCG CCT GTT TT (Xho1)	Reverse primer for *oxyR*

Table 2 - Vectors used in this study

***E. coli* OxyR**	**Description**
m-pET21d-o*xyR*	Modified pET21 vector with *E. coli* OxyR insertion Contains a 6x His-tag on N-terminal Contains a TEV cleavage site to remove His-tag
pFC20K-*oxyR*	pFC20K vector with *E. coli* OxyR insertion Attaches a Halo-tag to C-terminal Contains a TEV cleavage site to remove Halo-tag
***P. gingivalis* OxyR**	**Description**
m-pET21d-*oxyR*	Modified pET21 vector with *P. gingivalis* OxyR insertion Contains 6x His-tag on N-terminal Contains a TEV cleavage site to remove His-tag
pFC20K-*oxyR*	pFC20K vector with *P. gingivalis* OxyR insertion Attaches a Halo-tag to C-terminal Contains a TEV cleavage site to remove Halo-tag

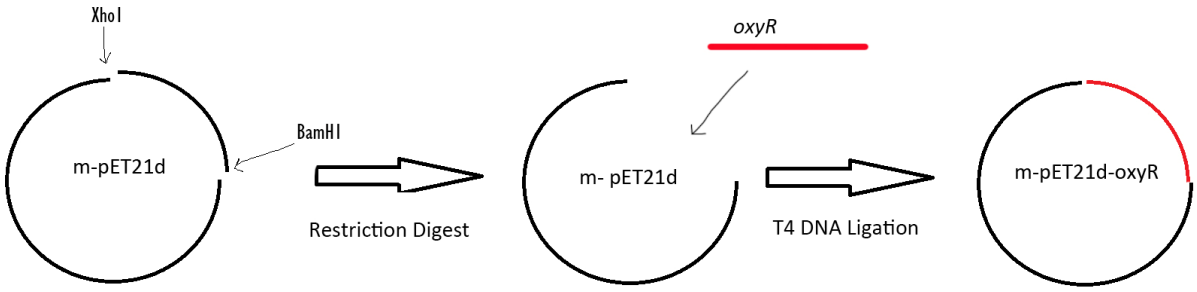

Figure 2 – Cloning strategy to insert *E. coli oxyR* into m-pET21d vector

A double digestion was performed using BamH1 and Xho1 restriction enzymes were used to cleave the vector at the specified restriction sites. T4 DNA ligation was used to insert *E. coli oxyR* into the m-pET21d vector. The *oxyR* insert was PCR amplified using primers designed to contain restriction sites for BamH1 and Xho1.

3.3 Purification of OxyR

The m-pET21d-*oxyR* and pFC20K-*oxyR* (both *E. coli* and *P. gingivalis*) were grown in either auto-induction (AI) media or Luria-Bertani (LB) with 10% Glycerol overnight at 37^{o}C at 225 RPM. When grown in LB media, the cultures were induced with 1mM IPTG at the mid log phase (0.6 OD at 660nm).

3.3.1 - His-Tag Purification of OxyR

After overnight growth, cell cultures were spun down at 8,000 RPM. The cells were washed with PBS buffer and then resuspended in His Binding Buffer (50mM NaH_2PO_4, 300mM NaCl, and 10mM Imidazole adjusted to pH 8). Lysozyme (10mg/mL) was resuspended in the His Binding Buffer when resuspending the cells. To facilitate lysis, CelLytic B cell Lysis Reagent (Sigma) was added. Benzonase was used to degrade the genomic DNA. The cells were incubated for 30 minutes at room temperature. After lysis, the cells were spun down at 15,000 RPM and the lysate (supernatant) was collected. The cell lysates were passed through a flow column containint Ni-NTA Resin (Qiagen) equilibrated with His Binding Buffer. The column was washed with His Wash Buffer (50mM NaH_2PO_4, 300mM NaCl, and 20mM IMD adjusted to pH 8). The His-tagged protein was eluted from the Ni-NTA Resin using His Elution Buffer (50mM NaH_2PO_4, 300mM NaCl, and 250mM IMD adjusted to pH 8). The elutions were run on a 10% Bis-Tris Denaturing gel to assess purity of protein.

3.3.2 - Halo-Tag Purification of OxyR

Cell cultures of pFC20K-*oxyR* were spun down at 8,000 RPM. The pellets were washed with PBS and then resuspended in Halo Binding Buffer (25mM HEPES, 150mM NaCl, and 1mM DTT adjusted to pH 7.5). The cells were lysed with Lysozyme

(10mg/mL) and CelLytic B cell lysis (Sigma). Benzonase was used to degrade the genomic DNA. The cells were incubated for 30 minutes at room temperature. The lysed cells were spun down at 15,000 RPM and the cell lysates collected. Halo Link Resin (Promega) was prepared and equilibrated with Halo Binding Buffer. The cell lysates were incubated with equilibrated Halo Link Resin with inversion for 1 hour at room temperature. The resin was added to a flow column and then washed with Halo Binding Buffer. The resin was incubated overnight with AcTEV protease (Thermo Fisher) at room temperature to cleave the Halo-tag off OxyR. The eluted protein was electrophoresed on a 10% Bis-Tris denaturing gel to assess for purity.

3.3.3 - Heparin-Affinity Chromatography Purification of OxyR

Cell cultures of m-pET21d-*oxyR* were spun down at 8,000 RPM. The pellets were washed with PBS and resuspended in Heparin binding buffer (200mM NaCl, 25mM Tris, 10% Glycerol, and 1mM DTT adjusted to pH 8). The cells were lysed with Lysozyme (10mg/mL), Cellytic B cell lysis reagent, and Benzonase to degrade the genomic DNA. The cells were incubated in lysis solution for 30 minutes at room temperature. The cells were spun down at 15,000 RPM and the cell lysates collected. The cell lysate was loaded into a Superloop 50mL column (GE) and run across a HiTrap Heparin column equilibrated with binding buffer on an ÄKTA pure HPLC machine. The Heparin column was washed with the Heparin binding buffer. OxyR was eluted using Heparin Elution Buffer (1M NaCl, 25mM Tris, 10% Glycerol, and 1mM DTT adjusted to pH 8). An elution profile was generated and the corresponding fractions collected and run on a 10% Bis-Tris denaturing gel to assess purity. After electrophoresis, the gel was stained using a Pierce 6x His Protein Tag Stain Reagent kit (ThermoFisher) to detect

the presence of the His-tagged protein. The elutions containing the 6x His tag were saved for further studies.

3.4 - Size Exclusion Chromatography Studies

Proteins were purified from the three methods detailed above (His tag, Halo, and Heparin). The purified protein was run on a Superdex 200 (10/300 GL) column (GE Healthcare) on an ÄKTA pure HPLC machine. The Superdex 200 column was equilibrated with binding buffer (200mM NaCl, 25mM Tris, 10% Glycerol, and 1mM DTT). The protein was collected off the column using the generated elution profile based on UV absorption at 280nm. The collected elutions were run on a 10% Bis-Tris denaturing gel. The His-tag and Heparin purified elutions from the Superdex 200 (purified from the m-pET21d-*oxyR*) were stained for the presence of the His-tag.

Molecular weight markers were run on the Superdex 200 using the same binding buffer to generate a calibration curve based on the volume at which the markers and proteins eluted off the column. Using the curve, an equation was derived and used to determine the experimental molecular weight of eluted proteins. The following molecular markers were used: Blue Dextran (2000 kda), Beta-Amylase (200 kDa), Alcohol Dehydrogenase (150 kDa), Albumin (66 kDa), and Carbonic Anhydrase (29 kDa).

3.5 – Sedimentation Velocity Experiment of OxyR

OxyR was purified from both His-tag and Halo-tag purification systems. The His-tagged OxyR was dialyzed into the Halo binding buffer: 25mM Hepes, 150mM NaCl, and 1mM DTT adjusted to pH 7.5. The Halo buffer was used to prepare the sample in a buffer that did not interfere with the optics and absorption profiles. Samples were prepared at various concentrations (0.1 – 1.06 mg/mL). The samples were analyzed on

a Beckman Optima XL-I analytical ultracentrifuge. The samples were run at either 45,000 or 50,000 RPM.

3.6 - Electromobility Shift Assay (EMSA) with OxyR

Fluorescent and nonfluorescent primers were designed using the EcoGene 3.0 database for *E. coli* genes for binding targets of OxyR (Table 3). The primers were designed to amplify the promoter region for each gene of interest. A set of forward primers were designed with a 5' IRDye® 700 tag (IDT). A set of identical forward primers were designed without the fluorescent tag for inhibition studies. Reverse primers were designed without a fluorescent tag. The binding targets were PCR amplified for gel shift studies. Both the His-tagged and Tagless OxyR were used for these assays. HcpR from *P. gingivalis* was purified using the His-tag purification system from a pET30 vector to run as a negative control. Two types of shifts were performed: uninhibited shifts and shifts with competitive inhibitor.

3.6.1 - Uninhibited Shift Assays

OxyR was purified from the His-tag and the Halo-tag purification systems. Increasing concentrations of OxyR ranging from 0-100pM was incubated with only the fluorescent-tagged target DNA under the following binding conditions: 0.1pM fluorescent DNA, 25mM Tris (pH 8), 6mM $MgCl_2$, 10% Glycerol, 0.5mM EDTA, 50mM NaCl, and 1mM DTT to a final volume of 25uL (adapted from Tartaglia, et al. 1992). The protein was incubated with the target DNA in binding buffer for 30 minutes at room temperature with minimal exposure to light. After incubation, the samples were electrophoresed on a thin 1% Agarose gel. The gel was imaged on an Odyssey Clx imager (Li-COR), to visualize the shifts.

3.6.2 - Competitive Inhibitor Shift Assays

Purified OxyR was incubated with fluorescent and nonfluorescent (cold) target DNA. The fluorescent and nonfluorescent target sequences were identical with the exception of the 5' IRDye® 700 fluorescent tag. OxyR at a working concentration of 100pM was incubated with fluorescent and nonfluorescent DNA under the following binding conditions: 0.1pM fluorescent DNA, 0.025-0.2pM nonfluorescent DNA, 1ug/uL Poly Poly (dI•dC), 25mM Tris (pH 8), 6mM $MgCl_2$, 10% Glycerol, 0.5mM EDTA, 50mM NaCl, and 1mM DTT at a final volume of 25uL. The concentration of nonfluroescent DNA increased with each reaction—starting from 25% of the fluorescent DNA concentration all the way to 200% (0.025, 0.05, 0.075, 0.1, and 0.2pM). The reactions were incubated in the dark for 30 minutes. Following incubation, the reactions were electrophoresed on a thin 1% Agarose gel and imaged on an Odyssey Clx imager to visualize the shifts.

Table 3 - EMSA Primers

Name	Sequence	Description
ahpCF- F.F	/5IRD700/GGTTGTAAGGTAAAACTTATCGA	Fluorescent forward primer for *ahpCF*
ahpCF - Forward	GGTTGTAAGGTAAAACTTATCGATTTGAT	Nonfluorescent forward primer for *ahpCF*
ahpCF - Reverse	CCCGGGAGCTTACACAAGTA	Reverse primer for *ahpCF*
hcp - F.F	/5IRD700/TGCACTGGGCTTATGCGGTGCC	Fluorescent forward primer for *hcp*
hcp - Forward	TGCACTGGGCTTATGCGGTGCC	Nonfluorescent forward primer for *hcp*
hcp - Reverse	CAGCCGTTTCCTGCCGGAGTACGG	Reverse primer for *hcp*
hemH - F.F	/5IRD700/CGAAAGTTGACGGCACCAAGC	Fluorescent forward primer for *hemH*
hemH - Forward	CGAAAGTTGACGGCACCAAGC	Nonfluorescent forward primer for *hemH*
hemH - Reverse	TACCGCCTCTTATCGATTCAACTTGTTG	Reverse primer for *hemH*
katG - F.F	/5IRD700/GGGCGGGAAAATAAGGTTATCA	Fluorescent forward primer for *katG*
katG - Forward	GGGCGGGAAAATAAGGTTATCAGCC	Nonfluorescent forward primer for *katG*
katG - Reverse	CAA TGT GCT CCC CTC TAC AG	Reverse primer for *katG*

3.7 - *in vitro* Pulldown of OxyR

Tagless OxyR was purified using the Halo purification system. The protein was dialyzed into Epoxy buffer A (0.1M Sodium phosphate adjusted to pH 7.4). Dynabeads M-270 Epoxy (Invitrogen) was prepared and equilibrated with Epoxy binding buffer. The dialyzed protein was incubated with the equilibrated Epoxy beads with Epoxy buffer A and Epoxy buffer B (3M ammonium sulfate) overnight with inversion at 37^{o}C to immobilize the proteins on the beads according to protocol. A working concentration of 100ug protein per 5mg of beads was used. The beads were washed and equilibrated with Pulldown Binding Buffer (200mM NaCl, 25mM Tris, 10% Glycerol, and 1mM DTT adjusted to pH 8).

Genomic DNA was prepared and sonicated to generate fragments <1kb in size using a Branson 250 Sonicator (6 minutes at 30% power, 30% duty cycle, at 20 seconds on and off). The equilibrated Epoxy-OxyR beads were incubated with the sonicated (<1kb) DNA in binding buffer (6mM $MgCl_2$, 1mM DTT, and 10% glycerol) with inversion for 1 hour at room temperature. Beads immobilized with *E.* coli OxyR were incubated with *E. coli* genomic DNA. Beads immobilized with *P. gingivalis* OxyR were incubated with *P. gingivalis* genomic DNA.

Following incubation, the beads were washed with wash buffer (200mM NaCl, 25mM Tris, 5% Glycerol, and 1ug/mL BSA adjusted to pH 8). The target DNA was eluted using elution buffer (1M NaCl, 25mM Tris, and 5% Glycerol adjusted to pH 8). The eluted DNA was PCR purified for genomic library generation.

3.8 - *in vitro* Pulldown of HcpR

P. gingivalis HcpR was purified from pET30-*hcpR* using His-tag purification. The protein was immobilized on the Epoxy beads using the same methods described above. The Epoxy-HcpR beads was incubated with sonicated *P. gingivalis* DNA. The pulldown assay was performed as described above.

3.9 - Genomic Library Generation for Pulldowns

The elutions from *in vitro* pulldown experiments were used to generate a genomic library to determine the regulon of the target proteins. The libraries were generated the ThruPlex DNA-Seq Kit and according to the protocol provided. The cycles during the library amplification step were adjusted accordingly based on concentration of input DNA (i.e. 5 cycles for 50ng input DNA). The samples were run on a Bio-Analyzer (VCU Sequencing Center) to assess for quality of the libraries generated before processing. Following adequate bio-analyzer reads, qPCR was performed on the genomic libraries and sent for sequencing. The samples were sequenced on a NextSeq Series System (Illumina).

The results were demultiplexed and aligned with the whole genome of the respective organism. *E. coli* OxyR libraries were aligned with the *E. coli* genome. The *P. gingivalis* OxyR and HcpR librares were both aligned with the *P. gingivalis* genome. The peaks were analyzed to determine what gene targets the proteins interacted with. The size of the peaks indicated the relative number of reads for that particular region on the genome. The larger the peak, the more number of reads, which indicates strong interactions between protein and DNA at that particular sequence on the genome.

Chapter 4 – Results

4.1 - Cloning and Expression of *Escherichia coli* OxyR

The OxyR gene was cloned into the m-pET21d vector to generate m-pET21d-*oxyR*. A restriction digest was performed on both the m-pET21d vector and *oxyR.* The results were run on a 1% Agarose gel. The m-pET21d vector is approximately 5.4 kB in size. The OxyR gene is approximately 900 bp in size. Following digestion, a gel extraction was performed to clone *oxyR* into the m-pET21d vector. T4 DNA ligation was performed to insert *oxyR* into the m-pET21d vector. The result were run on a 1% agarose gel to verify successful cloning of OxyR into m-pET21d vector (Figure 3). Successful clones were screened using Carbenicillin for antibiotic screening. A successful clone was also plasmid purified and sent for sequencing to verify the identity the *oxyR* insertion. When the sequence was verified for successful generation of m-pET21d-*oxyR*, the m-pET21d-OxyR was transformed into Top10 cells and subsequently into BL21(DE3) cells for expression.

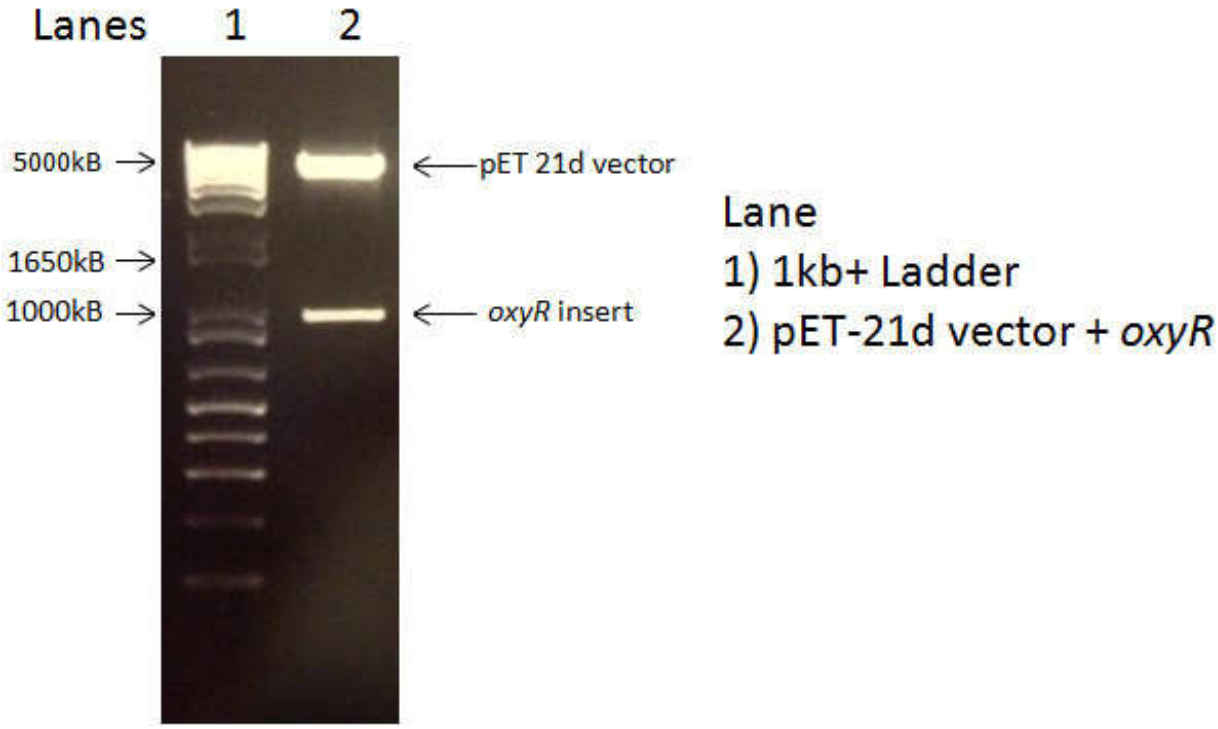

Figure 3: Insertion of *E. coli oxyR* into the m-pET21d vector

A double digestion of m-pET21d-*oxyR* using BamH1 and Xho1 restriction enzymes to determine insertion of *oxyR* into the vector. Lane 1 contains the ladder. Lane 2 contains the digestion of the m-pET21d-*oxyR* vector. The vector is approximately 5.4kb in size. The *oxyR* insert is 918bp in size. The digestion was electrophoresed on a 1% agarose gel and illuminated on a UV transilluminator.

4.2 Purification of *E. coli* OxyR

4.2.1 – His-Tag Purification of *E. coli* OxyR

OxyR was purified via His-tag purification system using Ni-NTA resin. The purified OxyR was run on a 10% Bis-tris denaturing gel with MES running buffer. The purified OxyR with a 6x His tag appears approximately 34 kDa in size on a denaturing gel, indicating a monomeric form (Figure 4a).

4.2.2 – Halo-Tag Purification of *E. coli* OxyR

E. coli OxyR was purified using HaloTag Affinity Purification from pFC20K-*oxyR*. The HaloTag was cleaved off from OxyR using AcTEV Protease to generate the tagless form of the protein. The tagless protein was ran on a 10% Bis-Tris denaturing gel to assess purity. The purified OxyR from the pFC20K vector was approximately 34 kDa in size (Figure 4b).

4.2.3 – Heparin Affinity Chromatography Purification of *E. coli* OxyR

E. coli OxyR was purified using Heparin Affinity Chromatography from m-pET21d-*oxyR*. An elution profile was generated and the corresponding elutions run on a 10% Bis-tris denaturing gel. Two major bands appeared on the gel, indicating a potentially overexpressed protein (Figure 4c). One of the major bands appearing on the gel runs at approximately 34 kDa in size. This band size matches the band sizes for OxyR purified from both His-tag and Halo-tag purifications. The other major band runs much higer at approximately 100 kDa in size.

The elutions were stained using a 6x His Protein Tag Stain kit to detect for the presence of the His-tag. The His-tag was detected in both major bands (Figure 4d).

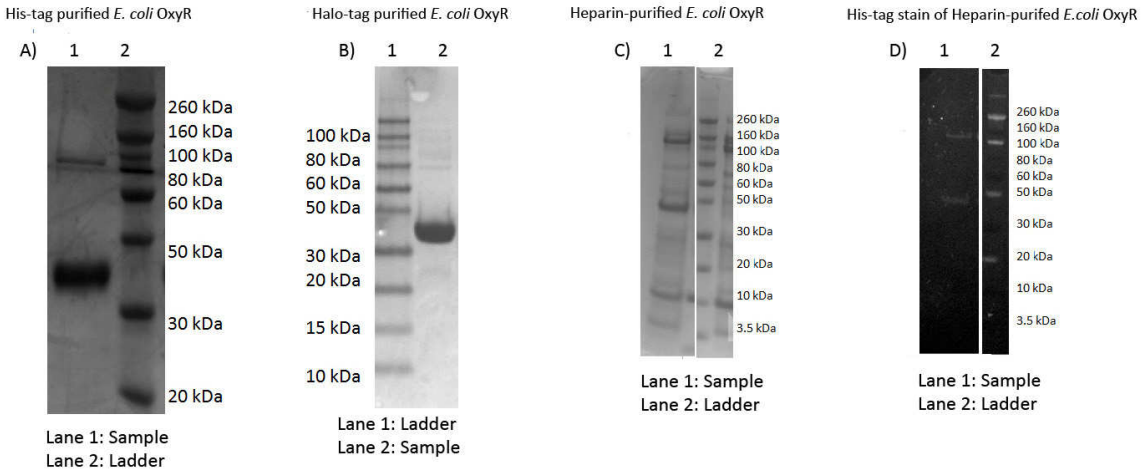

Figure 4 – Purification results of *E. coli* OxyR

The results for each of these purifications were run on a 10% Bis-tris denaturing gel in MOPS running buffer. Tris-Glycine SDS was added to each sample. A) Lane 1 contains the His-tag purified *E. coli* OxyR. Lane 2 contains protein ladder. B) Lane 1 contains protein ladder. Lane 2 contains the Halo-tag purified (tagless) *E. coli* OxyR after overnight TEV treatment. C) Lane 1 contains the Heparin purified *E. coli* OxyR with a two major bands at approximately 34 and 100 kDa. Lane 2 contains protein ladder D) Lane 1 contains protein ladder. Lane 2 contains the His-tag stain of the Heparin purified *E. coli* OxyR of Gel C to detect the presence of a His-tag. The protein was concentrated down before electrophoresis in order to get a working concentration usable to detect for the presence of the His-tagged protein. The His-tag appears in both major bands.

4.3 Purification of *P. gingivalis* OxyR

4.3.1 – Bioinformatic Comparison between *E. coli* and *P. gingivalis* OxyR

Comparisons were made between the amino acid sequences of OxyR of *E. coli* and *P. gingivalis* OxyR. These comparative studies revealed a 34% sequence similarity (Supplemental S1).

4.3.2 – His Tag Purification of *P. gingivalis* OxyR

Recombinant *P. gingivalis* OxyR was purified from m-pET21d-*oxyR*. The purified *P. gingivalis* OxyR with the 6x His-tag is approximately 34 kDa in size (Figure 5a). The purified protein appears as a monomer according to protein size on the denaturing gel.

4.3.3 – HaloTag Purification of *P. gingivalis* OxyR

Recombinant *P. gingivalis* OxyR was purified from pFC20k-*oxyR*. AcTEV protease was used to cleave the HaloTag from the protein to purify the tagless form. The purity of the protein was verified on a 10% Bis-Tris denaturing gel. The purified *P. gingivalis* OxyR runs at approximately 34 kDA in size (Figure 5b).

4.3.4 – Heparin Affinity Chromatography Purification of *P. gingivalis* OxyR

OxyR was purified using Heparin affinity chromatography from m-pET21d-*oxyR*. An elution profile was generated and the elutions run on a 10% Bis-tris denaturing gel to assess purity. Many bands appear on the denaturing gel, however a rather large major species band runs at approximately 100 kDa in size (Figure 5c). The gel was stained using a 6x His Tag Stain kit to detect the presence of a 6x His tag in order to identify which band contained the His-tagged OxyR. The major band appearing at 100 kDa was shown to contain a His-tagged protein which indicates this is the His-tagged OxyR (Figure 5d).

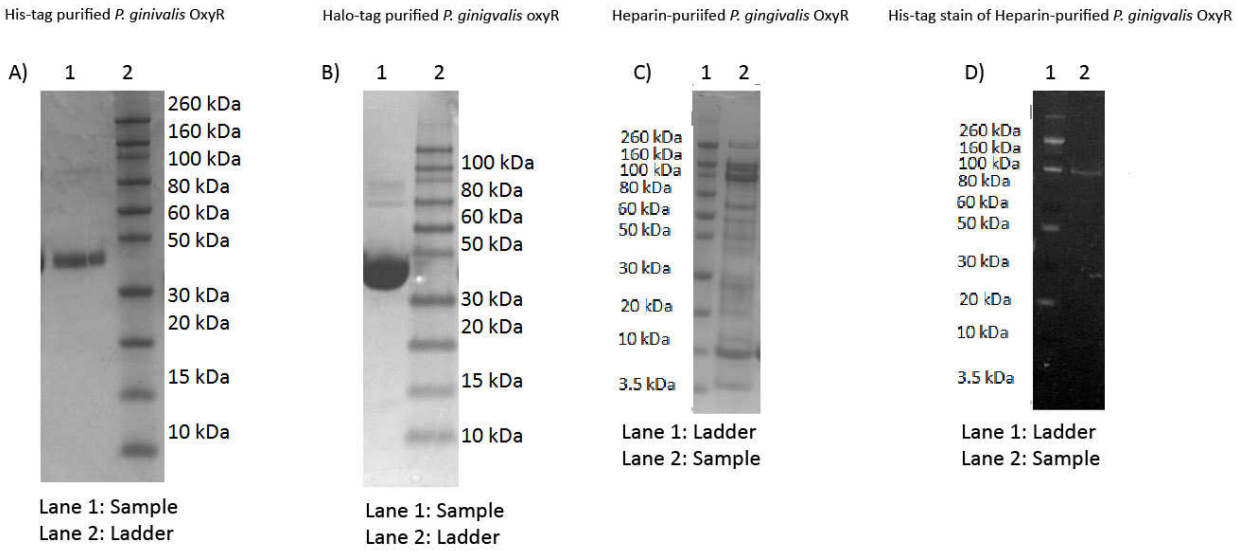

Figure 5 – Purification Results of *P. gingivalis* OxyR

The results for each of these purifications were run on a 10% Bis-tris denaturing gel in MOPS running buffer. Tris-Glycine SDS was added to each sample. A) Lane 1 contains the His-tag purified *P. gingivalis* OxyR. Lane 2 contains protein ladder. B) Lane 1 contains protein ladder. Lane 2 contains the Halo-tag purified (tagless) *P. gingivalis* OxyR after overnight TEV treatment. C) Lane 1 contains the Heparin purified *P. gingivalis* OxyR with a major band at approximately 100 kDa. Lane 2 contains protein ladder D) Lane 1 contains protein ladder. Lane 2 contains the His-tag stain of the Heparin purified *P. gingivalis* OxyR of Gel C to detect the presence of a His-tag. The protein was concentrated down before electrophoresis in order to get a working concentration usable to detect for the presence of the His-tagged protein. The His-tag appears in the major band seen in Gel C.

4.4 – Size Exclusion Chromatography Studies of *E. coli* OxyR

E. coli OxyR was purified from the three methods: His tag, Halo tag, and Heparin affinity. The resulting purifications were run on a Superdex 200 (10/300GL) column using an ÄKTA pure HPLC machine. Molecular weight markers were also run on the Superdex 200 column. An elution profile was generated (Figure 6) and used to create a standard calibration curve (Figure 7) based on the volume at which the markers eluted off the column (Table 4). The molecular weight of OxyR was calculated using both the standard calibration curve equation and the volume at which the protein elutes off the column (Table 4)**.**

4.4.1 – His-Tag Purified *E. coli* OxyR on Superdex 200 column

His-tagged *E. coli* OxyR was purified from the His-tag purification system and run on a Superdex 200 column. An elution profile was generated and the fractions collected (Figure 8). The protein was found to elute at approximately 13.1mL (Table 4). Using the equilibration curve and the volume at which OxyR eluted, the protein was calculated to be approximately 154 kDa in size, indicating it runs as a tetramer. This elution had the largest peak based on absorbance at the 280nm wavelength. All the elutions were run and run on a 10% Bis-tris denaturing gel. Two major bands appeared on the gel. The larger band appears to run at approximately 80kDa and the other at approximately 34 kDa (Figure 9a).

4.4.2 – Halo-Tag Purified *E. coli OxyR* on Superdex 200 column

Tagless *E. coli* OxyR was purified from pFC20k-*oxyR*. The purified protein was run on the S200 column. An elution profile was generated (Figure 8) and the fractions collected. The tagless protein eluted at a volume of 13.5 mL (Table 4). Using the

Standard calibration curve, the tagless OxyR was calculated to be approximately 140 kDa in size, which indicates it runs as a tetramer. This elution had the largest peak based on the absorbance at the 280nm wavelength. However, this was a rather weak and small absorbance peak. All the collected fractions were run on a 10% Bis-tris denaturing gel. However, the eluted protein was not concentrated enough to be visualized on the gel.

4.4.3 – Heparin Affinity Purified *E. coli* OxyR on Superdex 200 column

E. coli OxyR was purified using Heparin Affinity Chromatography from m-pET21d-*oxyR*. The elution containing the larger major band at 100 kDa (verified to contain His-tagged OxyR) was chosen to run on the S200 column. An elution profile was generated and all the fractions collected. Using the equilibration curve, the heparin affinity purified OxyR eluted from the Superdex 200 column was calculated to be approximately 170 kDa in size. Though larger than expected, the results indicate OxyR purified through a Heparin column runs as a tetramer in solution.

The collected fractions were run on a 10% Bis-tris denaturing gel (Figure 9b). A major band appeared at approximately 100 kDa in size from the fraction containing the elution with the largest peak based on absorbance at the 280nm wavelength. Boiling the protein and the addition of reducing agents (DTT) produced a new band at approximately 34 kDa. The samples were run concentrated down (Figure 9c) and stained to detect the presence of the 6x His tag. After staining the gel, both major bands contained a His tagged protein, indicating these bands contain the His-tagged OxyR (Figure 9d).

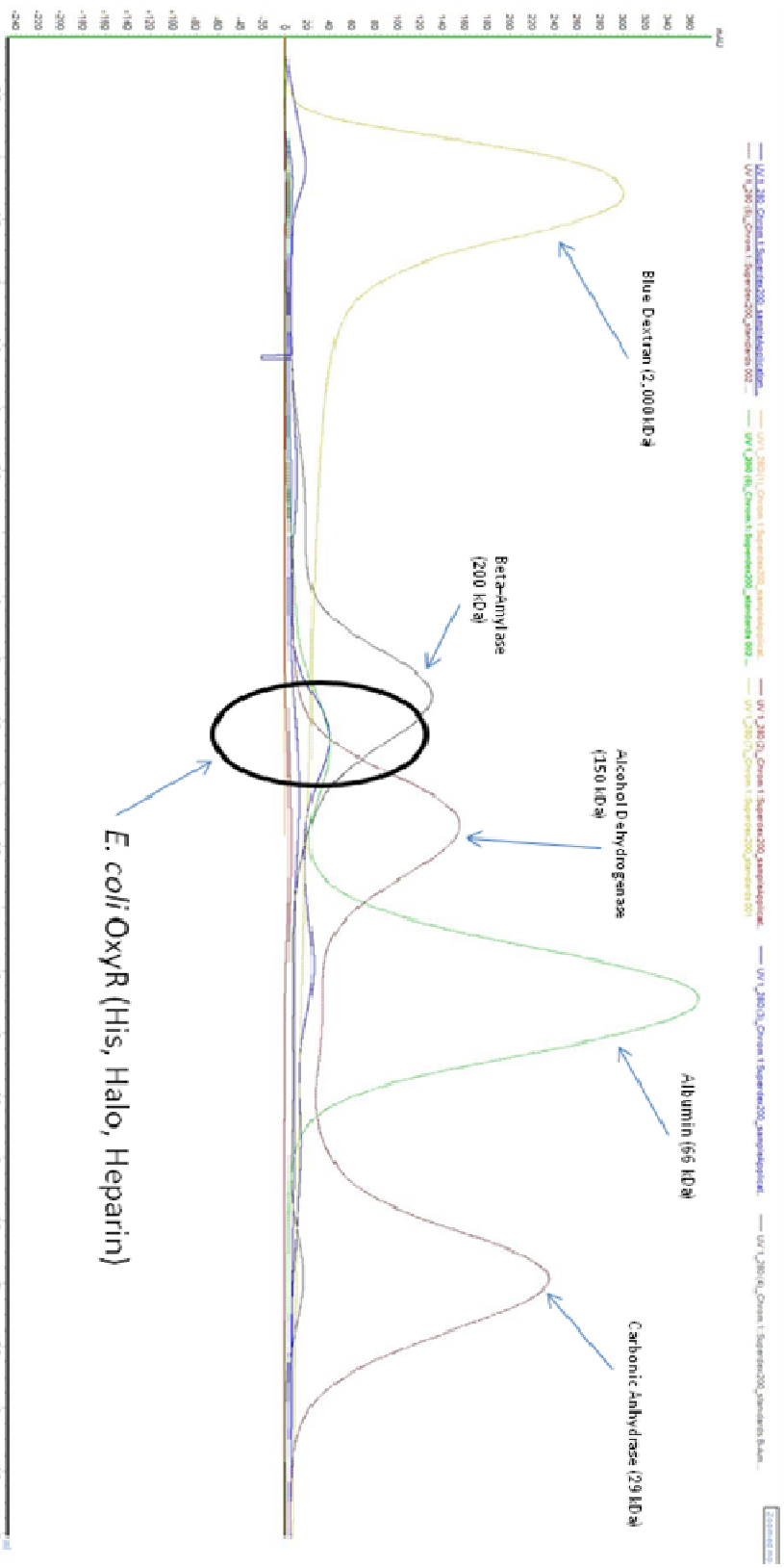
Blue Dextran (2,000 kDa)
Beta-Amylase (200 kDa)
Alcohol Dehydrogenase (150 kDa)
Albumin (66 kDa)
Carbonic Anhydrase (29 kDa)
E. coli OxyR (His, Halo, Heparin)

Figure 6 – Superdex Elution Profile of *E. coli* OxyR and Molecular Weight Standards

The elution profiles of *E. coli* OxyR (circled) purified from His-tag, Halo-tag, and Heparin affinity chromatography run on the Superdex 200 column overlaid with the elution profiles of the molecular weight standards. The elution profiles were overlaid to determine the approximates molecular weights using the markers as reference points. Blue Dextran (2000 kDa) was used to determine the void volume. The molecular weight for the His-tag and the Heparin purified protein lies between 150 and 200 kDa. The molecular weight for the Halo-tag purified protein is slightly below 150 kDa.

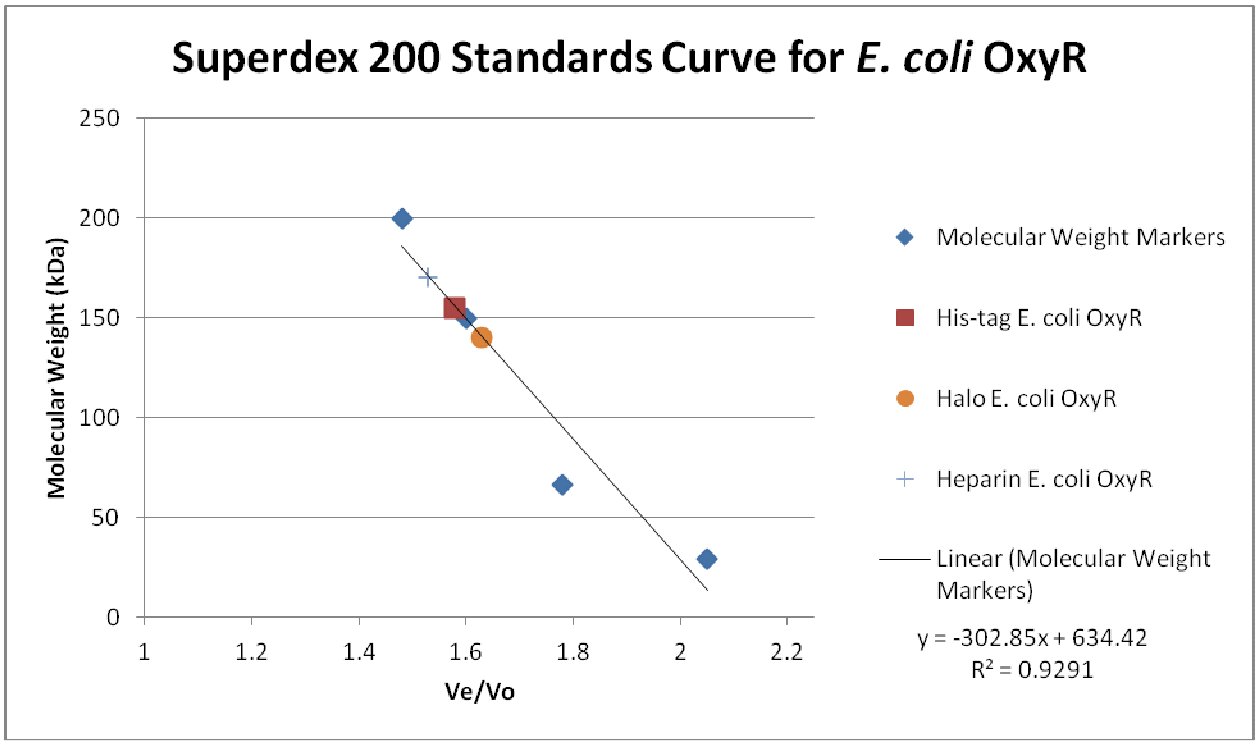

Figure 7 – Superdex 200 Standards Curve for *E. coli* OxyR

A standard calibration curve was generated using the V_e/V_o ratio (Table 5) for the molecular weight standards. V_e is the elution volumes of the markers and V_o is the elution volume for the voild volume. A best fit line was generated and the derived equation used to calculate the molecular weight of the OxyR elutions. The "Halo *E. coli* OxyR" was the smallest protein in size when compared to the His-tag and Heparin purified protein.

Table 4 - Gel Filtration Chromatography Elution Volumes for *E. coli* OxyR

Name	kDa	Elution Volume	Ve/Vo Value
Blue Dextran	2000	8.28	1
B-Amylase	200	12.23	1.48
Alcohol Dehydrogenase	150	13.35	1.6
Albumin	66	14.72	1.78
Carbonic Anhydrase	29	17	2.05
	Calculated kDa		
His-Tag Purified *E. coli* OxyR	155.92	13.1	1.58
Heparin Purified *E. coli* OxyR	171.06	12.7	1.53
Tagless *E. coli* OxyR	140.78	13.5	1.63

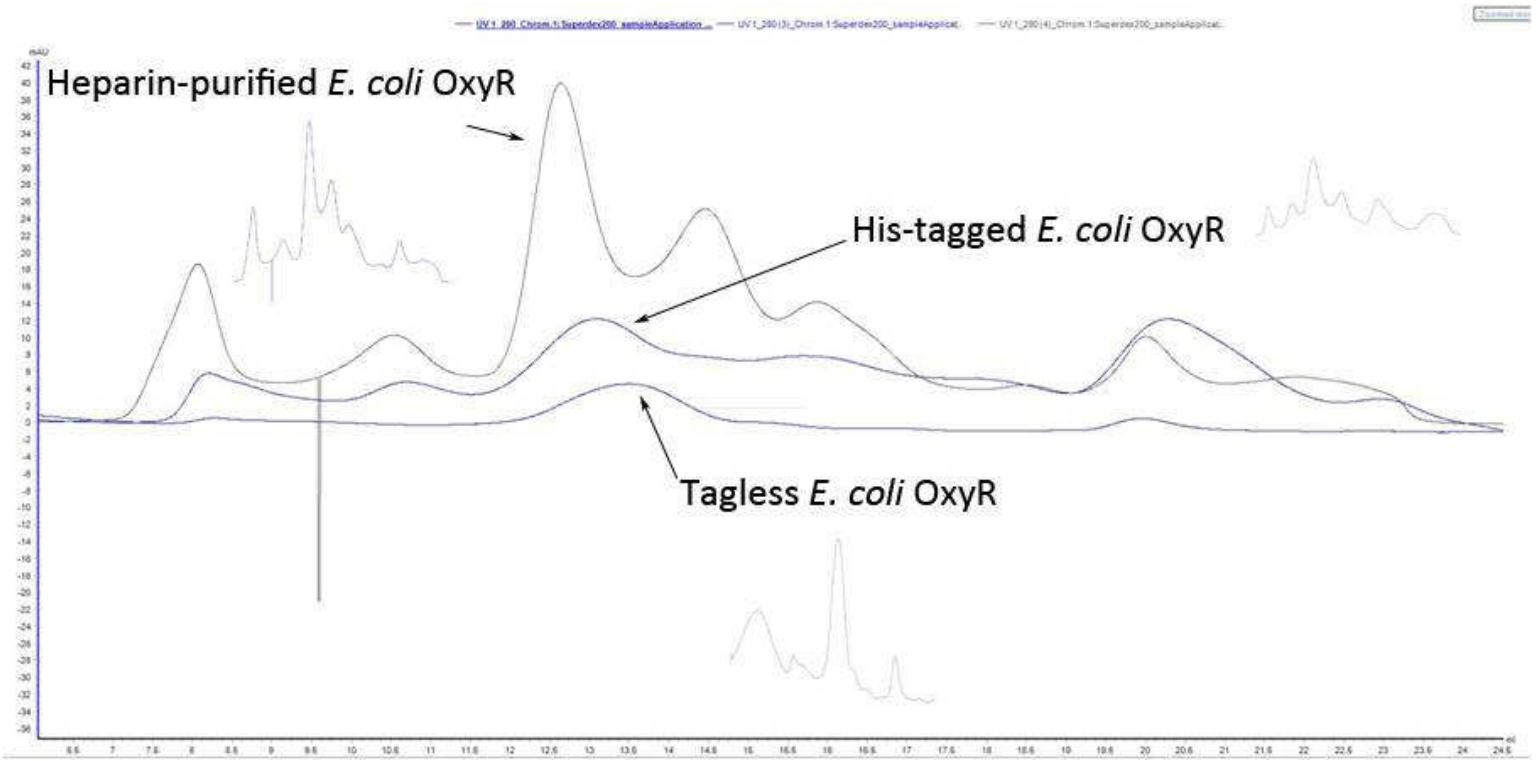
Heparin-purified *E. coli* OxyR
His-tagged *E. coli* OxyR
Tagless *E. coli* OxyR

Figure 8 – Superdex 200 Elution Profiles for *E. coli* OxyR

The elution profiles for His-tag, Halo-tag, and Heparin affinity purified *E. coli* OxyR samples run on the Superdex 200 were overlaid with one another for comparison. The major peak containing the OxyR protein all occurred around the same elution volume. The proteins eluted at between 12.5-13.5 mL. The size of the peaks indicate the absorption strength at 280nm. A larger peak corresponds to a more concentrated protein.

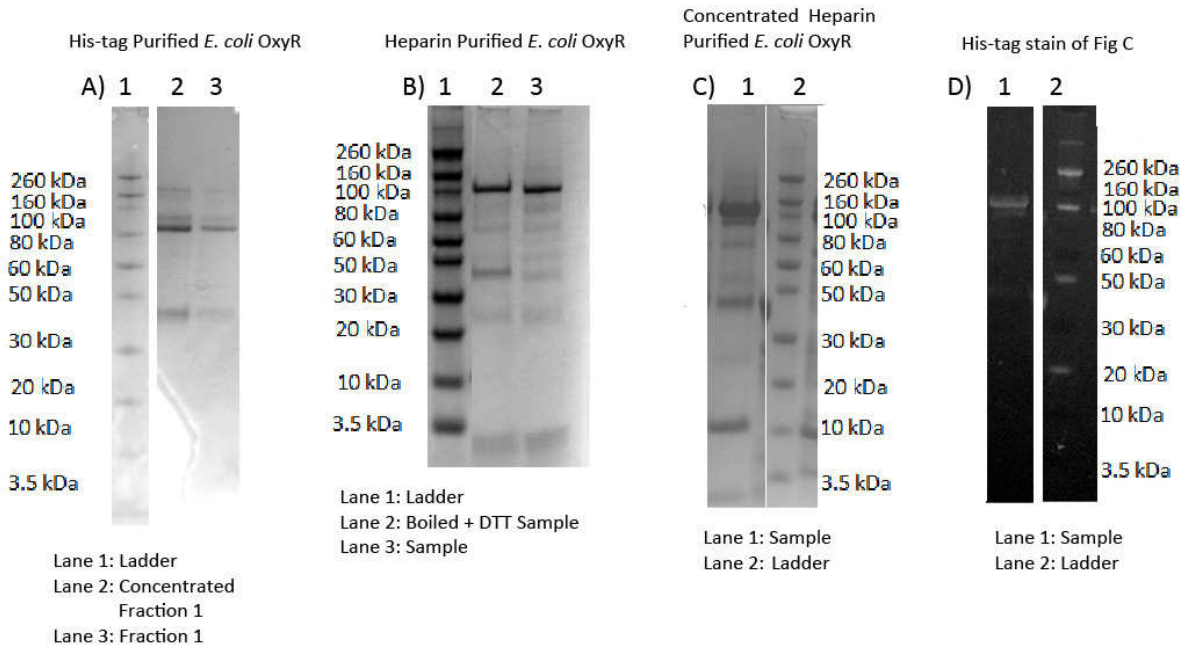

Figure 9 – Gel Filtration Results of *E. coli* OxyR on S200 column

The protein elutions were collected and run on a 10% Bis-tris denaturing gel. Tris-Glycine-SDS was added to each sample. A) Lane 1 contains the protein ladder. Lane 2 contains the His-tagged OxyR concentrated down to ensure detection on the gel. Lane 3 contains the protein taken straight from the column. B) Lane 1 contains protein ladder. Lane 2 contains OxyR that was boiled with the addition of reducing agents. Lane 3 contains the protein eluted straight from the column without any modifications.C) Lane 1 contains the Heparin- purified OxyR elution after it was concentrated down for His-tag detection. Lane 2 contains protein ladder. D) This Gel C that has been His-tag stained. Lane 1 contains the Heparin-purified OxyR elution. The His-tag appears at approximately 100 kDa. Lane 2 contains the protein ladder.

4.5 – Size Exclusion Chromatography Studies of *P. gingivalis* OxyR

P. gingivalis OxyR was purified from three methods: His-tag, Halo, and Heparin affinity. Following purification, the samples were run on a Superdex 200 (10/300GL) column using an ÄKTA pure HPLC machine. A standard calibration curve (Figure 10) was generated using molecular weight markers to determine the size of the protein eluting from the column. The elution profiles of the proteins were overlaid with the elution profile of the markers to determine the relative molecular weights (Figure 11a).

4.5.1 – His Tag Purified *P. gingivalis* OxyR on Superdex 200

His-tagged OxyR was purified from m-p21d-*oxyR* using the His-tag purification system. The protein ran at approximately 34 kDa. The purified protein was run on the Superdex 200 column. An elution profile was generated (Figure 11b) and the fractions collected. The protein eluted at approximately 12.8mL. Using the standard calibration curve, the molecular weight of the protein was calculated to be approximately 167 kDa in size (Table 5), indicating that OxyR runs as a tetramer. The fractions from the S200 column were run on a 10% Bis-tris denaturing gel. The protein was found to run at approximately 34 kDa (Figure 12a).

4.5.2 – Halo Tag Purified *P. gingivalis* OxyR on Superdex 200

Tagless *P. gingivalis* OxyR was purified from the pFC20k-*oxyR* and run on the Superdex 200. The protein was found to elute at approximately 12.8mL. It was calculated to be approximately 167 kDa in size (Table 5). This indicates that OxyR runs as a tetramer. This elution had the largest absorbance peak at the 280nm wavelength. The protein ran at approximately 34 kDa on a denaturing gel (Figure 12b).

4.5.3 – Heparin Affinity Purified *P. gingivalis* OxyR on Superdex 200

OxyR was purified from m-pET21d-*oxyR* using the Heparin affinity purification system on an ÄKTA pure HPLC machine. An elution containing a major bad at 100 kDa containing the His-tag protein (verified through His tag stain) was chosen and run on the Superdex 200 column. The elution profile showed that the protein eluted at approximately 12.88 mL (Table 5). This elution had the largest absorbance peak at the 280nm wavelength. Using the Standards calibration curve, the protein was calculated to be approximately 161 kDa in size.

The S200 elutions were run on a 10% Bis-tris denaturing gel. The eluted protein was found to run at approximately 100 kDa in size (Figure 12c). Boiling the protein and the addition of reducing agents (DTT) did not affect the protein (Figure 12c). The eluted protein was concentrated down stained for the presence of the His-tag to verify the identity of the protein. The major band at 100 kDa contained the His-tag, which indicates that the major band contains the OxyR (Figure 12de).

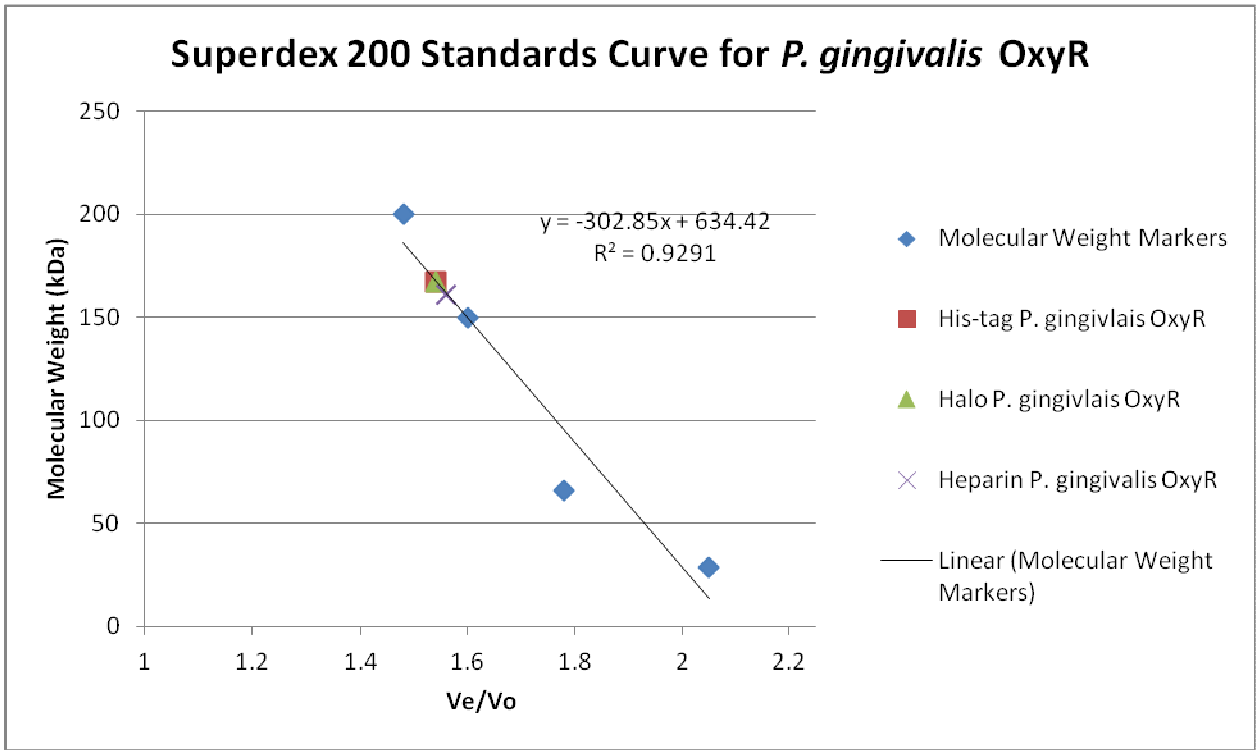

Figure 10 – Superdex 200 Standards Curve for *P. gingivlais* OxyR

The calibration curve was generated from the molecular weight markers using the V_e/V_o ratio. A best fit line was created and the derived equation used to calculate the molecular weight of the *P. gingivalis* OxyR samples eluted from the Superdex 200 column. All three forms of the protein appeared to be of the similar molecular weights.

A)

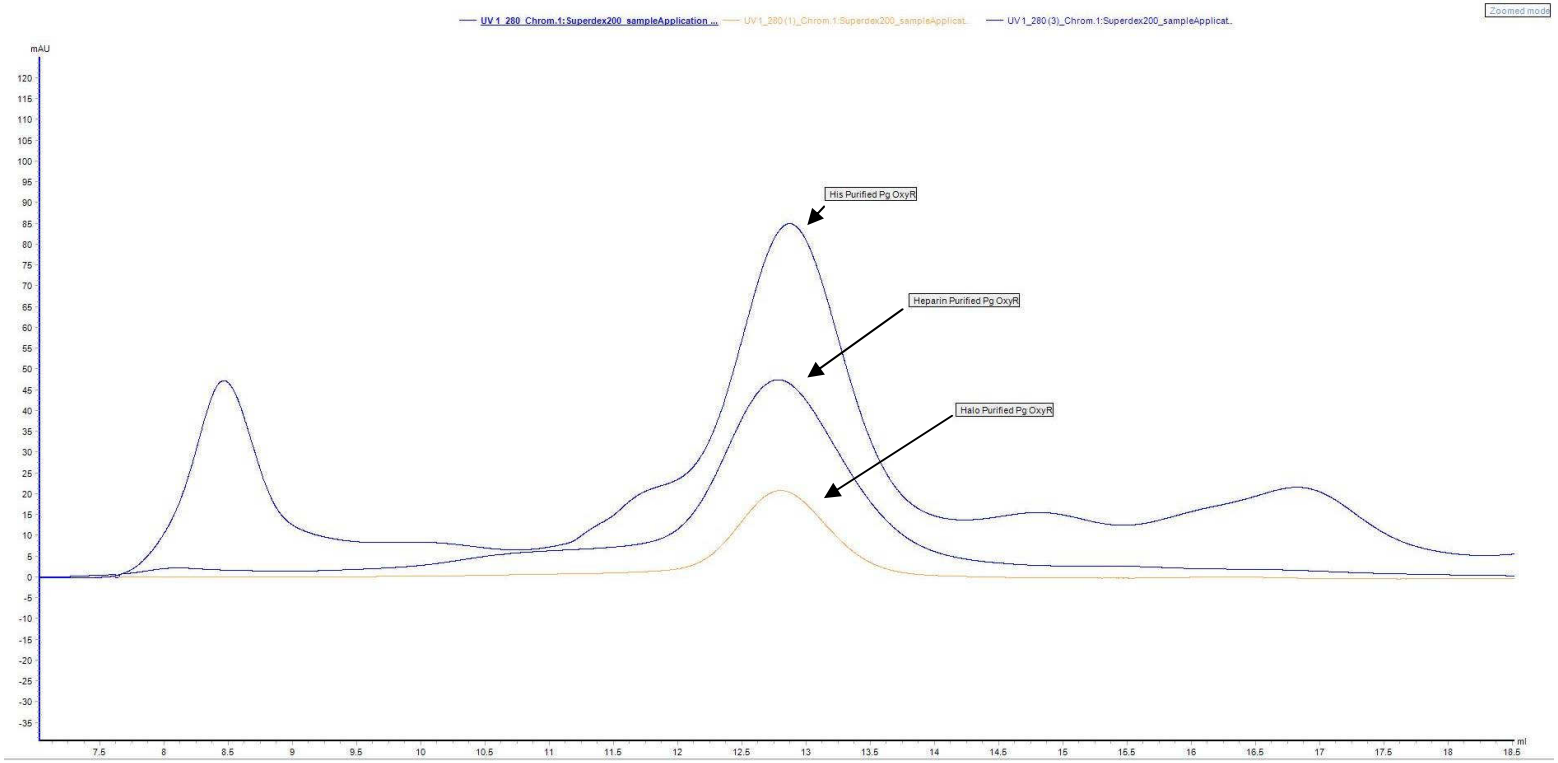
UV 1_280_Chrom.1:Superdex200_sampleApplication ...
UV 1_280 (1)_Chrom.1:Superdex200_sampleApplicat...
UV 1_280 (3)_Chrom.1:Superdex200_sampleApplicat...
Zoomed mode
mAU
His Purified Pg OxyR
Heparin Purified Pg OxyR
Halo Purified Pg OxyR
ml

B)

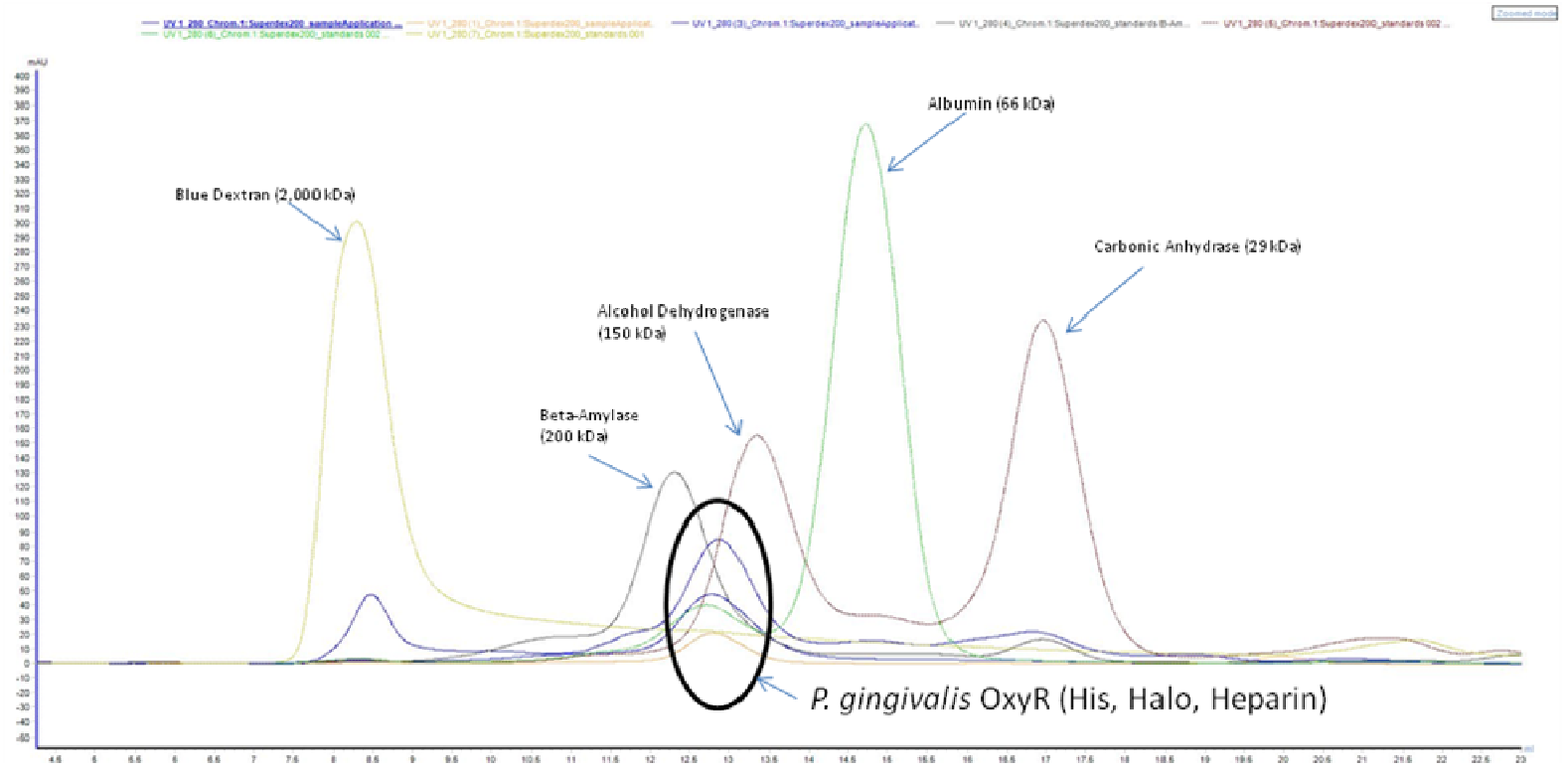
Albumin (66 kDa)
Blue Dextran (2,000 kDa)
Carbonic Anhydrase (29 kDa)
Alcohol Dehydrogenase
(150 kDa)
Beta-Amylase
(200 kDa)
P. gingivalis OxyR (His, Halo, Heparin)

Figure 11 – Superdex 200 Elution Profiles for *P. gingivalis* OxyR

A) The elution profiles generated for *P. gingivalis* OxyR from His-tag, Halo-tag, and Heparin affinity purifications run on the Superdex 200 column. The elution profile from each of these purification sources were overlaid with each other for comparision. The proteins all eluted at approximately 12.8mL from the column. When comparing the profiles, the results indicate the proteins are all very similar in size. B) The elution profiles of His-tag, Halo-tag, and Heaprin affinity purified *P. gingivalis* OxyR run on the Superdex 200 overlaid with the the profiles for the molecular weight markers. The profiles were overlaid with the markers to determine the approximate molecular weight. All three forms of the protein are between 150 and 200 kDa.

Table 5 - Gel Filtration Chromatography Elution Volumes for *P. gingivalis* OxyR

Name	kDa	Elution Volume	Ve/Vo Value
Blue Dextran	2000	8.28	1
B-Amylase	200	12.23	1.48
Alcohol Dehydrogenase	150	13.35	1.6
Albumin	66	14.72	1.78
Carbonic Anhydrase	29	17	2.05
	Calculated kDa		
His-Tag Purified *P. gingivalis* OxyR	168.03	12.8	1.54
Heparin Purified *P. gingivalis* OxyR	161.97	12.88	1.56
Tagless *P. gingivalis* OxyR	168.03	12.8	1.54

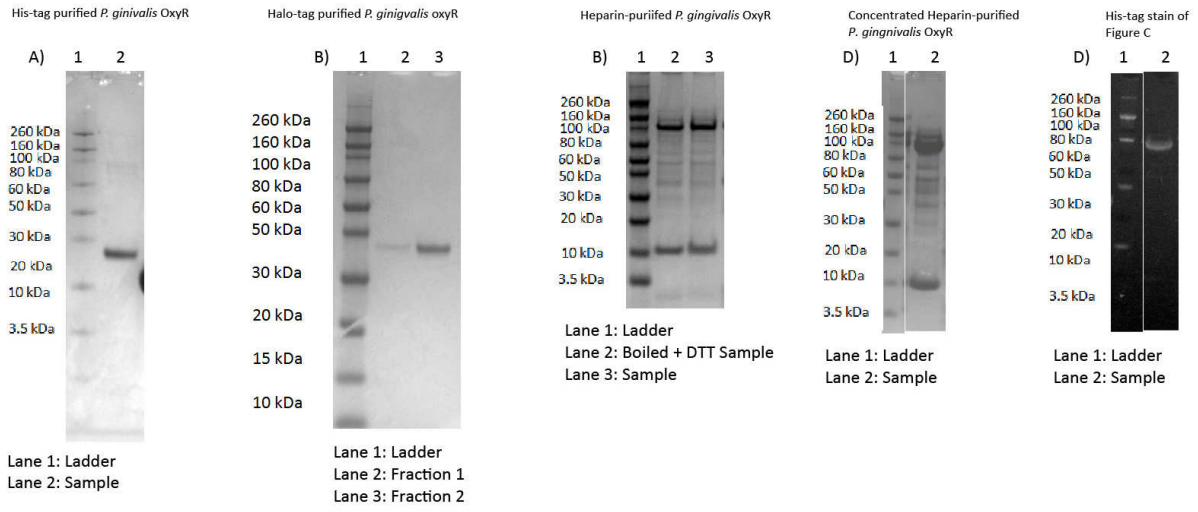

Figure 12 – Gel Filtration Results of *P. gingivalis* OxyR on S200 column

The protein elutions were collected and run on a 10% Bis-tris denaturing gel. Tris-Glycine-SDS was added to each sample. A) Lane 1 contains the protein ladder. Lane 2 contains the His-tagged OxyR concentrated down to ensure detection on the gel. Lane 3 contains the protein taken straight from the column. B) Lane 1 contains the protein ladder. Lane 2 contains Fraction 1 from the Halo-tag purified OxyR. Lane 3 contains Fraction 2 from the Halo-tag purified OxyR. These fractions were chosen based on the elution profile generated for the Halo-tag purified OxyR. C) Lane 1 contains protein ladder. Lane 2 contains Heparin-purified OxyR that was boiled with the addition of reducing agents. Lane 3 contains the protein eluted straight from the column without any modifications.D) Lane 1 contains the Heparin- purified OxyR elution after it was concentrated down for His-tag detection. Lane 2 contains protein ladder. E) This Gel C that has been His-tag stained. Lane 1 contains the Heparin-purified OxyR elution. The His-tag appears at approximately 100 kDa. Lane 2 contains the protein ladder.

4.6 – Sedimentaion Velocity Experiment Studies of *E. coli* OxyR

4.6.1 – Sedimentation Velocity Experiment of tagless *E. coli* OxyR

A sedimentation velocity experiment was performed on the tagless form of OxyR purified from pFC20k-*oxyR* using the Halo-tag purification. The OxyR was prepared at a concentration of 0.55 mg/mL. The results reveal two distinct forms of OxyR. One form exists at approximately 145 kDa and the other form at approximately 40-45 kDa (Figure 13). This indicates that *E. coli* OxyR exists as a tetramer or monomer in solution. Based on the size of the peaks, it appears the tetramer form is favored over the monomer.

4.6.2 – Sedimentation Velocity Experiments of His-Tag Purified *E. coli* OxyR

A sedimentation velocity experiment was performed on the His-tagged *E. coli* OxyR from m-pET21d-*oxyR*. The results from this experiment with the His-tagged OxyR were inconclusive due to salt or solvent interactions. Initial sedimentation values hinted at a tetramer in solution.

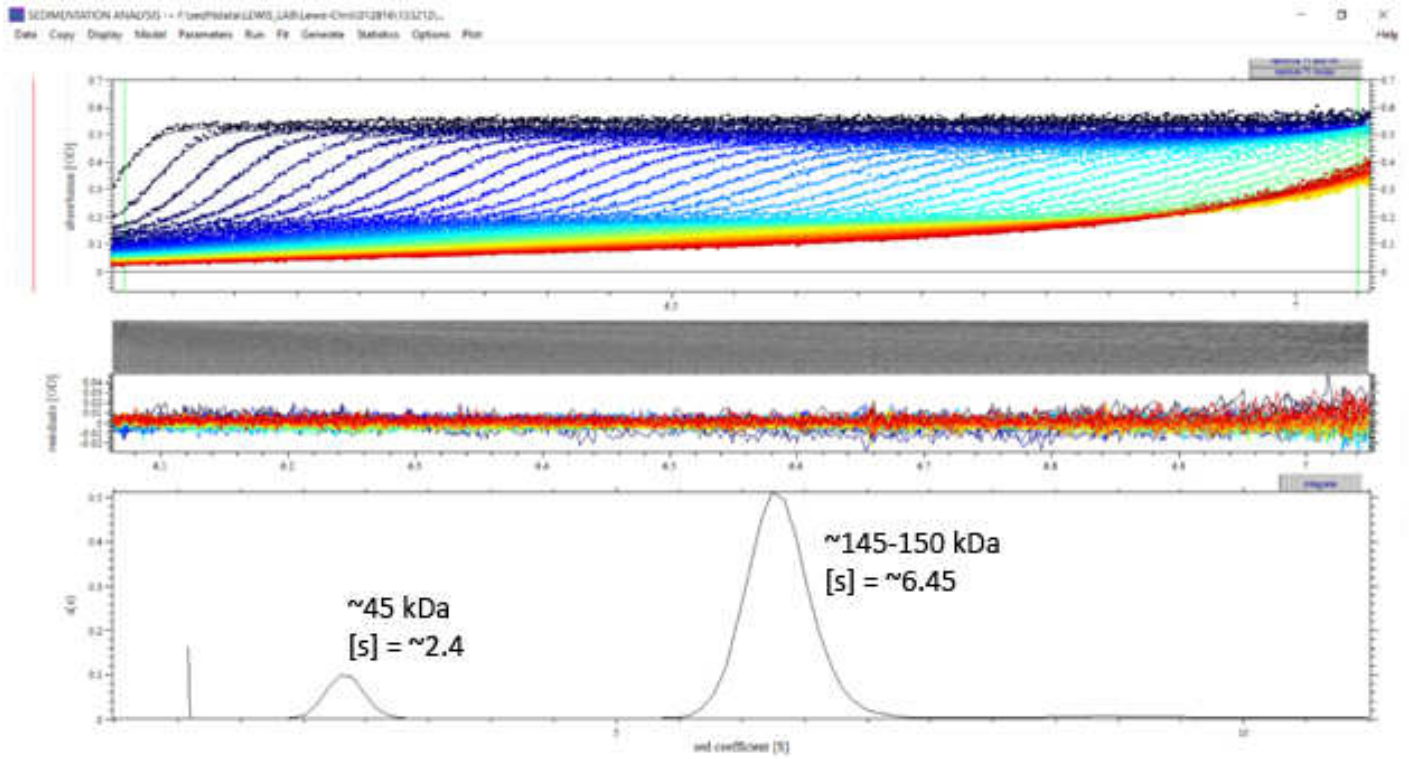

Figure 13 – **Sedimentation Velocity Experiment with tagless *E. coli* OxyR**

Sedimentation velocity experiment results of tagless *E. coli* OxyR purified from pFC20k-*oxyR.* The concentration of protein was 0.55 mg/mL. The top graph (color) depicts the OD absorbance data. The middle graph is the interference data. The gray color indicates the standard of error for the interference data is very little to no error. The interference data validates the results produced. The bottom graph is the sedimentation coefficient graph. The [s]-values were determined and used to calculate the approximate size of the protein. Bufer: 25mM HEPES, 150mM NaCl, 1mM DTT adjusted to pH 7.5.

4.7 – Sedimentation Velocity Experiment Studies of *P. gingivalis* OxyR

4.7.1 – Sedimentation Velocity Experiment of Tagless *P. gingivalis* OxyR

Tagless OxyR was purified from pFC20k-*oxyR* using the Halo-tag purification under anaerobic conditions. An undiluted sample of OxyR (1.06 mg/mL) and a 1:2 dilution (0.59 mg/mL) of OxyR sample was prepared for these experiments (Figure 14). The results from both samples reveal that *P. gingivalis* OxyR exists primarily as a tetramer (approximately 137-145 kDa) in solution (Figure 14). The absorbance peaks for OxyR appear very sharp and strong. Tagless *P. gingivalis* OxyR (0.66 mg/mL) was also purified under aerobic conditions. The result from this sample also shows that *P. gingivalis* OxyR exists as a tetramer in solution.

4.7.2 – Sedimentation Velocity Experiment of His-Tag Purified *P. gingivalis OxyR*

His-tagged OxyR was purified from m-pET21d-*oxyR* using the His-tag purification method. The centrifugation was performed on a dilute sample of His-tagged OxyR. The results show three species existing at various molecular weights: 40 kDa, 80 kDa, and 140 kDa (Figure 15). These results suggest His-tagged *P. gingivalis* OxyR exists as a tetramer, dimer, and monomer in solution when at low concentration. The absorbance peaks for these three species are connected, indicating transition between the three forms. The 140 kDa species possesses the greatest peak. The 40 kDa species has the second greatest whereas the 80kDa species has the smallest peak.

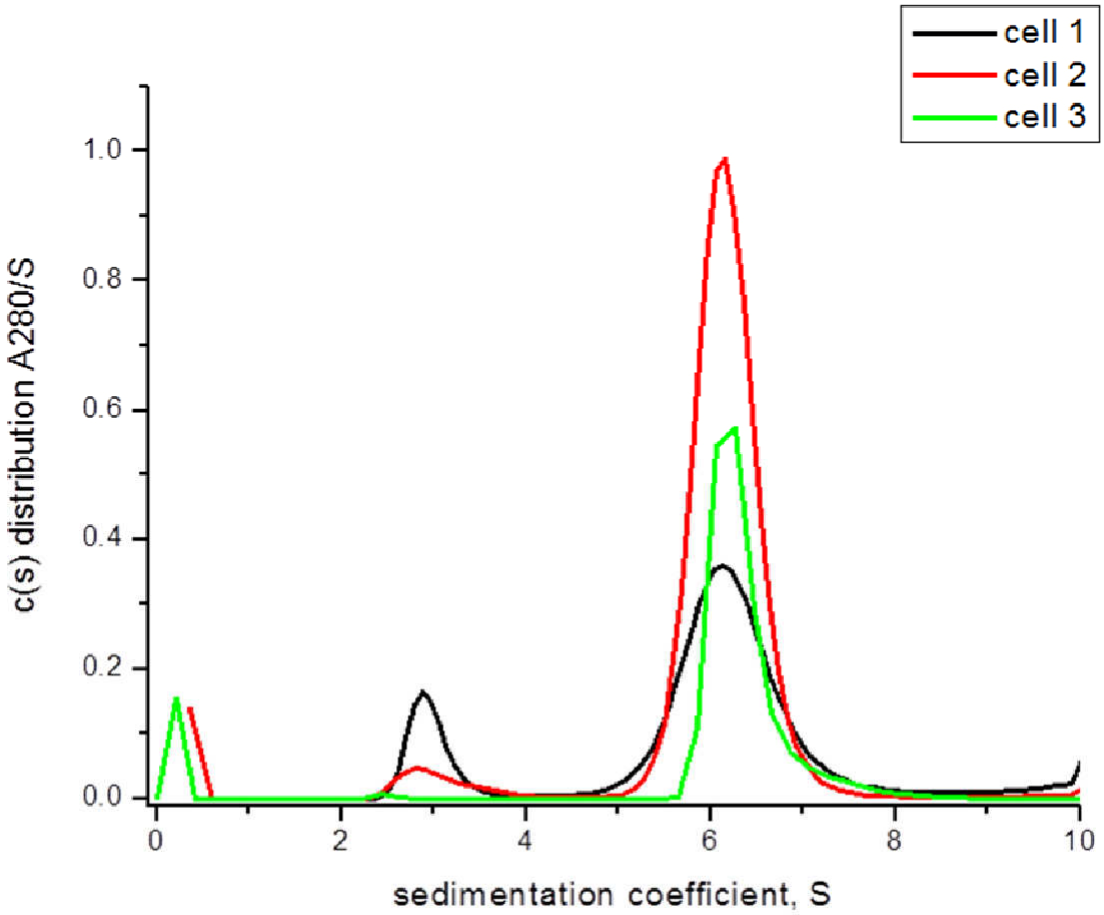

Figure 14 – Sedimentation Velocity Experiment with tagless *P. gingivalis* OxyR

Absorbance profile for tagless *P.* gingivalis OxyR. Cell 1 and 2 are tagless *P. gingivalis* OxyR purified under anaerobic conditions at 0.59 mg/mL and 1.06 mg/mL respectively. Cell 3 is OxyR purified under aerobic conditions at 0.66 mg/mL. Buffer: 25mM HEPES, 150mM NaCl, and 1mM DTT adjusted to pH 7.5).

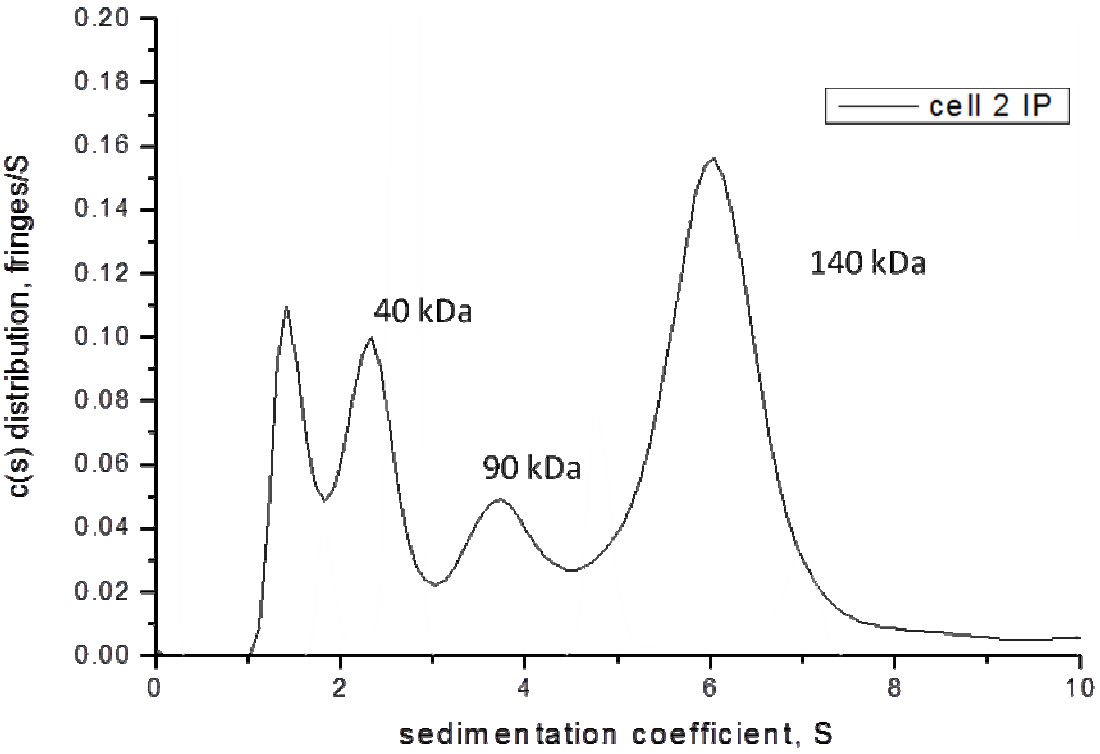

Figure 15 – Sedimentation Velocity Experiment of His-tagged *P. gingivalis* OxyR

The interference profile for His-tagged *P. gingivalis* OxyR at 0.1 mg/mL. His-tagged OxyR was dialyzed into 25mM Hepes, 150mM NaCl, and 1mM DTT adjusted to pH 7.5. This profile shows *P. gingivalis* OxyR at 3 different sizs: ~40 kDa, 90 kDa, and 140 kDa.

4.8 Electromobility Shift Assays (EMSA) with *E. coli* OxyR

Purified OxyR was tested for binding with 4 gene promoters: the *ahpCF* promoter, the *hcp* promoter, the *katG* promoter and the *hemH* promoter. Each forward primer was designed with a fluorescent tag. After incubating increasing concentrations of OxyR with target DNA in binding buffer for 30 minutes in the dark, the reactions were run on a thin 1% agarose gel. OxyR was purified from both His-tag and Halo-tag purifications.

4.8.1 – Shift Assays with tagless OxyR

4.8.1.1 – Shift Assay with the *ahpCF* promoter

For the uninhibited shift assays, increasing concentrations of tagless OxyR (0 – 120 pM) was incubated with just the fluorescent-tagged *ahpCF* gene promoter in binding buffer. A visible shift was seen between OxyR and *ahpCF* gene promoter (Figure 16a). A shifted band appears when OxyR at a concentration of 60pM is incubated with the fluorescent promoter. The shifted bands showed increased fluorescence intensity with increasing concentrations of OxyR. Likewise, the nonshifted or unbound DNA bands had a decrease in fluorescence intensity with increasing concentrations of OxyR.

For the competitive inhibition studies, increasing concentrations of OxyR was incubated with both fluorescent and nonfluorescent *ahpCF* gene promoter in binding buffer. Both promoter sequences were identical with the only difference being the fluorescent tag. A visible shift was seen between OxyR and the *ahpCF* gene promoter. With the addition of the competitive inhibitor, there is a visble difference in fluorescence intensity when compared to the uninhibited shift assays (Figure 16b). The free or

unbound DNA bands in the competitive inhibition shift assays fluoresced more intensely compared to unbound DNA bands in the uninhibited shift assay at the same concentration of OxyR. The shifted DNA bands in the competitive inhibition shift assays were less intense than the uninhibited shift assays. The same concentration of fluorescent DNA was used in both uninhibited shift assay and competitive shift assay.

4.8.1.2 – Shift Assay with the *hcp* promoter

For the uninhibited shift assay, a visible shift is seen between OxyR and fluorescent *hcp* promoter in binding buffer (Figure 16c). The visible shift appears when OxyR at a concentration of 40pM is incubated with the *hcp* promoter. The shifted bands show an increase in fluorescence intensity with increasing concentration of OxyR. At the same time, the shifted bands appear higher in the gel with increasing concentration of OxyR. The higher the concentration of OxyR, the higher up the shifted band is on the gel. The corresponding free DNA bands decrease in intensity as the concentration of OxyR increases.

Competitive inhibition studies with the *hcp* promoter and OxyR was performed with fluorescent and nonfluorescent (cold) *hcp* promoter. The fluorescence of the free DNA bands increased as the concentration of nonfluorescent *hcp* increased (Figure 16d). Likewise, the intensity of the shifted DNA did not fluoresce as intensely when compared to the uninhibited shift assays at the same concentration of fluorescent DNA. The cold probe outcompetes for binding with the fluorescent DNA.

4.8.1.3 – Shift Assay with the *katG* promoter

A visible shift was seen between OxyR and the *katG* promoter in an uninhibited shift assay. The visible shift appears when OxyR is at a working concentration of 60pM

(Figure 16e). The unshifted free DNa decrease in fluorescence as the concentration of OxyR increases. The shifted DNA bands appear to increase in intensity as the concentration of OxyR increases.

4.8.1.4 – Shift Assay with the *hemH* promoter

A visible shift was also seen between OxyR and fluorescent-tagged *hemH* promoter when performing the uninhibited shift assay (Figure 16f). The shifted DNA bands appear when *hcp* is incubated with OxyR starting at a concentration of 20pM. There is an increase in fluorescence intensity in the shifted bands as the concentration of OxyR increases. The shifted bands appear higher in the gel as the concentration of OxyR increases. The higher the concentration of OxyR, the higher up the shifted band appears on the gel. The free DNA band decreases in intensity as the concentration of OxyR increases.

The addition of competitive inhibitor appears to show a decrease in the shifted band fluorescence as the concentration of nonfluorescent inhibitor increases. However, the shift is poorly resolved (Figure 16g).

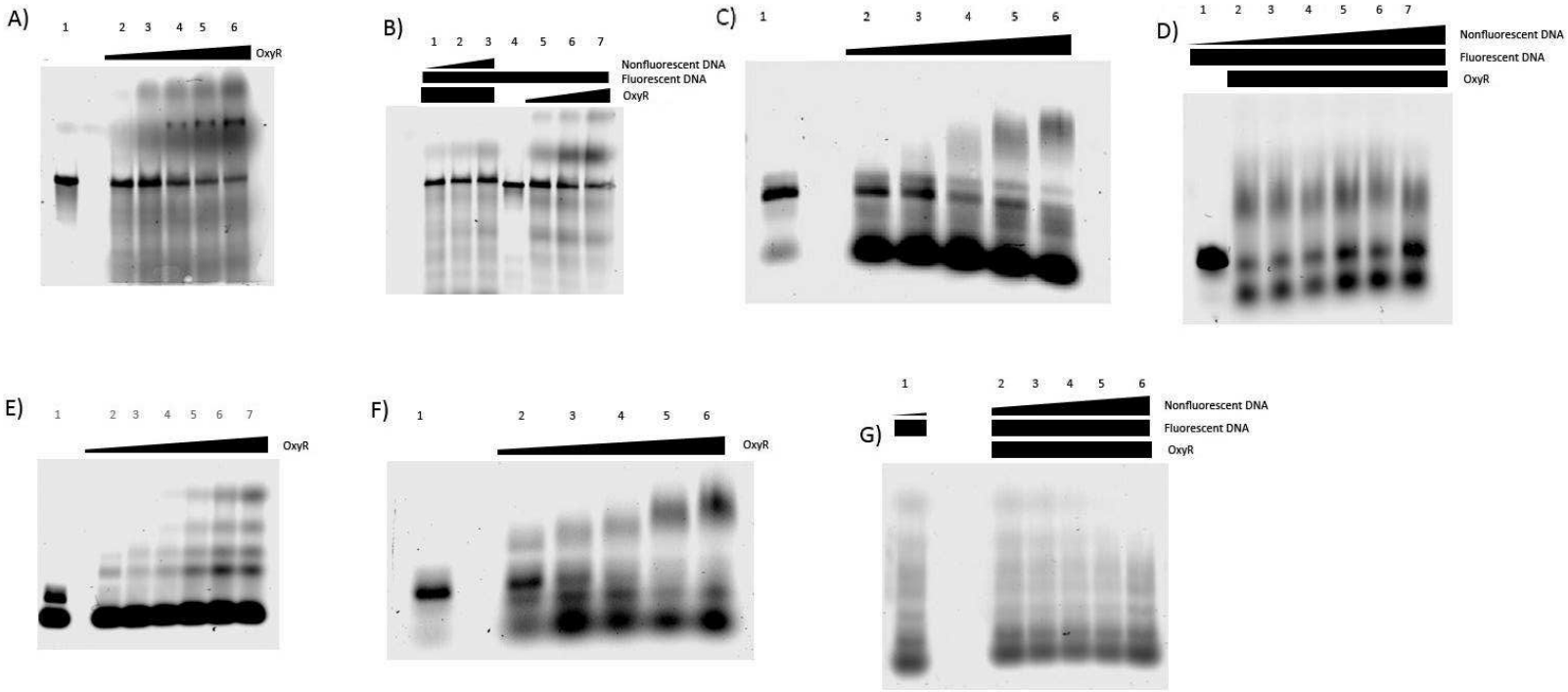
A)
1
2 3 4 5 6
OxyR
B)
1 2 3 4 5 6 7
Nonfluorescent DNA
Fluorescent DNA
OxyR
C)
1
2 3 4 5 6
D)
1 2 3 4 5 6 7
Nonfluorescent DNA
Fluorescent DNA
OxyR
E)
1
2 3 4 5 6 7
OxyR
F)
1
2 3 4 5 6
OxyR
G)
1
2 3 4 5 6
Nonfluorescent DNA
Fluorescent DNA
OxyR

Figure 16 – Electromobility Shift Assays with tagless *E. coli* OxyR

Details of binding conditions can be found under “Materials and Methods”. Reactions were electrophoresed on a thin 1% agarose gel imaged on an Odyssey Clx imager. Control lanes contain just the fluorescent-tagged target DNA in binding buffer.
A) Fluorescent-tagged *ahpCF* promoter DNA was incubated with increasing amounts of tagless *E. coli* OxyR. Lane 1 is the control lane. B) Competitive inhibition study with *ahpCF* promoter. In addition to 0.1pM fluorescent-tagged *ahpCF* promoter, Lanes 1-3 contain 0.025, 0.05, and 0.075pM nonfluorescent DNA incubated with increasing amounts of OxyR. Lane 4 serves as a control. Lanes 5-7 contain just 0.1pM fluorescent-tagged *ahpCF* promoter DNA with increasing [OxyR]. C) Fluorescent-tagged *hcp* promoter DNA was incubated with increasing concentrations of tagless *E. coli* OxyR. Lane 1 serves as a control. D) Competitive inhibition study with *hcp* promoter. Lane 1 serves as the control. Lanes 2-7 all contain 100pM *E. coli* OxyR and 0.1pM fluorescent-tagged *hcp* promoter with increasing concentrations of nonfluorescnet *hcp* promoter (0, 0.025, 0.05, 0.075, 0.1 and 0.2pM). E) Fluorescent-tagged *katG* promoter DNA was incubated with increasing amounts of OxyR. Lane 7 serves as a control. F) Fluorescent-tagged *hemH* promoter DNA was incubated with increasing amounts of OxyR. Lane 1 serves as the control. G) Competitive inhibition study with *hemH* promoter. Lane 6 serves as a control. Lanes 1-5 contain 0.1 pM fluorescent DNA and 100pM OxyR wich decreasing amounts of nonfluroescent *hemH* promoter DNA (0.1, 0.075, 0.05, 0.025, and 0pM).

4.8.2 – Gel Shift Assay with His-tagged *E. coli* OxyR

For each of these shift assays, the His-tag purified OxyR still contained the 6x His-tag on the N-terminal.

4.8.2.1 – Shift Assay with the *ahpCF* promoter

For the uninhibited shift assay, a potential shift was seen between His-tag purified OxyR and fluorescent-tagged *ahpCF* promoter (Figure 17a). As the concentration of OxyR increases, the intensity of the unbound DNA decreases. The potential shifted bands were very faint, but appear to increase in intensity as the concentration of OxyR increases ranging from 0 – 100pM. The supposed shifted bands appear in the same region on the gel.

4.8.2.2 – Shift Assay with the *hcp* promoter

A potential shift was seen between the His-tag purified OxyR and fluorescent-tagged *hcp* promoter (Figure 17b) in the uninhibited shift assay. The intensity of the free DNA bands appear to get fainter as the concentration of OxyR increases. However, the presence of shifted DNA is hard to discern. The potential shifted bands ran very close to the free DNA and have poor resolution. The appearance of the alleged shifted DNA bands may simply be the result of smearing in the gel or some kind of nonspecific interaction

4.8.2.3 – Shift Assay with the *katG* promoter

A potential shift was seen with His-tagged OxyR and the fluorescent-tagged *katG* promoter. A shift was seen when the His-tagged OxyR is at a concentration of 60pM (Figure 17c). The potential shifted bands are faint, but appear to increase in intensity as the concentration of OxyR is increased.

4.8.2.4 – Shift Assay with the *hemH* promoter

When incubating *hemH* promoter with His-tagged OxyR at concentrations ranging from 0-100pM, a potential shift is seen on the gel (Figure 17d). Increasing the concentration of OxyR resulted in a decrease in fluorescent intensity of the unbound, free DNA bands. Within this same range, a very faint band appears higher up in the gel starting at 40pM of OxyR. These bands do appear to increase in intensity as the concentration of OxyR increase, which indicates a potential shift.

To better resolve these bands higher up in the gel, the concentration range of OxyR was increased from 0-100pM to 100-250pM OxyR (Figure 17e). Despite the large increase in OxyR, no definitive shift was produced. The faint bands at the top of the gel did not increase in intensity despite the increase in the concentration of OxyR. These faint bands appear even lighter and only appear at 200-250 pM OxyR. No faint bands were seen when OxyR is at a concentration of 100pM despite appearing on the gel previously at this concentration. It is possible these faint bands are a result of gel composition and orientation. As a result, there was no definitive shift between the His-tag purified OxyR and the fluorescent-tagged *hemH* promoter in the uninhibited shift assay.

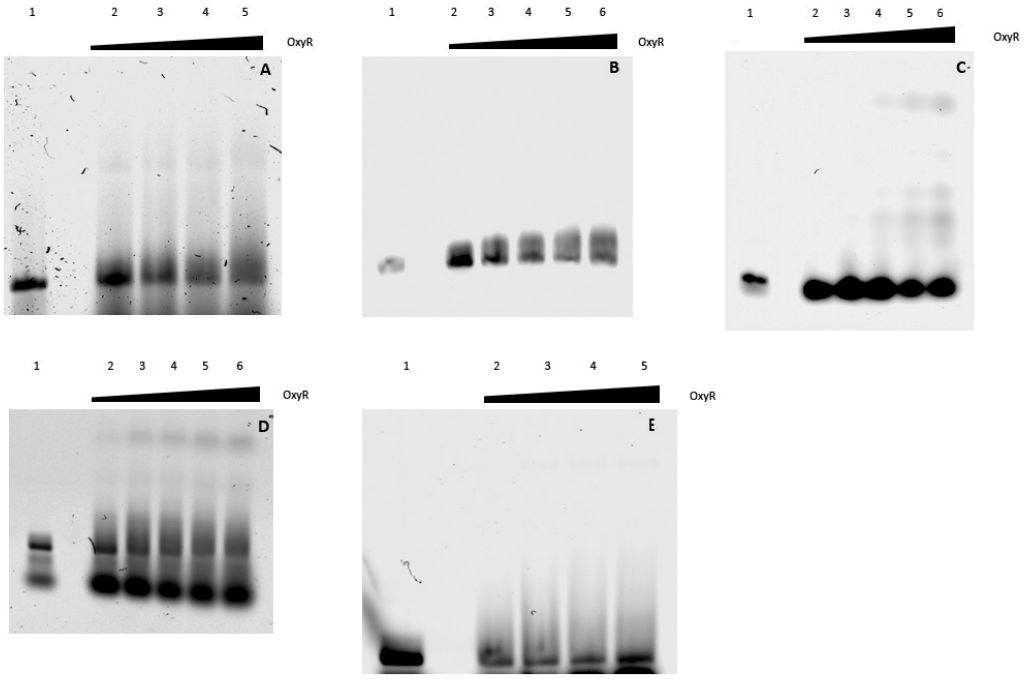

Figure 17 – Electromobility Shift Assays with His-tagged *E. coli* OxyR

Binding conditions can be found under “Materials and Methods”. Reactions were electophoresed on a thin 1% Agarose gel. Control lanes contained fluorescent target DNA only in binding buffer. A) Fluorescent-tagged *ahpCF* promoter DNA with increasing amounts of *E. coli* OxyR. Lane 5 serves as a control. B) Fluorescent-tagged *hcp* promoter DNA was incubated with increasing amounts of *E. coli* OxyR. Lane 1 serves as a control. C) Fluorescent-tagged *katG* was incubated with increasing amounts of *E. coli* OxyR. D) Fluroescent-tagged *hemH* promoter DNA was incubated with increasing amounts of *E. coli* OxyR. Lane 6 serves as a control. Fluorescent-tagged *hemH* promoter DNA was incubated with increased amounts of His-tagged *E. coli* OxyR. Concentrations were greatly increased from the standard amount. Lane 1 serves as a control.

4.9 – Electromobility Shift Assay (EMSA) with *P. gingivalis* OxyR

4.9.1 – Gel Shift Assay with tagless *P. gingivalis* OxyR

P. gingivalis OxyR was purified from the Halo-tag purification system. The Halo-tag was cleaved off resulting in the tagless form of *P. gingivalis* OxyR. When incubated with the same promoters under the same binding conditions, no visible shifts occurred with any of the four promoters (Figure 18a-d). Longer incubation time did not produce a shift either (data not shown). Increasing the concentration range of the tagless *P. gingivalis* OxyR did not produce any shifts either.

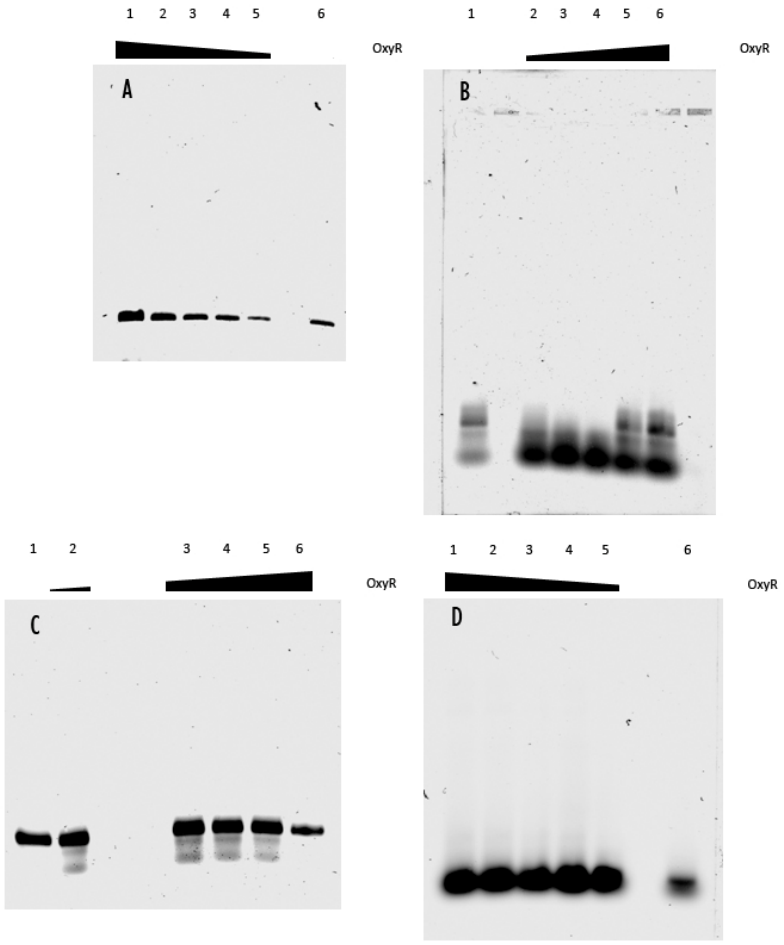

Figure 18 – Electromobility Shift Assay with tagless *P. gingivalis* OxyR

Binding conditions can be found under “Materials and Methods”. Reactions were electrophoresed on a thin 1% Agarose gel and imaged on an Odyssey Clx. Control lanes contained only fluorescent target DNA. A) Fluorescent-tagged *ahpCF* promoter was incubated with increasing amounts of OxyR. Lane 6 was the control. B) Fluorescent-tagged *hcp* promoter DNA was incubated with increasing amounts of OxyR. Lane 1 was the control. C) Fluroescent-tagged *hemH* was incubated with increasing amounts of OxyR. Lane 1 was the control. D) Fluorescent-tagged *katG* was incubated with increasing amounts of OxyR. Lane 6 was the control.

4.9.2 – Gel Shift Assay with His-Tag purified *P. gingivalis* OxyR

For each of these assays, the purified OxyR still retains the 6x His-tag on the N-terminus.

4.9.2.1 – Shift Assay with *ahpCF* promoter

When running the uninhibited shifts with His-tagged *P. gingivalis* OxyR with the *ahpCF* promoter, it seems that a nonspecific or potential shift occurs. The shift appears at when OxyR is running at a concentration of 20pM (Figure 19a). These shifted bands all appear in the same region of the gel. The shifted bands increase in intensity as the concentration of OxyR increases. The nonshifted free DNA bands decrease in intensity as the concentration of OxyR increases.

4.9.2.2 – Shift Assay with the *hcp* promoter

When incubating *P. gingivalis* OxyR with the *hcp* promoter, it appears that a very weak shift occurs (Figure 19b). The shifted bands start to appear very faintly when the concentration of OxyR is at 40pM. These bands appear to increase in intensity as the concentration of OxyR increases. The nonshifted free DNA bands decrease in intensity as the concentration of OxyR increases.

4.9.2.3 – Shift Assay with the *hemH* promoter

A shift appears to occur when performing a shift assay with *P. gingivalis* OxyR and the *hemH* promoter. The shift appears when the concentration of OxyR is at 20pM (Figure 19c**).** The shifted bands increase in intensity and vise versa the unbound DNA bands decrease in intensity as the concentration of OxyR increases. The shifted DNA bands all appear at the same region in the gel. In order to better resolve the potential shifted bands, the working concentration range of OxyR was increased from 0 – 100pM

to 100 – 250pM. However, there was no discernible effect on the shift assay (data not shown).

4.9.2.4 – Shift Assay with the *katG* promoter

No visible shift occurs when between His-tagged *P. gingivalis* OxyR and the *katG* promoter (Figure 19d).

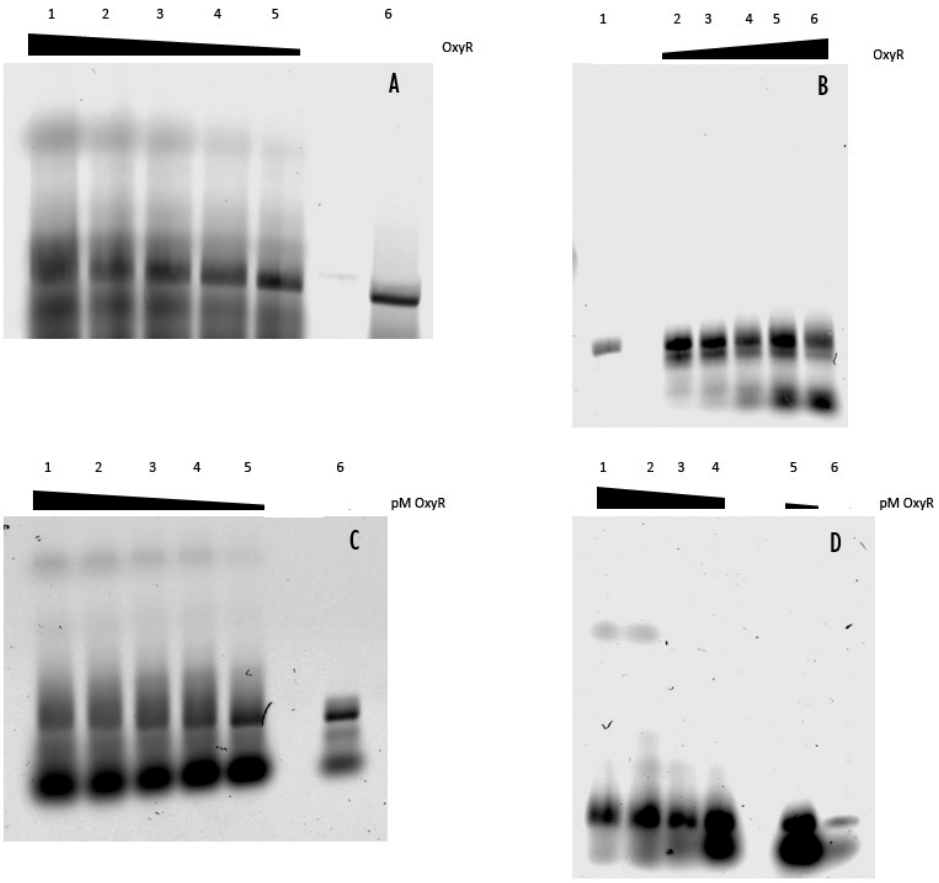

Figure 19 – Electromobility Shift Assay with His-tagged *P. gingivalis* OxyR

Binding conditions can be found under “Materials and Methods”. Each reaction contained increasing concentrations of OxyR (0-100pM). Control lanes contained just the fluorescent-tagged DNA in binding buffer. A) Fluorescent-tagged *ahpCF* promoter DNA was incubated with increasing amounts of OxyR. Lane 6 was the control. B) Fluorescent-tagged *hcp* promoter DNA was incubated with increasing amounts of OxyR. Lane 1 is the control C) Shift assay with *hemH* promoter DNA with increasing amounts of OxyR. Lane1 is the control. D) Shift assay with *katG* promoter DNA with increasing OxyR. Lane 6 is the control lane.

4.10 – Electromobility Shift Assay (EMSA) with *P. gingivalis* HcpR

P. gingivalis HcpR was purified from pET30-*hcpR* using the His-tag purification method. The pET30 vector contains a larger His-tag than the His-tag found in the m-pET21d vector used for OxyR. The HcpR used in these experiments still retained the His-tag. HcpR was incubated with the same promoters used for OxyR under the same binding conditions in order to test for nonspecific binding. No visible shift occurred when HcpR was incubated with the promoters (Figure 20a-d).

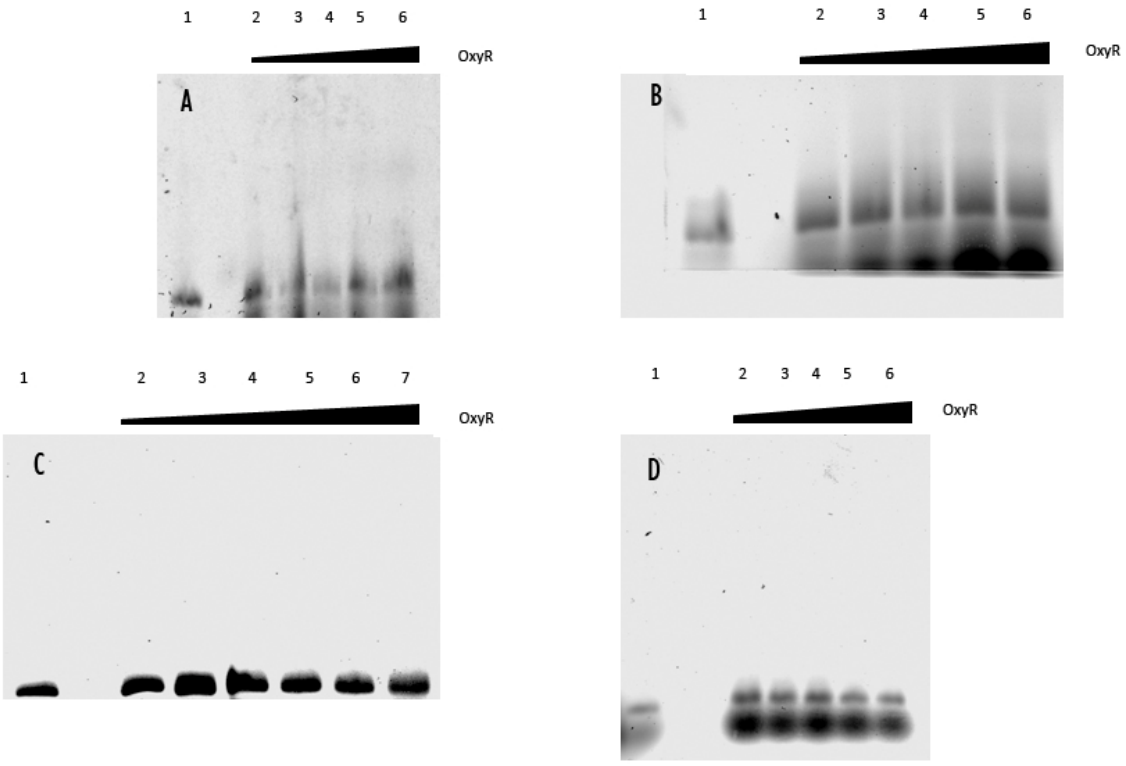

Figure 20 – Electromobility Shift Assays with His-tagged *P. gingivalis* HcpR

Gel Shift assays with His-tagged HcpR. Binding conditions can be found under "Materials and Methods". Reactions were electrophoresed on a 1% Agarose gel in the dark. Reaction controls contained just the fluorescent-tagged DNA in binding buffer. A) Fluorescent-tagged *ahpCF* promoter DNA was incubated with increasing amounts of His-tagged HcpR. Lane 1 served as the control. B) Fluorescent-tagged *hcp* promoter DNA was incubated with increasing amounts of His-tagged HcpR. Lane 1 was the control. C) Fluorescent-tagged *hemH* promoter DNA was incubated with increasing amounts of His-tagged HcpR. Lane 1 served as the control. D) Fluorescent-tagged *katG* promoter DNA was incubated with increasing amounts of HcpR.Lane 1 served as the control.

4.11 - *in vitro* Pulldown Genomic Libraries with *E. coli* OxyR

A total of 6 genomic libraries were generated from pulldown assays with Epoxy-OxyR generated from tagless *E. coli* OxyR. Each library was generated with a distinct barcode or index containing a specific sequence of nucleotides in order to identify each sample (Table 6). The quality of each library generated was assessed on a Bio-analyzer (Figure 21). All 6 of the genomic libraries generated appeared to have quality data based on Bio-analyzer results (see Supplemental for the rest of the data).

After running the libraries on a Bio-analyzer, qPCR was performed on each sample to further assess the quality of the samples (Table 7). Of the samples generated, only 4 out of 6 libraries had sequenceable results. The concentrations of these 4 libraries were all >1nM. The concentration of the rest the libraries (3 out of 7) were deemed too low for sequencing (<1nM).

The genomic sequencing data was aligned with the whole genome of BL21 *E. coli* in order to assess which genes had increased number of reads (Figure 22). The peaks correspond to OxyR-DNA interactions on the genome that were pulled down. The larger the size of the peak, the increased interaction between OxyR and DNA. Of the peaks examined, one peak at 3,946,260 on the genome, pertained to the promoter region of *mobB* (Figure 23). The gene codes for molybdenum cofactor protein, which has a role in GTP-binding and GTPase activity. The rest of the peaks examined pertained to intergenic regions within genes. Analysis of these peaks can be found in the Supplemental Data.

Table 6 - List of Indexes used for Library Generation

Sample Name	Index	Sequence
EC 1	2	CGATGTTT
EC 12.4	8	ACTTGATG
EC 211	9	GATCAGCG
EC 219	11	GGCTACAG
EC 225	1	ATCACGTT
EC 226	4	TGACCACT
PG 218	10	TAGCTTGT
PG 219	12	CTTGTACT
PG 226	3	TTAGGCAT
PG 229	5	ACAGTGGT
HcpR 1	6	GCCAATGT
HcpR 2	7	CAGATCTG
HcpR 3	A1	TATAGCCT; ATTACTCG

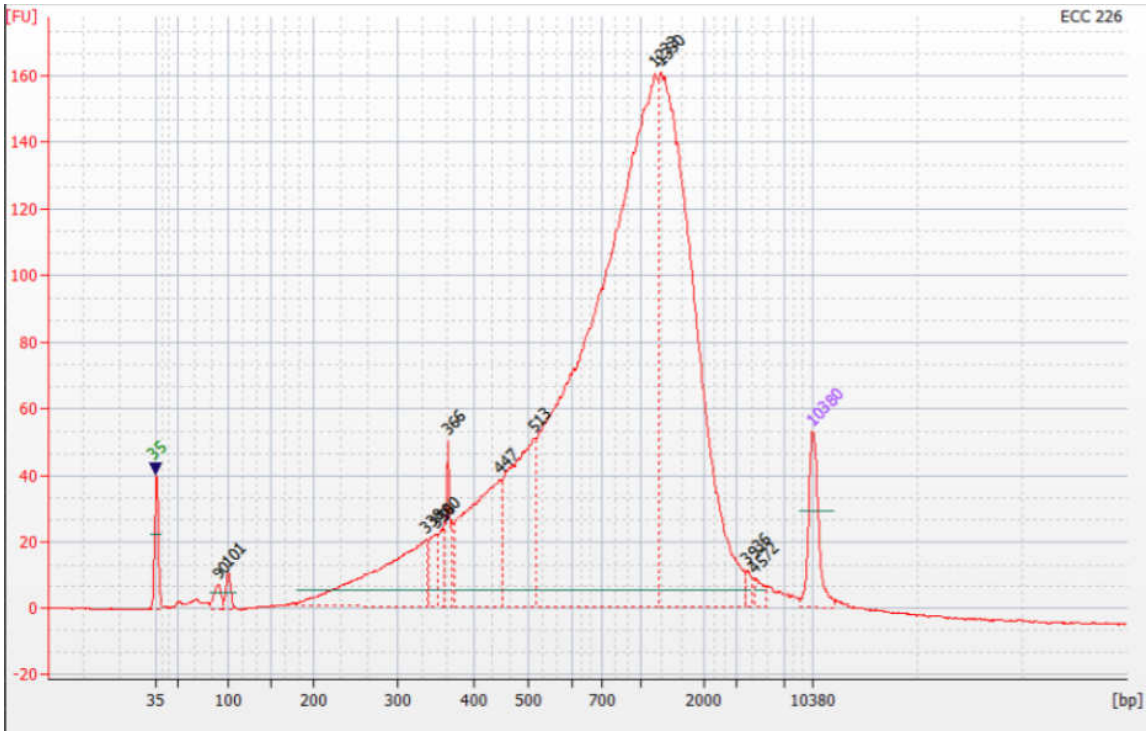

Figure 21 – Bio-analyzer result for *E. coli* OxyR Library: EC 226

Example of results expected when running genomic library on an Bio-analyzer to asses quality the genomic libraries. See supplemental data for the bio-analyzer results of all the samples.

Table 7 - qPCR results of genomic libraries

Name	nM
EC 1	0.0312
EC 12.4	2.315
EC 211	1.23
EC 219	0.072
EC 225	1.435
EC 226	1.14
PG 218	3.12
PG 219	2.9
PG 226	1.98
PG 229	0.0177
HcpR1	1.94
HcpR2	2.26
HcpR3	2.34

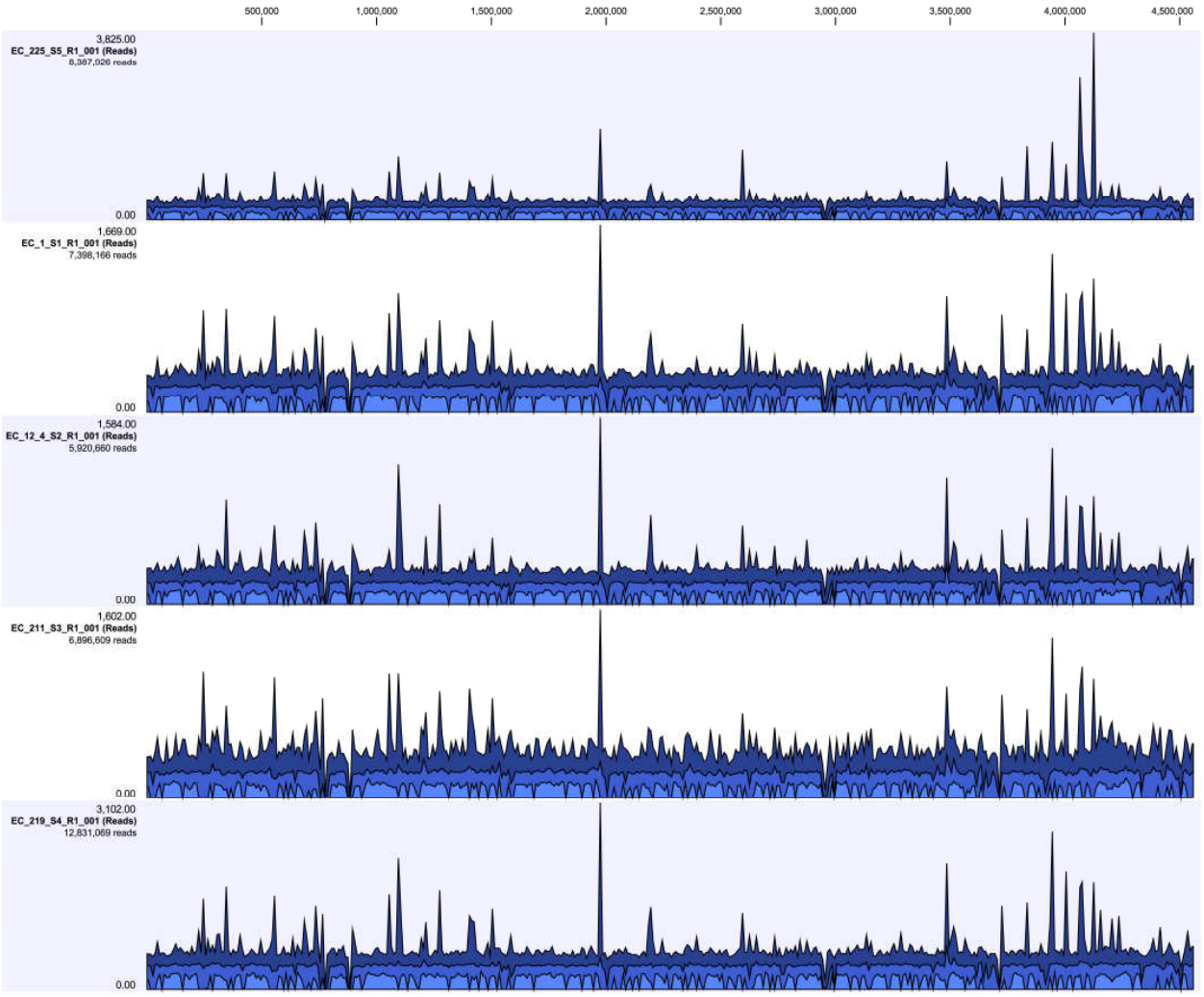

Figure 22 – Genomic Library Sequencing Data of *E. coli* OxyR

Sequencing data reads for each genomic library generated with *E. coli* OxyR are aligned with the whole genome of *E. coli*. Experimental reads are the top layer (dark blue) in each figure. The peak sizes indicate the number of hits for individual genes. The larger the size of the peaks, the more number of reads for that particular region, which indicates increased interaction and thus gene expression.

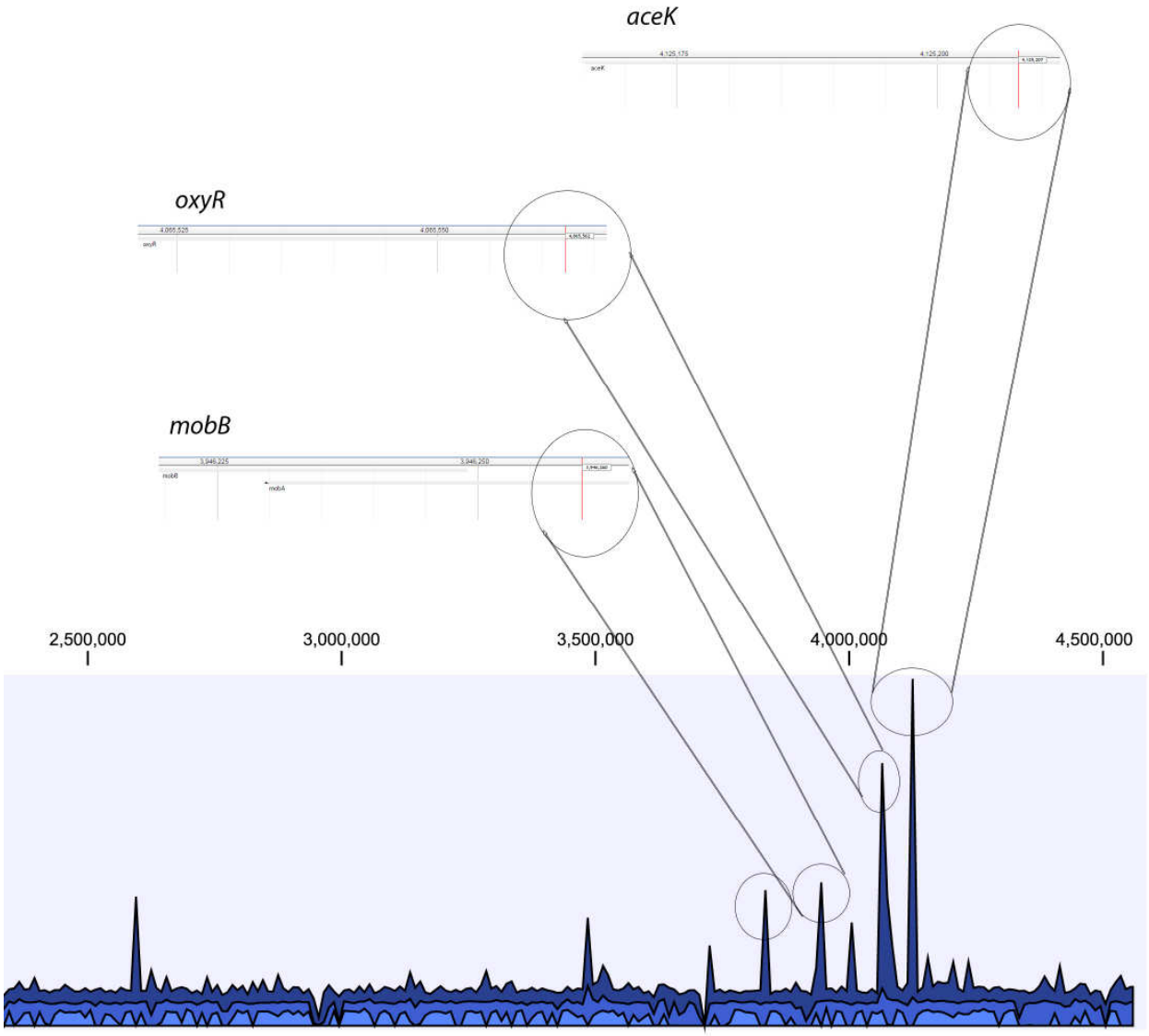

Figure 23 – Peak Analysis of EC 225 Genomic Library

Sequencing data for “EC 225” genomic library lined up with the genome of BL21 *E. coli.* The coordinates of the OxyR-DNA interactions were examined to determine the binding targets of OxyR. Three interesting peaks are shown here: *mobB, oxyR,* and *aceK*. The *mobB* peak pertains to the promoter region. The two other peaks pertain to intergenic regions within those genes. Peak analysis for the rest of the peaks can be found in the Supplemental data.

4.12 - *in vitro* Pulldown Genomic Libraries with *P.gingivalis* OxyR

A total of 4 genomic libraries were generated from Epoxy-OxyR generated from Halo-tag purified *P. ginigvalis* OxyR. Distinct barcodes were used for each library generated (Table 5**)**. Bio-analyzer results showed that all 4 libraries submitted had quality data (Figure 25). The results from qPCR showed that 3 of the 4 libraries submitted had concentrations high enough for sequencing (>1nM) **(**Table 6).

Sequencing data for *P. ginigvalis* OxyR was demultiplexed to sort out the libraries based on index sequence. The genomic library sequencing data was aligned with the whole genome of *P. gingivalis* in order to assess the approximate number of peaks for individual genes of interest (Figure 26). The larger the peak, the more number of reads for that particular gene indicating increased expression of that gene.

The exact location of OxyR-DNA binding pertaining to the various peaks was closely-examined. The sequencing results of *P. gingivalis* OxyR libraries were reproducible across the various samples submitted. Of all the peaks examined, the peak coming in at 1,287,432 on the genome showed that *P. gingivalis* OxyR appeared to bind to the promoter region of the PG 1209 gene (Figure 27). The rest of the peaks examined appeared to be nonspecific binding to various genes rather than the gene promoter.

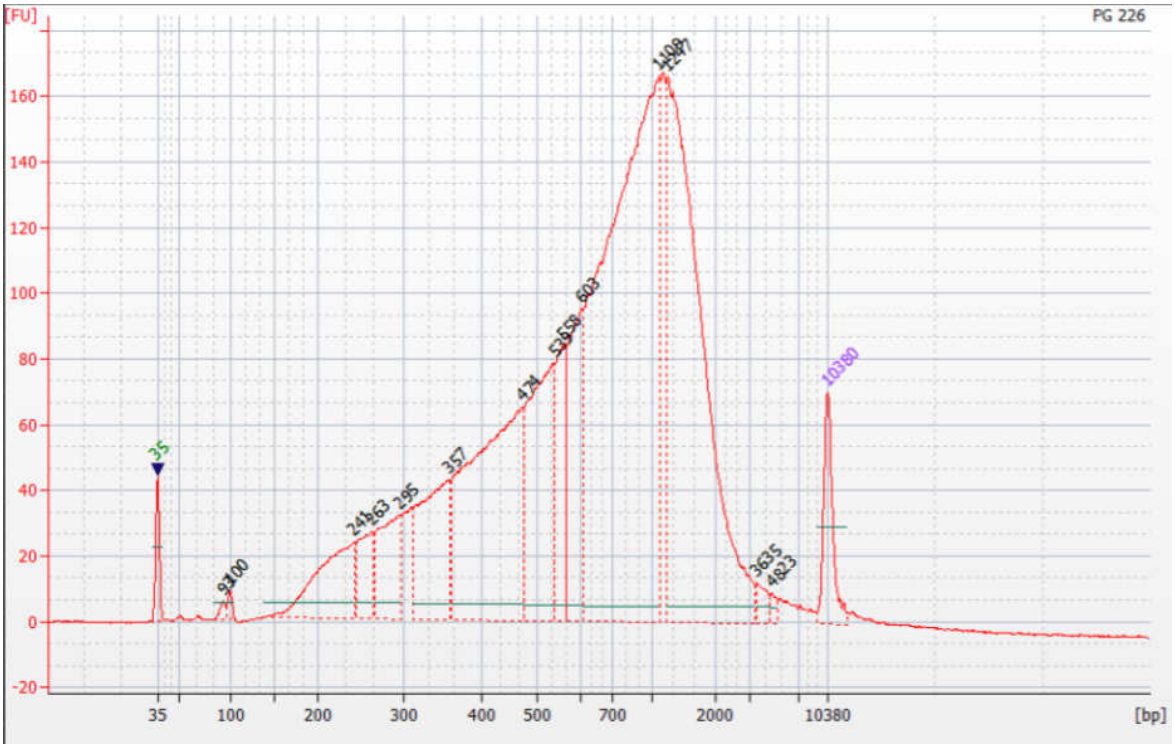

Figure 24 – Bio-analyzer result for *P. gingivalis* OxyR Library: PG 226

Example of bio-analyzer results for *P. gingivlalis* OxyR libraries. See supplemental data for the rest of the libraries.

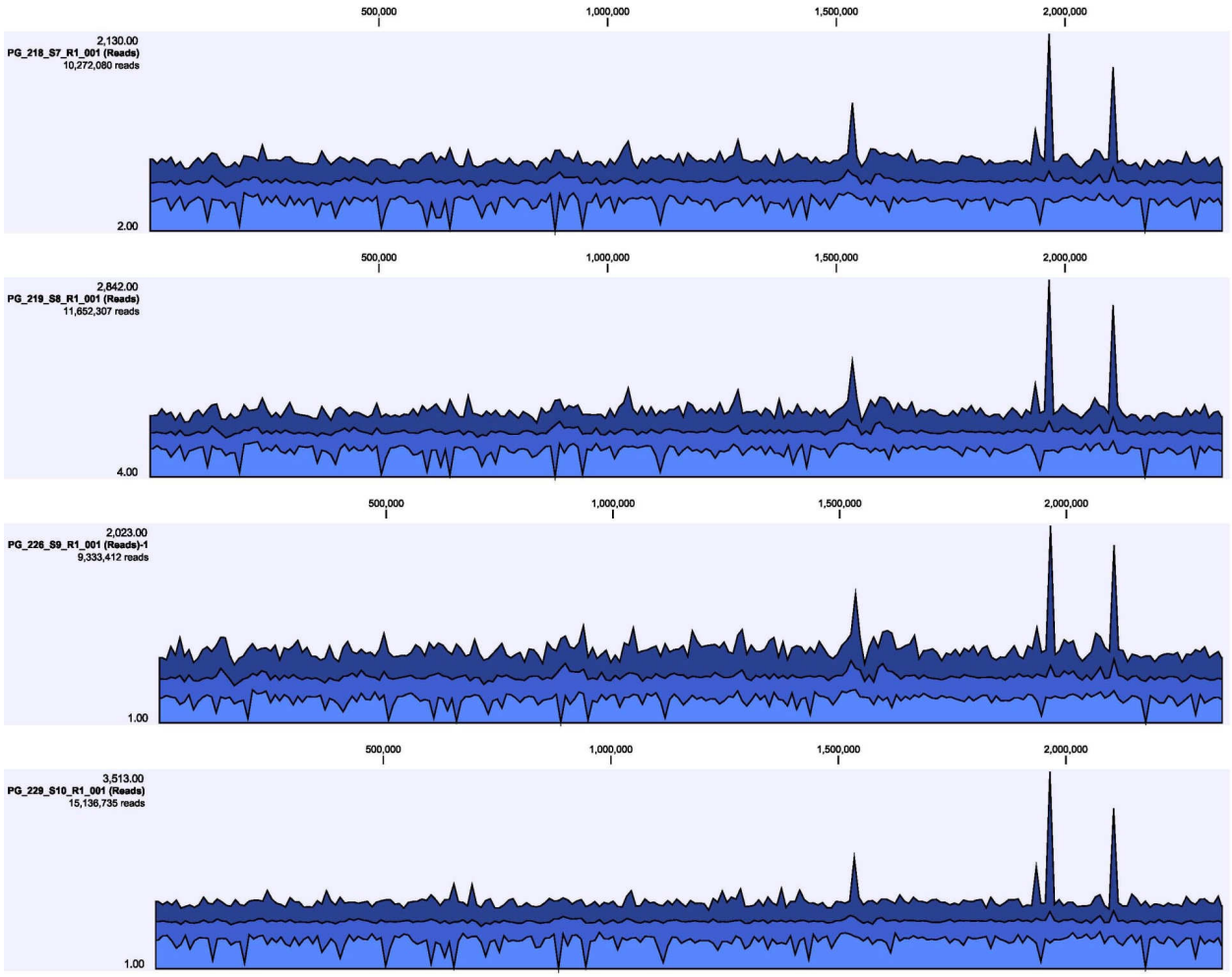

Figure 25 – Genomic Library Sequencing Data for *P. gingivalis* OxyR

Sequencing data reads for each genomic library generated with *P. gingivalis* OxyR is overlaid with the whole genome for *P. gingivalis*. The experimental reads are shown in dark blue for each figure. The peaks indicate the number of reads for individual genes.

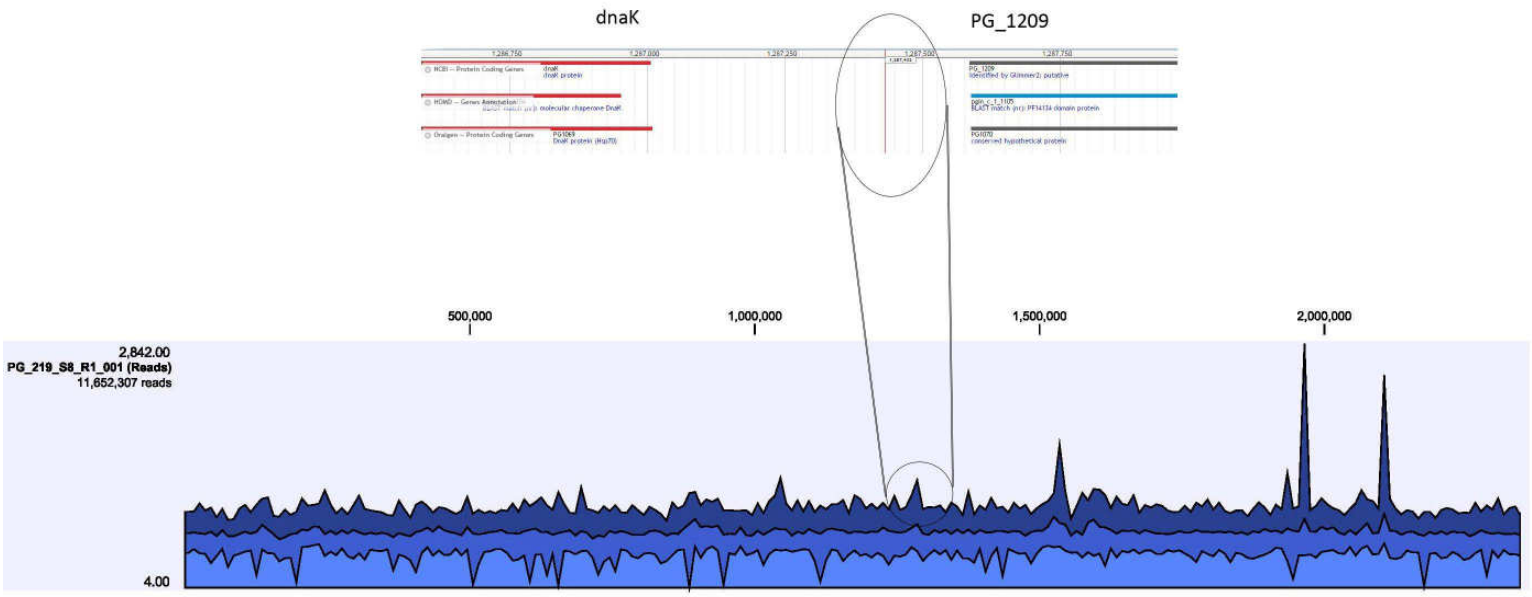

Figure 26 – Peak Analysis of PG 218 Genomic Library

Sequencing data for “PG 218” genomic library lined up with the genome of *P. gingivalis*. The location of OxyR-DNA interactions was examined to determine the binding targets of OxyR. See supplemental figures for analysis of the other peaks.

4.13 - *in vitro* Pulldown Genomic Libraries with *P.gingivalis* HcpR

Three genomic libraries were generated from Epoxy-HcpR. HcpR purified using His-tag purification and immobilized on Epoxy beads. Distinct barcodes were used for the libraries (Table 5**)**. Bio-analyzer results showed that all 3 libraries contained quality data (Figure 27). The qPCR results (Table 6) showed that all 3 of the libraries had concentrations high enough for sequencing (>1nM).

Sequencing data for HcpR Libraries was demultiplexed to sort out the libraries based on index sequence. The genomic library sequencing data was aligned with the whole genome of *P. gingivalis* in order to assess the approximate number of peaks for individual genes of interest (Figure 28). The larger the peak, the more number of reads for that particular gene and thus increased expression for those genes.

The exact location of HcpR-DNA binding pertaining to the various peaks was closely-examined. The sequencing results of *P. gingivalis* HcpR were largely similar with the exception of a very large peak in the HcpR 2 library (Figure 29). The HcpR 2 Library was chosen for close-examination. The large peak coming in at 955,987 on the genome showed that HcpR binds to the promoter region of PG0893, which encodes for hydroxylamine reductase (Figure 28).

Side-by-side comparisons were made between the PG 218 and the HcpR 2 libraries (Figure 30). There was a large number of reads for the promoter region of PG0893 or *hcp* in the HcpR 2 library. This finding was not seen in the PG218 library. At the same time, there was a large number of reads for the promoter region of PG1209 that was not seen in the HcpR 2 library. The other major peaks are present in both libraries.

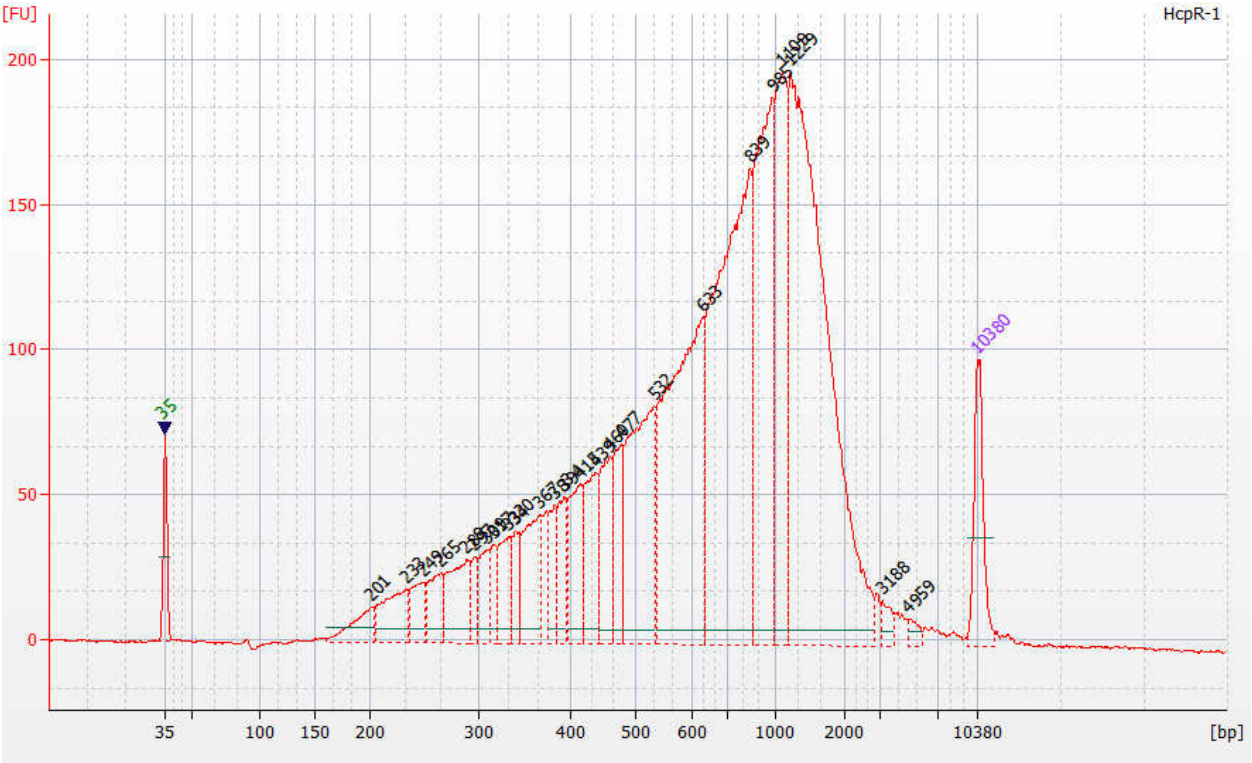

Figure 27 – Bio-analyzer esult for *P. gingivalis* HcpR Library: HcpR 1

Example of bio-analyzer results of HcpR. See supplemtanl figures for the rest of the bio-analyzer results.

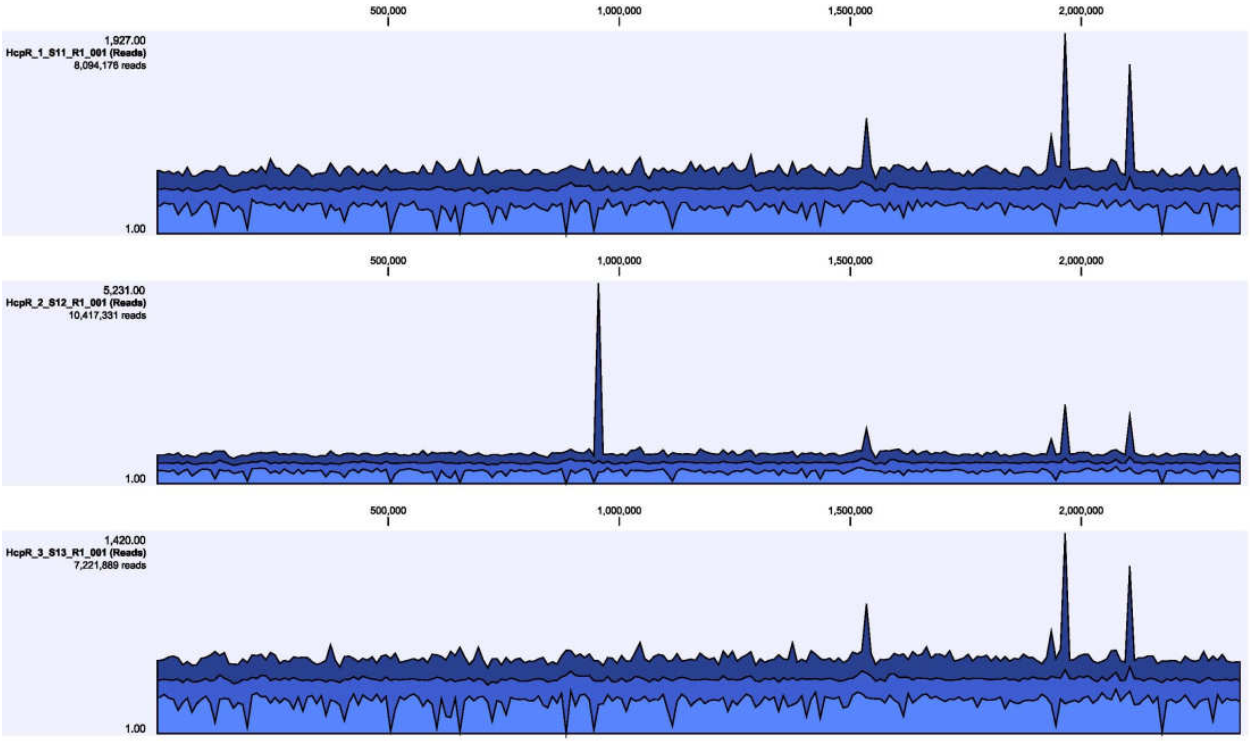

Figure 28 – Genomic Library Reads for *P. gingivalis* HcpR

Sequencing data reads from libraries generated from *P. gingivalis* HcpR was aligned with the whole genome of *P. gingivalis*. The experimental reads are shown in dark blue for each figure. The peak sizes indicate the approximate number of reads for individual genes.

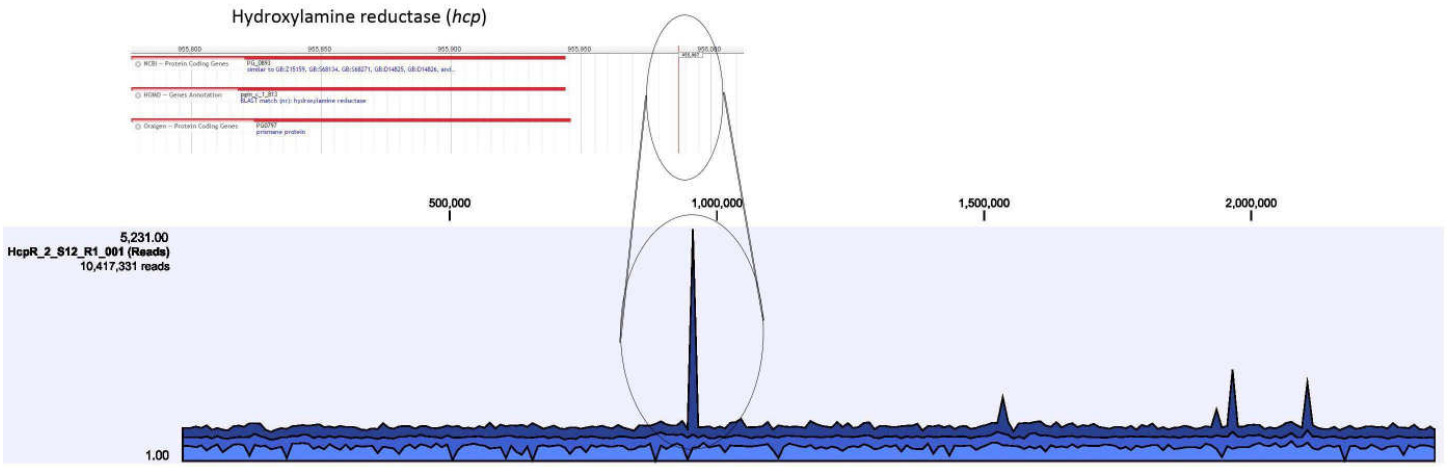

Figure 29 – Peak Analysis of HcpR 2Genomic Library

Sequencing data for the “HcpR 2” genomic library lined up with the genome of *P. gingivalis*. The location of HcpR-DNA interactions was examined to determine the binding targets of HcpR. (See supplemental figures for analysis of the other peaks)

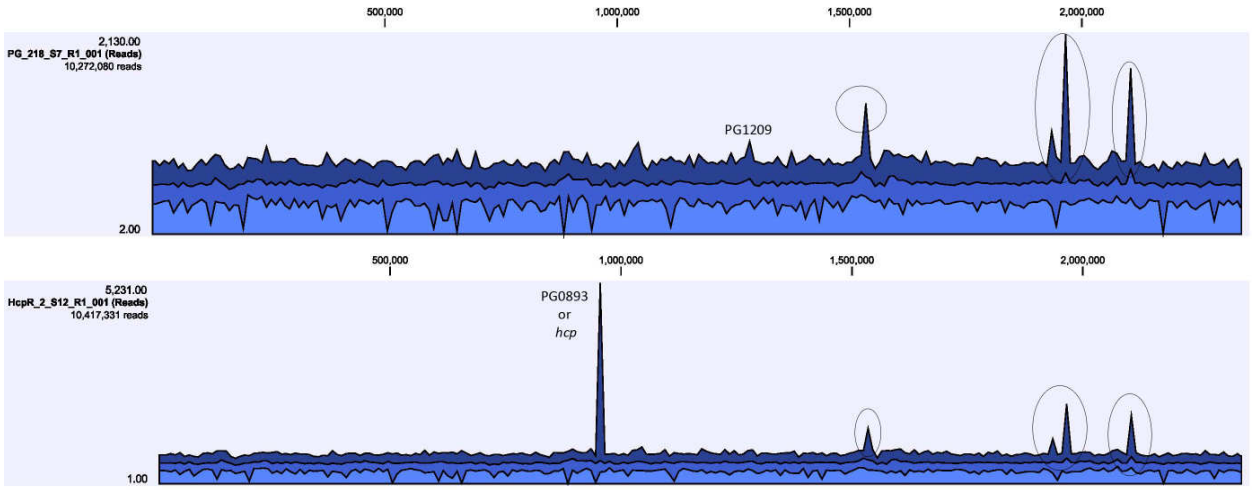

Figure 30 – Comparison of PG 218 and HcpR 2 Genomic Libraries

Side-by-side comparison of the PG218 and HcpR2 Sequencing Data. Both were generated using *P. gingivalis* genomic DNA. The circled peaks are similar peaks found in both the OxyR and HcpR libraries for *P. gingivalis*. When the peaks for these peaks were examined, they contained similar coordinates on the genome.

Chapter 5 – Discussion

The majority of the studies conducted of *E.* coli OxyR focus primarily on the redox switch and the oxidative stress response regulated. The oligomeric state of *E. coli* OxyR has not been extensively studied and thus not not well-defined. Evidence exists suggesting that *E. coli* OxyR behaves as a tetramer in solution (Kullik et al., 1995). As a transcriptional regulator, OxyR binds to the promoter region upstream of the genes it regulates. OxyR appears to recognize a binding motif made of an ATAG sequence followed by CTAT thereafter and another repeat of ATAGnnnnCTAT shortly after (Toledano et al., 1994). The oxidized or active form of OxyR appears to interact with DNA at four major grooves at these ATAGnnnCTAT binding motifs (Kullik et al., 1995; Toledano et al., 1994). This evidence suggests OxyR exists as a tetramer in solution. However, the reduced or inactive form of OxyR was shown to interact with DNA at two points at these binding motifs. This evidence suggests the possibility of a dimer in the reduced form. Crystal structures of the regulatory domain (redox switch) of OxyR have shown both dimer and tetramer forms (Choi et al., 2001). In addition, cross-linking indicated that OxyR exists as a dimer in solution (L. Tartaglia et al., 1992). Because there are different reports regarding the conformational structure of OxyR, we sought to determine the oligomeric state of *E. coli* OxyR.

After successful insertion of *E. coli* m-pET21d-*oxyR* into BL21 cells, OxyR was purified using His-tag purification in large scale for extensive studies. His-tag purifications produced an over-expressed protein that we verified as *E. coli* OxyR through Mass Spectrometry. The protein runs as a monomer at approximately 34-35 kDa on a denaturing gel (Figure 4a). The attempts to cleave the 6x His-tag from the N-

terminal using TEV protease treatment failed to remove the His-tag to generate the tagless form of OxyR. While this should not be a problem, the N-terminal domain has been identified as the DNA-binding domain of OxyR (Kullik et al., 1995). The presence of the His-tag on the DNA-binding domain of the protein may interfere with DNA binding and oligomerizaiton studies. The presence of the His-tag could also cause the protein to behave or fold differently as well. As a result, an alternative purification method was used to purify OxyR.

Tagless *E. coli* OxyR was purified from pFC20k-*oxyR* using the Halo-tag purification method. Halo-tag purification produced a highly expressed and very pure sample that runs as a monomer on a denaturing gel (34-40kDa) (Figure 4b). Unfortunately, the Halo-tag purification method is a rather time-consuming method because it requires overnight TEV protease treatment. At the same time, this method does not produce large quantities of protein compared to His-tag purifications.

E. coli OxyR was also purified using Heparin Affinity Chromatogrpahy in an attempt to purify the DNA-binding form of OxyR for our studies. Because Heparin can mimic the negatively-charged phosphate backbone of DNA, heparin affinity chromatography can be used to purify the DNA-binding form of proteins (Fenner, Oppegard, Hiasa, & Kerns, 2013; Ishii, Futaki, Uchiyama, Nagasawa, & Andoh, 1987). The resulting purification produced number of species when run on a denaturing gel due to the nature of the purification. This purification method was not as selective compared to the His-tag and Halo-tag purification methods in purifying the protein of interest. Two major species appeared more concentrated, indicating an over-expressed protein

(Figure 4c). His-tag stain confirmed that these bands contained the His-tagged protein (Figure 4d).

The gel filtration studies show that *E. coli* OxyR exists as a tetramer in solution. OxyR from all three purification methods all eluted at similar volumes (12.7mL – 13.5mL) from the S200 column (Table 4). All three purifications produced proteins that gave similar elution profiles despite different purification methods (Figure 8). Molecular weight markers were run on the S200 column to determine the approximate molecular weight of the eluted proteins. When comparing the OxyR elution profiles to the profile of the molecular weight standards, the data indicates OxyR exists as a tetramer in solution. Likewise, molecular weight calculations using the equation generated from the standards calibration curve support these results. The tagless OxyR has a moleccular weight of approximately 140 kDa, which is what the expected tetramer is calculated to be.

Despite similar elution profiles, interesting variations arise when the eluted proteins are electrophoresed on a denaturing gel (Figures 9a-d). When tagless OxyR was run on the Superdex 200, the absorbance peak produced was very small (>5mAU) compared to the absorbance profiles of the His-tagged OxyR. However, the peak was very sharp and defined which indicates that it is very likely our protein of interest. A low absorbance indicates the sample coming off the column is very dilute which was evident by an empty gel (data not shown). Perhaps a more concentrated sample of tagless OxyR is needed to run on gel filtration using the S200 column in order to detect the results on a denaturing gel.

The eluted His-tag purified OxyR appears to run as both at both 34-40 kDa and 100 kDa on a denaturing gel which indicates it runs as a monomer and a dimer (Figure 9a). The Heparin purified OxyR runs at primarily at 100 kDa. However, boiling the protein sample and the addition of reducing agents produced a band running at 35-40 kDa (Figure 9b). It is interesting to note that despite boiling the sample and adding reducing agents, Heparin-purified OxyR run on an S200 column still runs primarily at 100kDa. His-tag staining confirms that the band appearing at 100 kDa contains the His-tagged protein (Figure 9d). A faint band can be seen for the band running between 30-50 kDa which indicates this second band also contains the His-tagged protein. However, the majority of the protein runs at approximately 100 kDa.

Sedimentation velocity experiments of the tagless form of *E. coli* OxyR show that it exists as both a tetramer at approximately 140-145 kDa and a monomer at approximately 45 kDa in solution (Figure 13). The top (colored) graph depicts the absorbance values, which are nice and clean. The middle graph depicts the interference data. The grey color indicates standard error, in which there is little to no error. The bottom graph depicts the S-values for our protein. The expected value of a tetramer is approximately 137.6 kDa. The expected value of the monomer is approximately 34 kDa. The molecular weights are right around the expected weights with room for error. The peaks of the tetramer and monomer species are spread apart from one another, which indicates the protein is very stable at these configurations. If there were any transitions between the two forms, it would occur very slowly. This result is both very interesting and very unusual. It is rare in nature for a protein to transition from a monomer to tetramer or vice versa with no intermediates in between. Perhaps the dimer form does

exist, but too brief to be detected during centrifugation. Based on peak size, it appears that the tetramer form of *E. coli* OxyR is the more favored form of the two.

When comparing the amino acid sequences between *E. coli* OxyR and *P. gingivalis* OxyR, there is only a 34% sequence similarity (Supplemental S1). However, the regulatory domain of *P. gingivalis* OxyR has been studied and a truncated form has been crystallized (Svintradze et al., 2013). The structure of the regulatory domain of *P. gingivalis* OxyR has been shown to be very similar to the regulatory domain of *E. coli* OxyR. Beyond the crystallization these studies of the truncuated form, the oligomeric state of the full-length *P. gingivalis* OxyR has not been determined. Because we showed that the oligomeric state of *E. coli* OxyR is a tetramer in form, we have increased reasons to believe *P. gingivalis* OxyR also exists as a tetramer in solution. In our study, we sought to characterize the oligomeric state of *P. gingivalis* OxyR to better understand the protein.

P. gingivalis OxyR was purified from m-pET21d-*oxyR* using His-tag purification. This method produced a highly concentrated and pure protein that runs as a monomer (35kDa) on a denaturing gel (Figure 5a). Like *E. coli* OxyR from m-pET21d-*oxyR*, TEV cleavage to remove the His-tag was not successful. Once again, we turned to using Halo-tag purification to purify *P. gingivalis* OxyR from pFC20k-*oxyR*. Halo-tag purification produced a very pure and concentrated sample of OxyR (Figure 5b).

P. gingivalis OxyR was also purified from m-pET21d-*oxyR* using Heparin Affinity chromoatogrpahy in hopes of obtaining the DNA-binding form. Like the Heparin purification with *E. coli* OxyR, many species appeared when the elutions were run on a denaturing gel (Figure 5c). However, one of the bands on the gel appeared to be more

concentrated indicating the possibility of an over-expressed protein. His-tag staining confirmed that these bands contained the His-tagged protein (Figure 5d).

Gel Filtration Chromatography shows that *P. gingivalis* OxyR exists as a tetramer in solution. The results from all three purifications (His-tag, Halo-tag, and Heparin affinity) generated similar elution profiles (Figure 11a). Purified protein from all three purification systems elutes off the column at approximately 12.8mL. When comparing the elution profiles to the elution profiles of molecular weight markers, the data indicates OxyR exists as a tetramer in solution. Molecular weight calculations using the standard calibration curve also shows that OxyR exists as a tetramer in solution (Table 5).

When the S200 elutions of *P. gingivalis* OxyR were run on a denaturing gel, there was a small difference with OxyR purified from Heparin compared to the tagless and His-tag purified OxyR. The His-tagged OxyR runs as a monomer on a denaturing gel at approximately 35 kDa (Figure 12). Tagless OxyR also runs as a monomer on a denaturing gel at approximately 35 kDa (Figure 12b). The S200 elutions of Heparin purified OxyR were run on a denaturing gel, runs at approximately 100 kDa on the denaturing gel. Boiling the sample and addding reducing agents had no effect on the protein (Figure 12c**)**. This result is different from the Heparin-purified *E. coli* OxyR run on the S200 column. Boiling and the addition of reducing agents to the *E. coli* OxyR sample resulted in a second band appearing at approximately 35 kDa.

Sedimentation velocity experiments also show that *P. gingivalis* OxyR exists as a tetramer in solution. Tagless OxyR was purified both aerobically and anaerobically using the Halo-tag purification system and run on an analytical ultracentrifugation. The protein was purified anaerobically in order to obtain a more biologically relevant form of

OxyR because *P. gingivalis* is an anaerobic bacterium. Only one major peak appears on the absorbance profile for both aerobic and anaerobic purified OxyR (Figure 14**).** The results indicate that this protein has a molecular weight of approximately 140 kDa, indicating that *P. gingivalis* OxyR exists as a tetramer in solution.

Sedimentation velocity experiments show that the His-tagged *P. gingivalis* OxyR appears to exists in three oligomeric states: tetramer (140 kDa), dimer (90 kDa), and monomer (40kDa) (Figure 15). The peaks of the His-tagged OxyR are not as sharp compared to the tagless OxyR results. Rather, these peaks are connected to one another indicating a dynamic equilibrium between the three conformational states. Of the three states, the tetramer form has the largest peak, indicating it is the most favored or abundant form. The monomer peak is the next largest peak with the dimer running as the smallest peak. We believe the dynamic equilibrium favors the monomer form over the dimer form due to the size and strength of the peaks. Two conclusions can be drawn from this result. Either the equilibrium favors more rapid change from dimer to monomer or there is a slower change from monomer to a dimer. However, it is interesting to note that this is only seen when the His-tagged OxyR is run at a much lower concentration compared to the tagless OxyR. Further studies at various concentrations can help clarify and better define the oligomeric state of His-tagged OxyR. Nevertheless, the results from both analytical ultracentrifugation and gel filtration indicate that *P. gingivalis* exists primarily as a tetramer in solution.

E. coli OxyR is a transcriptional regulator that is oxidized in the presence of hydrogen peroxide. The oxidized form of OxyR is the active form in which it begins turns on transcription of the genes it regulates. OxyR has been shown to bind upstream at the

promoter regions of the genes it regulates to initiate transcription (Zheng et al., 2001). Most of the known OxyR binding targets are the oxidative stress response (Storz, Tartaglia et al., 1990b; Tao et al., 1991). We wanted to confirm that we purified fully functional OxyR by showing DNA-binding through gel shift assays. At the same time, we wanted to compare the protein purification methods to determine which method to use for regulon studies. We chose and designed primers for the gene promoters of *ahpCF, hcp,* and *katG* because they have been shown to be under OxyR regulation as part of the oxidative stress response (Almeida, Romão, Lindley, Teixeira, & Saraiva, 2006; Seth et al., 2012; L. A. Tartaglia et al., 1989). By showing binding, we hoped to determine and optimize the binding conditions for OxyR for regulon studies. We also designed a gene promoter for the *hemH* gene, which was recently found to be induced by *E. coli* OxyR (Mancini & Imlay, 2015). This gene codes for ferrochetalase, which plays a role in heme synthesis. This ferrochetalase is responsible for the final step in heme synthesis by inserting iron into the protoporphyrin ring to generate heme B. We wanted to demonstrate binding with this gene, which has not been shown previously.

Gel shift assays were performed with both the His-tagged and tagless forms of *E. coli* OxyR. The shifts with the tagless form of OxyR are more physiologically relevant the His-tagged forms which retain the His-tag on the DNA-binding domain of OxyR (the N-terminal). The presence of the tag on the DNA binding may or may not affect the binding activities of OxyR.

Reproducible shifts were shown between tagless OxyR and gene promoters we designed: *ahpCF, hcp,* and *katG* (Figure 16a-g). These results indicate the tagless OxyR from Halotag purification yields a functional protein that is capable of binding

DNA. The addition of nonfluorescent or cold DNA of same gene promoter served as competitive inhibitors. The competitive inhibitors competed with binding of the fluorescent-tagged DNA as indicated by the increased fluorescence intensity in the free DNA bands as the concentration of cold DNA increased. The competitor studies also demonstrate that tagless *E. coli* OxyR is specifically binding to the promoters rather than nonspecific binding.

After showing binding with the known binding targets of OxyR, we tested for binding between OxyR and the gene promoter for *hemH* in order to confirm OxyR regulation. A reproducible shift was produced with tagless OxyR and *hemH* (Figure 16f). This was an interesting result because it shows the iron pathology side of the oxidative stress response. *hemH* is plays a role in heme synthesis by inserting free ferrous (Fe^{2+}) iron into the protoporphyrin IX (PPIX) ring to generate heme. This is beneficial because it limits the availability of free iron to react with hydrogen peroxide. At the same time, heme is required by KatG, which is the main catalase to drive down hydrogen peroxide when it reaches higher levels. By directly regulating *hemH*, OxyR is regulating another method to drive down levels of iron to prevent Fenton chemistry. This also helps promote KatG (catalase) activity to help detoxify the hydrogen peroxide.

Possible shifts are seen between His-tagged OxyR with *ahpCF, hcp,* and *hemH* gene promoters (Figure 17a-e). However, these shifts are not as well-defined as the shifts seen with the tagless form of OxyR and are thus inconclusive. The His-tag purifications do not yield as pure of a sample as the Halo-tag purifications. Any residual contaminant may cause a shift. At the same time, the His-tag may also affect the behavior of the protein, especially since the tag exists on the DNA-binding domain.

Even when the concentration of His-tagged OxyR is greatly increased, the purported shifts are still not well-defined and seems to be abolished (Figure17d and e). The addition of Poly Poly (dI•dC) did not seem to affect the shifts. Nevertheless, the shifts seen with the tagless form of OxyR are more physiologically relevant. We determined that Halotag purification method is the better method to purify OxyR because DNA-binding was shown. We also determined the best binding conditions for regulon studies.

The regulatory domain of *P. gingivalis* OxyR has been shown to very similar in structure to the regulatory domain of *E. coli* OxyR (Svintradze et al., 2013). We were curious if *P. gingivalis* OxyR would bind to the same promoters we used in the *E. coli* OxyR shift assays due to similarities between the structures. Shift assays were performed using both tagless and His-tagged *P. gingivalis* OxyR. No visible shifts were produced between tagless *P. gingivalis* OxyR with the *E. coli* gene promoters (Figure 18a-d). This result was expected because these genes are designed from *E. coli* DNA and not *P. gingivalis* DNA.

However, of these shifts performed, we were most interested the results of shifts performed with *ahpCF* and *hemH*. *P. gingivalis* relies on alkyl hydroperoxidase (from *ahpCF*) to combat hydrogen peroxide stress (Henry et al., 2012). It was shown that OxyR in *P. gingivalis* is required for the expression of *ahpCF* (Diaz et al., 2006). Because *hemH* plays a role in heme synthesis, we were curious to see if *P. gingivalis* OxyR regulates *hemH* because *P. gingivalis* is not capable of synthesizing heme. Unfortunately, no visible shifts were seen between *P. gingivalis* OxyR and the *E. coli* gene promoters. This was expected due to the shifting targets coming from different host organisms.

A possible shift was shown between His-tagged *P. gingivalis* OxyR with *ahpCF*, *katG,* and the *hemH* gene promoter (Figure 19a-d). However, these shifts are rather weak and poorly defined and thus are not conclusive. Doubling the concentration of His-tagged OxyR did not resolve the shifts any better. No shift was seen with the *hcp* gene promoter. The shifs seen with His-tagged *P. gingivalis* OxyR is most likely due to nonspecific binding because *P. gingivialis* does not have a *katG* homolog (Henry et al., 2012). Nonspecific binding is likely because tagless *P. gingivalis* OxyR did not produce shifts with any of these promoters. At the same time, the His-tagged *P. gingivalis* samples were not as pure as the tagless form. Any contaminants present may bind nonspecifically with the gene promoters. Nevertheless, the lack of shifts seen with the tagless *P. gingivalis* OxyR is more physiologically relevant.

The same shift assays were performed with *P. gingivalis* HcpR as a negative control. We wanted to make sure these probes we designed were not shifting with any protein we add. HcpR should not shift with any of these probes because of different regulons. As expected, no visible shifts were seen between HcpR and any of the gene promoters (Figure 20a-d), indicating these promoters are not binding to everything.

The pulldown assays were performed using the tagless *E. coli* and *P. gingivalis* OxyR because we were able to show binding with the tagless *E.coli* OxyR. The pulldown was also performed using His-tagged *P. gingivalis* HcpR as a negative control for the *P. gingivalis* libraries. The pulldown assays were performed using the same binding conditions used in the gel shift studies. Attempts to generate a library using *P. gingivalis* OxyR and *E. coli* genomic DNA as a negative control failed.

The sequencing data from the libraries generated from *E. coli* OxyR were reproducible. Each of the libraries generated similar peaks with similar coordinates. When these peaks were analyzed, one peak pertained to the promoter region of *mobB*. The gene product has a role in GTP-binding and GTPase activity. How and why OxyR may regulate this gene is unknown and will require further experimentation. The binding can be verified through gel shift assays. The oxidative stress response through OxyR may induce some unforeseen metabolic pathways. The rest of the peaks analyzed in from these libraries pertain to intergenic regions within various genes. Some of these genes include *oxyR* and *aceK.* The latter was recognized as a potential binding target through microarray data from previous members of the Lewis lab. The gene codes for an isocitrate dehydrogenase, which plays a role in the Krebs cycle. The Krebs cycle generates GTP as an energy source. These findings combined with the *mobB* findings (GTP-binding) may implicate OxyR having a role in cellular metabolism, possibly to regulate it to prevent further generation of reactive oxygen species. This is an interesting target and needs to be studied further. We believe these binding targets of *E. coli* OxyR may correspond to small RNAs or small proteins that are currently unknown. The databases for these targets is not complete and will require further investigation.

The sequencing data from the libraries generated from *P. gingivalis* OxyR appear to be reproducible. All four of the libraries generated contained similar peaks. When analyzing these peaks, only one peak stood out. This peak occurs at the 1,287,432 base pair on the genome and appears to pertain to the promoter region of the PG1209 (NCBI) gene (Figure 26). The exact function of this gene is unknown, but it is believed to involve NAD metabolism and is an ATPase/kinase (Nelson et al., 2003). If these

indings hold true, this may indicate that *P. gingivalis* OxyR may have role in regulating cellular metabolism. Further investigation of this binding target as well as its gene product needs to be conducted. The rest of the peaks appear to be nonspecific binding when compared to the results of libraries generated from *P.gingivalis* HcpR (Figure 30).

Sequencing data from all three libraries appear to be the same, with the exception of a very prominent peak seen in the HcpR 2 library. Analysis of this peak shows that it pertains to the promoter region of hydroxylamine reductase or PG0893, which encodes for Hcp, a hybrid cluster protein (Figure 27). HcpR has been shown to upregulate PG0893 (Lewis, Yanamandra, & Anaya-Bergman, 2012). It is interesting to see that this peak only appears in one out of the three libraries generated from HcpR. The purpose of generating libraries with HcpR was to serve as a negative control to determine nonspecific binding when comparing to the libraries generated from *P. gingivalis* OxyR. We found peaks present in libraries generated from both proteins, indicating these peaks are the result of nonspecific binding.

Chapter 6 – Conclusion

We were able to determine the oligomeric states for both *E. coli* and *P. gingivalis* OxyR. Our studies show that *E. coli* OxyR exist primarily as a tetramer in solution, but can also exist as a monomer in solution. We showed that *P. gingivalis* OxyR exists primarily as a tetramer in solution, which has not been shown before. We were able to show binding with the tagless *E. coli* OxyR. We discovered a potential binding target, PG1209 for *P. gingivalis* OxyR. We confirmed that HcpR regulates PG0893 or *hcp* as a byproduct of our studies. We discovered a potential binding target, *mobB* for *E. coli* OxyR. Many other targets were discovered for *E. coli* OxyR, all pertaining to the intergenic regions within various genes. Our findings indidcate that there are still unknown binding targets for OxyR. We sought to study OxyR to help us better understand the physiological characteristics of these bacteria. Before *P. gingivalis* can carry out its pathogenic functions, it must first survive in the ever-changing environment of the oral cavity during which it can be exposed to various reactive oxygen species. By understanding how it reacts to and survives with stressors such as oxidative stress can can help us better understand its pathogenicity in periodontal disease.

Bibliography

Aas, J. A., Paster, B. J., Stokes, L. N., Olsen, I., & Dewhirst, F. E. (2005). Defining the normal bacterial flora of the oral cavity. *Journal of Clinical Microbiology, 43*(11), 5721.

Almeida, C. C., Romão, C.,V., Lindley, P. F., Teixeira, M., & Saraiva, L. (2006). *The role of the hybrid cluster protein in oxidative stress defense*. Bethesda, Md. : doi:10.1074/jbc.M605888200

Amano, A., Nakagawa, I., Okahashi, N., & Hamada, N. (2004). *Variations of porphyromonas gingivalis fimbriae in relation to microbial pathogenesis*. Copenhagen,:

Anjem, A., Varghese, S., & Imlay, J. A. (2009). *Manganese import is a key element of the OxyR response to hydrogen peroxide in escherichia coli*. Oxford] : doi:10.1111/j.1365-2958.2009.06699.x

Bresgen, N., Jaksch, H., Lacher, H., Ohlenschläger, I., Uchida, K., & Eckl, P. M. (2010). *Iron-mediated oxidative stress plays an essential role in ferritin-induced cell death*. New York, NY] : doi:10.1016/j.freeradbiomed.2010.02.019

Choi, H., Kim, S., Mukhopadhyay, P., Cho, S., Woo, J., Storz, G., et al. (2001). Structural basis of the redox switch in the OxyR transcription factor. *Cell, 105*(1), 103-113. doi:http://dx.doi.org/10.1016/S0092-8674(01)00300-2

Christman, M. F., Morgan, R. W., Jacobson, F. S., & Ames, B. N. (1985). Positive control of a regulon for defenses against oxidative stress and some heat-shock proteins in salmonella typhimurium. *Cell, 41*(3), 753-762. doi:10.1016/S0092-8674(85)80056-8

Cummings, J. H., & Macfarlane, G. T. (1997). Role of intestinal bacteria in nutrient metabolism. *Clinical Nutrition, 16*(1), 3-11. doi:http://dx.doi.org/10.1016/S0261-5614(97)80252-X

Desvarieux, M., Demmer, R. T., Rundek, T., Boden-Albala, B., Jacobs, D. R., Sacco, R. L., et al. (2005). Periodontal microbiota and carotid intima-media thickness: The oral infections and vascular disease epidemiology study (INVEST). *Circulation, 111*(5), 576.

Diaz, P. I., Slakeski, N., Reynolds, E. C., Morona, R., Rogers, A. H., & Kolenbrander, P. E. (2006). Role of oxyR in the oral anaerobe porphyromonas gingivalis. *The Journal of Bacteriology, 188*(7), 2454.

Edlund, C., & Nord, C. E. (2000). *Effect on the human normal microflora of oral antibiotics for treatment of urinary tract infections*. Oxford, U.K. :

Escobar-Páramo, P., Clermont, O., Blanc-Potard, A., Bui, H., Le Bouguénec, C., & Denamur, E. (2004). *A specific genetic background is required for acquisition and expression of virulence factors in escherichia coli*. Chicago, Ill. : doi:10.1093/molbev/msh118

Fang, F. C. (2004). Antimicrobial reactive oxygen and nitrogen species: Concepts and controversies. *Nature Reviews Microbiology, 2*(10), 820-832. doi:10.1038/nrmicro1004

Fenner, A. M., Oppegard, L. M., Hiasa, H., & Kerns, R. J. (2013). *Selective inhibition of bacterial and human topoisomerases by N-arylacyl O-sulfonated aminoglycoside derivatives*. Washington, D.C. : doi:10.1021/ml3004507

Fridovich, I. (1978). The biology of oxygen radicals. *Science, 201*(4359), 875-880.

Graves, D. T., & Cochran, D. L. (2003). The contribution of interleukin-1 and tumor necrosis factor to periodontal tissue destruction. *Journal of Periodontology, 74*(3), 391-401.

Guarner, F., & Malagelada, J. (2003). Gut flora in health and disease. *The Lancet, 361*(9356), 512-519. doi:http://dx.doi.org/10.1016/S0140-6736(03)12489-0

Hajishengallis, G., Darveau, R. P., & Curtis, M. A. (2012). The keystone-pathogen hypothesis. *Nature Reviews Microbiology, 10*(10), 717. doi:10.1038/nrmicro2873

Hasegawa, Y., Mans, J. J., Mao, S., Lopez, M. C., Baker, H. V., Handfield, M., et al. (2007). *Gingival epithelial cell transcriptional responses to commensal and opportunistic oral microbial species*. Washington, DC : doi:10.1128/IAI.01957-06

Henry, L. G., McKenzie, R. M. E., Robles, A., & Fletcher, H. M. (2012). *Oxidative stress resistance in porphyromonas gingivalis*. London : doi:10.2217/fmb.12.17

Imlay, J. A., Chin, S. M., & Linn, S. (1988). Toxic DNA damage by hydrogen peroxide through the fenton reaction in vivo and in vitro. *Science, 240*(4852), 640-642.

Ishii, K., Futaki, S., Uchiyama, H., Nagasawa, K., & Andoh, T. (1987). *Mechanism of inhibition of mammalian DNA topoisomerase I by heparin*. London :

Katouli, M. (2010). Population structure of gut escherichia coli and its role in development of extra-intestinal infections. *Iranian Journal of Microbiology, 2*(2), 59-72.

Kim, S. O., Merchant, K., Nudelman, R., Beyer, W. F., Keng, T., DeAngelo, J., et al. (2002). OxyR: A molecular code for redox-related signaling. *Cell, 109*(3), 383-396. doi:10.1016/S0092-8674(02)00723-7

Kullik, I., Stevens, J., Toledano, M. B., & Storz, G. (1995). *Mutational analysis of the redox-sensitive transcriptional regulator OxyR: Regions important for DNA binding and multimerization*. Washington, D.C., etc.]:

Kullik, I., Toledano, M. B., Tartaglia, L. A., & Storz, G. (1995). Mutational analysis of the redox-sensitive transcriptional regulator OxyR: Regions important for oxidation and transcriptional activation. *The Journal of Bacteriology, 177*(5), 1275.

Lamont, R. J., & Yilmaz, O. (2002). *In or out: The invasiveness of oral bacteria*. Copenhagen, DK] :

Latchman, D. S. (1997). Transcription factors: An overview. *The International Journal of Biochemistry & Cell Biology, 29*(12), 1305-1312. doi:http://dx.doi.org/10.1016/S1357-2725(97)00085-X

Lee, C., Lee, S. M., Mukhopadhyay, P., Seung, J. K., Sang, C. L., Woo-Sung Ahn, et al. (2004). Redox regulation of OxyR requires specific disulfide bond formation involving a rapid kinetic reaction path. *Nature Structural & Molecular Biology, 11*(12), 1179. doi:10.1038/nsmb856

Lewis, J. P., Yanamandra, S. S., & Anaya-Bergman, C. (2012). *HcpR of porphyromonas gingivalis is required for growth under nitrosative stress and survival within host cells*. Washington, DC : doi:10.1128/IAI.00561-12

Loesche, W. J., Syed, S. A., Schmidt, E., & Morrison, E. C. (1985). Bacterial profiles of subgingival plaques in periodontitis. *Journal of Periodontology, 56*(8), 447.

Mancini, S., & Imlay, J. A. (2015). *The induction of two biosynthetic enzymes helps escherichia coli sustain heme synthesis and activate catalase during hydrogen peroxide stress*. Oxford] : doi:10.1111/mmi.12967

Martin, J. E., Waters, L. S., Storz, G., & Imlay, J. A. (2015). The escherichia coli small protein MntS and exporter MntP optimize the intracellular concentration of manganese. *PLoS Genetics, 11*(3) doi:10.1371/journal.pgen.1004977

McMahon, M. A., Xu, J., Moore, J. E., Blair, I. S., & McDowell, D. A. (2007). Environmental stress and antibiotic resistance in food-related pathogens. *Applied and Environmental Microbiology, 73*(1), 211.

Nelson, K. E., Fleischmann, R. D., DeBoy, R. T., Paulsen, I. T., Fouts, D. E., Eisen, J. A., et al. (2003). *Complete genome sequence of the oral pathogenic bacterium porphyromonas gingivalis strain W83*. Washington, D.C., etc.]:

Newman, M., Takei, H., Klokkevold, P., & Carranza, F. (2002). *Carranza's clinical periodontology* (9th ed.. ed.). Philadelphia: Philadelphia : W.B. Saunders Co.

Ogrendik, M., Kokino, S., Ozdemir, F., Bird, P. S., & Hamlet, S. (2005). Serum antibodies to oral anaerobic bacteria in patients with rheumatoid arthritis. *MedGenMed : Medscape General Medicine, 7*(2), 2.

Ren, B., Duan, X., & Ding, H. (2009). *Redox control of the DNA damage-inducible protein DinG helicase activity via its iron-sulfur cluster*. Bethesda, Md. : doi:10.1074/jbc.M807943200

Seaver, L. C., & Imlay, J. A. (2001). *Hydrogen peroxide fluxes and compartmentalization inside growing escherichia coli*. Washington, D.C., etc.]: doi:10.1128/JB.183.24.7182-7189.2001

Sekirov, I., Russell, S. L., Antunes, L. C., & Finlay, B. B. (2010). *Gut microbiota in health and disease*. Bethesda, MD : doi:10.1152/physrev.00045.2009

Seth, D., Hausladen, A., Wang, Y., & Stamler, J. S. (2012). *Endogenous protein S-nitrosylation in E. coli: Regulation by OxyR*. New York, N.Y. : doi:10.1126/science.1215643

Singh, A., Wyant, T., Anaya-Bergman, C., Aduse-Opoku, J., Brunner, J., Laine, M. L., et al. (2011). *The capsule of porphyromonas gingivalis leads to a reduction in the host inflammatory response, evasion of phagocytosis, and increase in virulence*. Washington, DC : doi:10.1128/IAI.05016-11

Slots, J. (1986). *Bacterial specificity in adult periodontitis. A summary of recent work*. Copenhagen,:

Storz, G., Tartaglia, L. A., & Ames, B. N. (1990a). Transcriptional regulator of oxidative stress-inducible genes: Direct activation by oxidation. *Science, 248*(4952), 189-194.

Storz, G., Tartaglia, L., & Ames, B. (1990b). The OxyR regulon. *Antonie Van Leeuwenhoek, 58*(3), 157-161. doi:10.1007/BF00548927

Svintradze, D. V., Peterson, D. L., Collazo-santiago, E. A., Lewis, J. P., & Wright, H. T. (2013). Structures of the porphyromonas gingivalis OxyR regulatory domain explain differences in expression of the OxyR regulon in escherichia coli and P. gingivalis. *Acta Crystallographica Section D, 69*(10), 2091-2103. doi:10.1107/S0907444913019471

Tao, K., Makino, K., Yonei, S., Nakata, A., & Shinagawa, H. (1991). Purification and characterization of the escherichia coli OxyR protein, the positive regulator for a hydrogen peroxide-inducible regulon. *Journal of Biochemistry, 109*(2), 262.

Tartaglia, L. A., Storz, G., Brodsky, M. H., Lai, A., & Ames, B. N. (1990). Alkyl hydroperoxide reductase from salmonella typhimurium. sequence and homology to thioredoxin reductase and other flavoprotein disulfide oxidoreductases. *The Journal of Biological Chemistry, 265*(18), 10535.

Tartaglia, L., Gimeno, C. J., Storz, G., & Ames, B. (1992). MULTIDEGENERATE DNA RECOGNITION BY THE OXYR TRANSCRIPTIONAL REGULATOR. *Journal of Biological Chemistry; J.Biol.Chem., 267*(3), 2038-2045.

Tartaglia, L. A., Storz, G., & Ames, B. N. (1989). Identification and molecular analysis of oxyR-regulated promoters important for the bacterial adaptation to oxidative stress. *Journal of Molecular Biology, 210*(4), 709-719. doi:10.1016/0022-2836(89)90104-6

Toledano, M. B., Kullik, I., Trinh, F., Baird, P. T., Schneider, T. D., & Storz, G. (1994). *Redox-dependent shift of OxyR-DNA contacts along an extended DNA-binding site: A mechanism for differential promoter selection*. Cambridge, Mass.],:

Turnbaugh, P. J., Ley, R. E., Hamady, M., Fraser, C. M., Knight, R., & Gordon, J. I. (2007). The human microbiome project. *Nature, 449*(7164), 804. doi:10.1038/nature06244

Unden, G., Becker, S., Bongaerts, J., Schirawski, J., & Six, S. (1994). Oxygen regulated gene expression in facultatively anaerobic bacteria. *Antonie Van Leeuwenhoek, 66*(1), 3-22. doi:10.1007/BF00871629

Varghese, S., Wu, A., Park, S., Imlay, K. R. C., & Imlay, J. A. (2007). *Submicromolar hydrogen peroxide disrupts the ability of fur protein to control free-iron levels in escherichia coli*. Oxford : doi:10.1111/j.1365-2958.2007.05701.x

Weiss, S. J., Young, J., LoBuglio, A. F., Slivka, A., & Nimeh, N. F. (1981). *Role of hydrogen peroxide in neutrophil-mediated destruction of cultured endothelial cells*. New York, N.Y. :

Wu, H., & Wu, E. (2012). The role of gut microbiota in immune homeostasis and autoimmunity. *Gut Microbes, 3*(1), 4. doi:10.4161/gmic.19320

Wu, J., Lin, X., & Xie, H. (2008). *OxyR is involved in coordinate regulation of expression of fimA and sod genes in porphyromonas gingivalis*. New York, NY] : doi:10.1111/j.1574-6968.2008.01116.x

Zheng, M., Åslund, F., & Storz, G. (1998). Activation of the OxyR transcription factor by reversible disulfide bond formation. *Science, 279*(5357), 1718-1721.

Zheng, M., Wang, X., Doan, B., Lewis, K. A., Schneider, T. D., & Storz, G. (2001). Computation-directed identification of OxyR DNA binding sites in escherichia coli. *The Journal of Bacteriology, 183*(15), 4571.

Vita

Christopher Khoa Pham was born on April 9, 1992, in Newport Beach, California and is an American citizen. He received his Bachelor of Arts in Neuroscience from the University of Southern California, Los Angeles, California in 2013. He completed the Pre-Medical Graduate Certificate Program at Virginia Commonwealth University in 2014. He received a Masters of Science in Biochemistry from Virginia Commonwealth University in 2016.

Supplemental Figures

```
34.2% identity in 301 residues overlap; Score: 462.0; Gap frequency: 0.3%

Ec              1 MNIRDLEYLVALAEHRHFRRAADSCHVSQPTLSGQIRKLEDELGVMLLERTSRKVLFTQA
Pg              1 MNIQQLEYIAALDKFRHFAKAADYCNVSQPTLSTMILKLEEELGAKLFDRSRQPIEPTSI
                  ***  ***  **   ***  *** * *******  * *** ***  *  *       *

Ec             61 GMLLVDQARTVLREVKVLKEMASQQGETMSGPLHIGLIPTVGPYLLPHIIPMLHQTFPKL
Pg             61 GALVVSQAKQILYDLNSITRIIEEEQQSLTGRLNIAVLPTIAPYLLPRVFPIWKKELAGL
                  * * * **   *                  * * *   **  *****   *        *

Ec            121 EMYLHEAQTHQLLAQLDSGKLDCVILALVKESEAFIEVPLFDEPMLLAIYEDHPWANREC
Pg            121 EIHVSEMQTSRCLASLLSGEIDMAIIASKAETEGLEDDLLYYEEFLGYVSRCEPLFEQDV
                  *    * **   ** * **  *  * *   * *      *  *  *       *

Ec            181 VPMADLAGEKLLMLEDGHCLRDQAMGFCFEAGADE-DTHFRATSLETLRNMVAAGSGITL
Pg            181 IRTTEVNPHRLWLLDEGHCFRDQLVRFCQMKGLHERQTAYSGGSMEAFMRLVESGQGITF
                        *  *  *** ***   **   *  *  *     * *     *  * ***

Ec            240 LPALAVPPERKRDGVVYLPCIKPEPRRTIGLVYRPGSPLRSRYEQLAEAIRARMDGHFDK
Pg            241 IPQLTVEQLSPSQKELVRPFGMPRPVREVRLAVRQDYSRRKLREQLIGLLRSAVPSDMHK
                   * * *            *   * * *   *  *     *   ***    *        *

Ec            300 V
Pg            301 L
```

Figure S1 – Sequence Similarity of *E. coli* and *P. gingivalis* OxyR

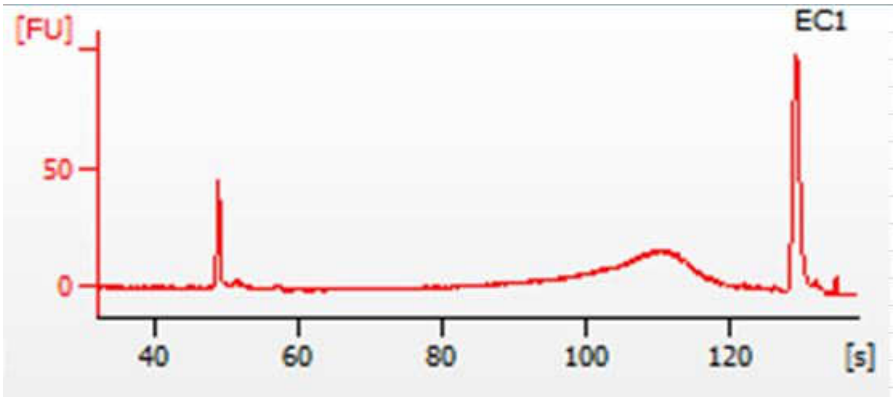

Figure S2 – Bio-analyzer result for *E. coli* OxyR Library: EC 1

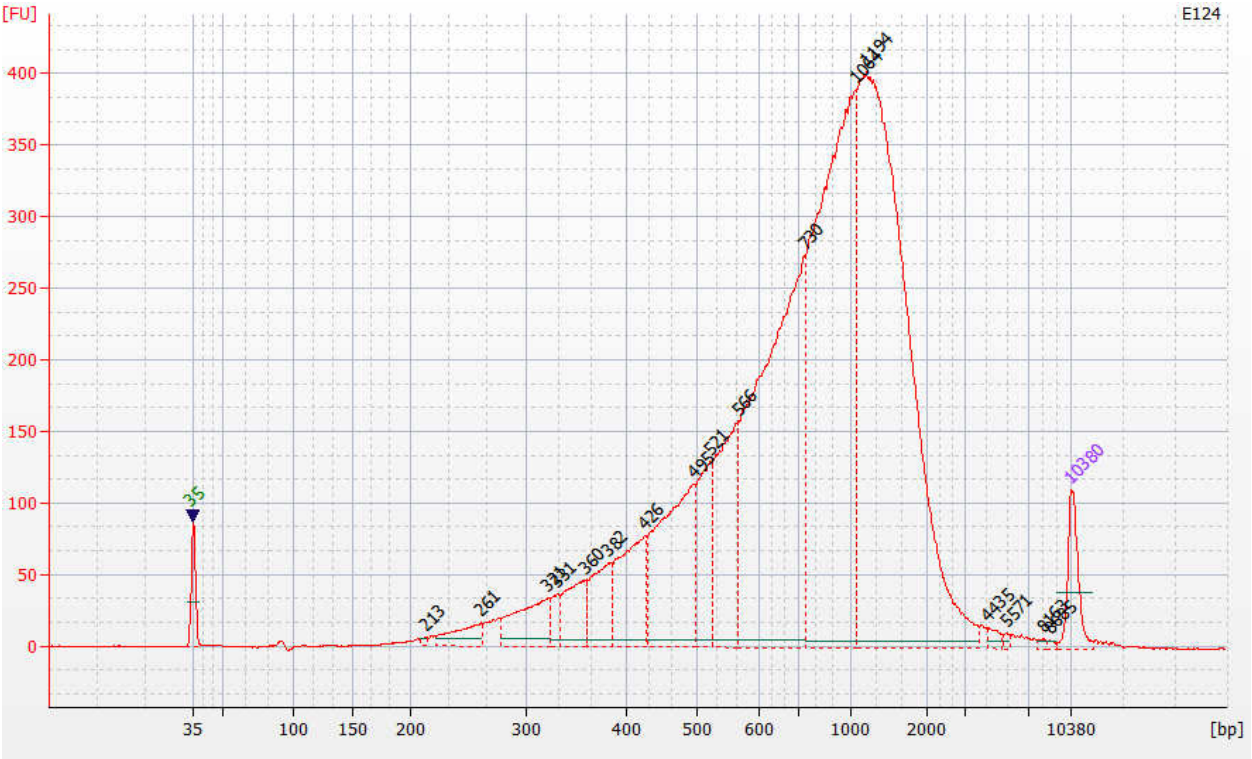

Figure S3 – Bio-analyzer Result for *E. coli* OxyR Library: EC 124

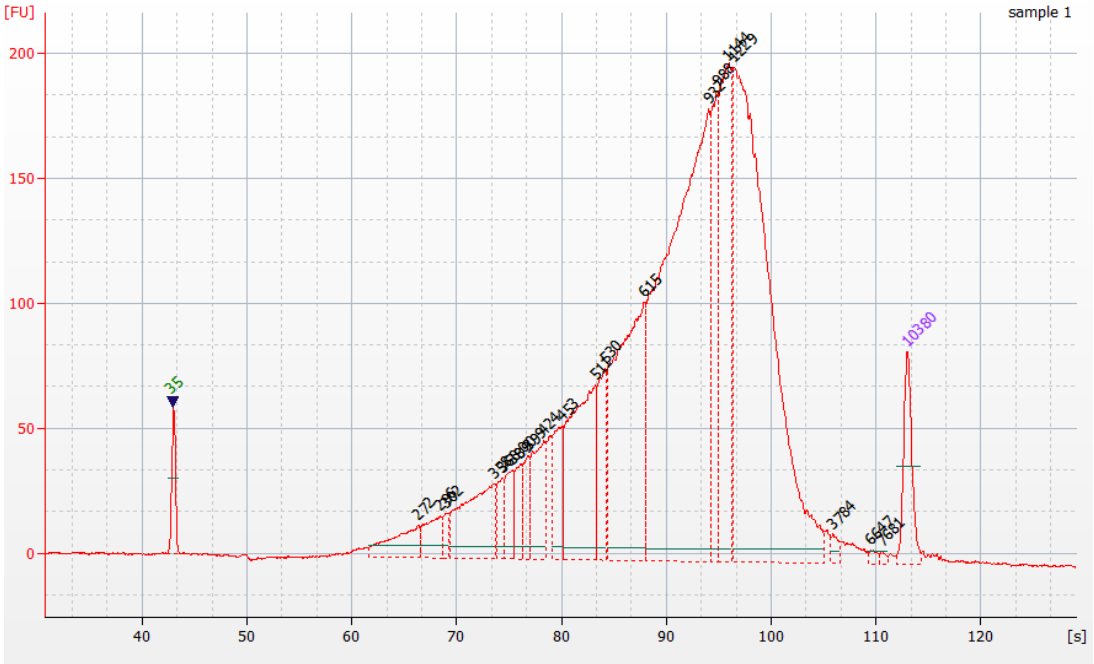

Figure S5: Bio-analyzer Result for *E. coli* OxyR Library: EC 211

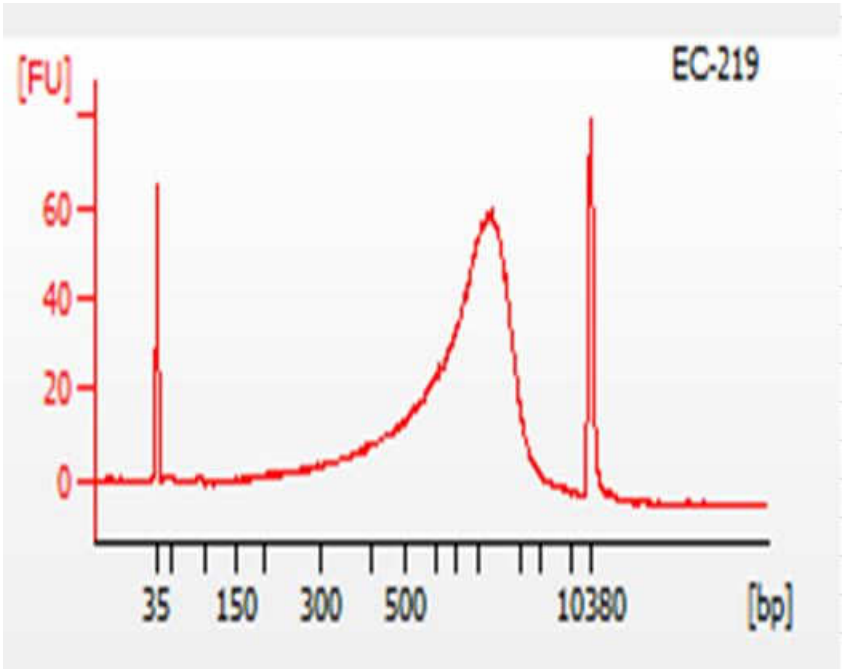

Figure S6: Bio-analyzer Result for *E. coli* OxyR Library: EC 219

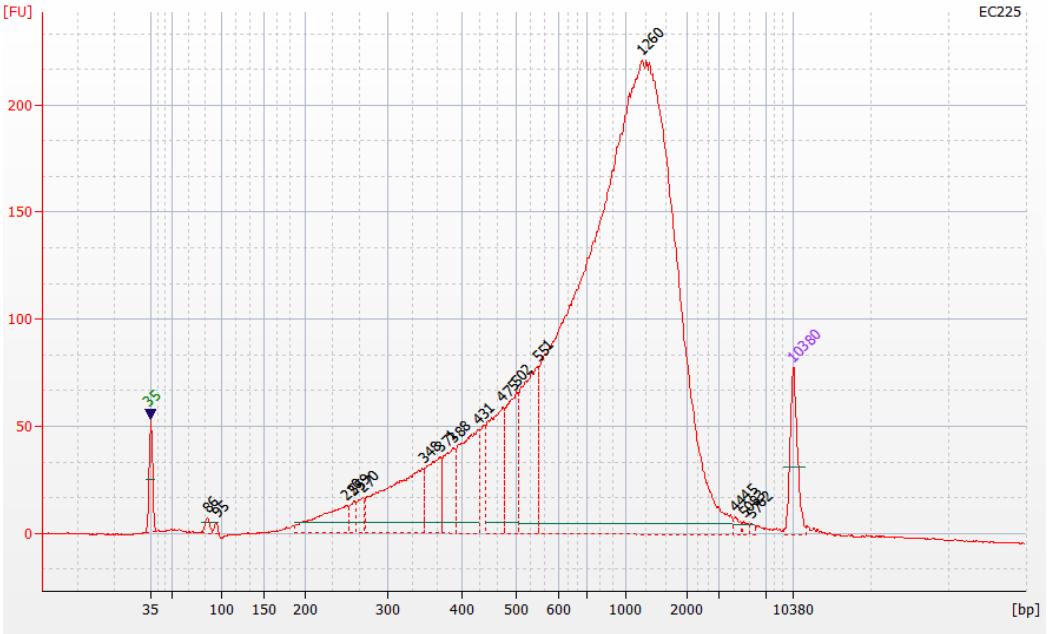

Figure S7: Bio-analyzer Result for *E. coli* OxyR Library: EC 225

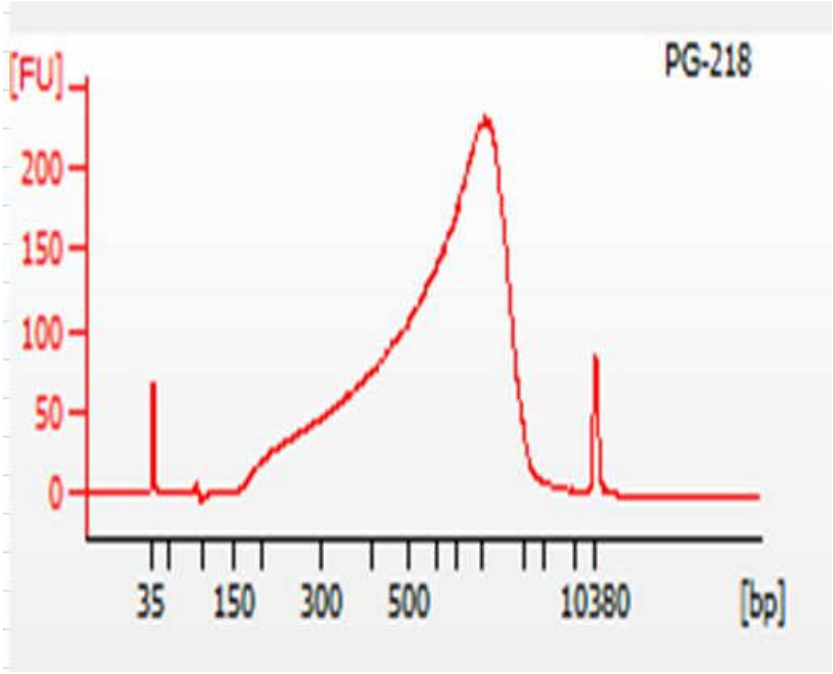

Figure S8: Bio-analyzer Result for *P. gingigvalis* OxyR Library: PG 218

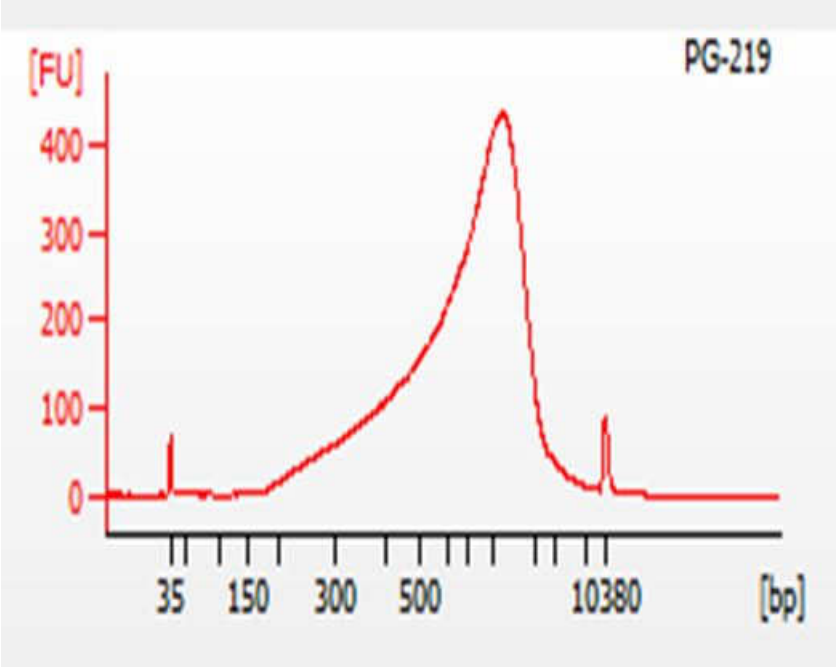

Figure S9: Bio-analyzer Result for *P. gingivalis* OxyR Library: PG 219

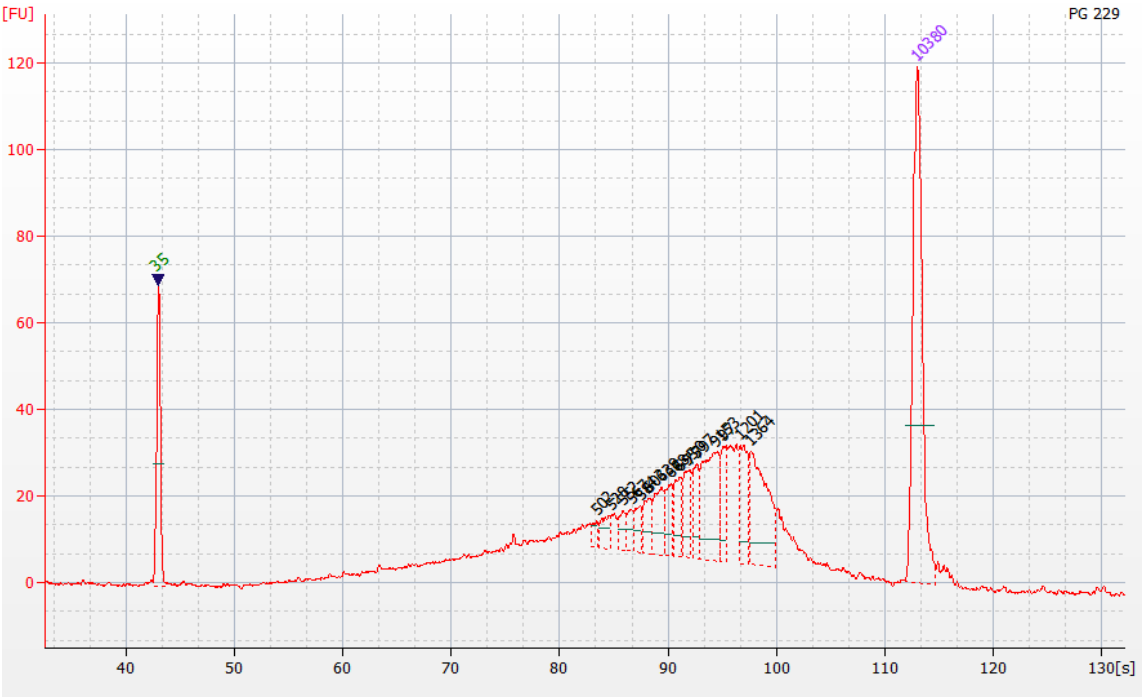

Figure S10: Bio-analyzer Result for *P. gingivalis* OxyR Library: PG 229

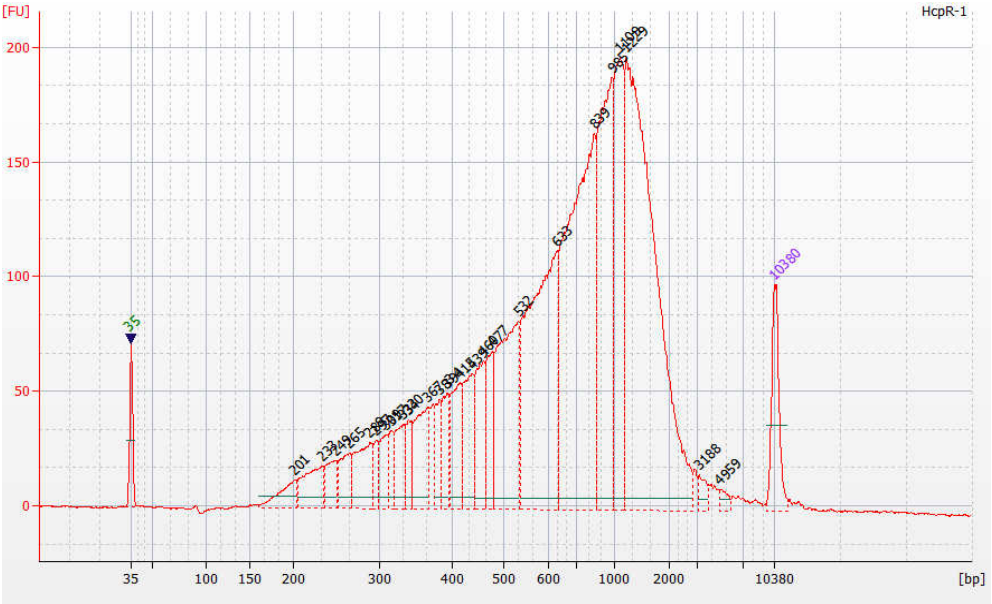

Figure S11: Bio-analyzer Result for *P. gingivalis* HcpR Library: HcpR 1

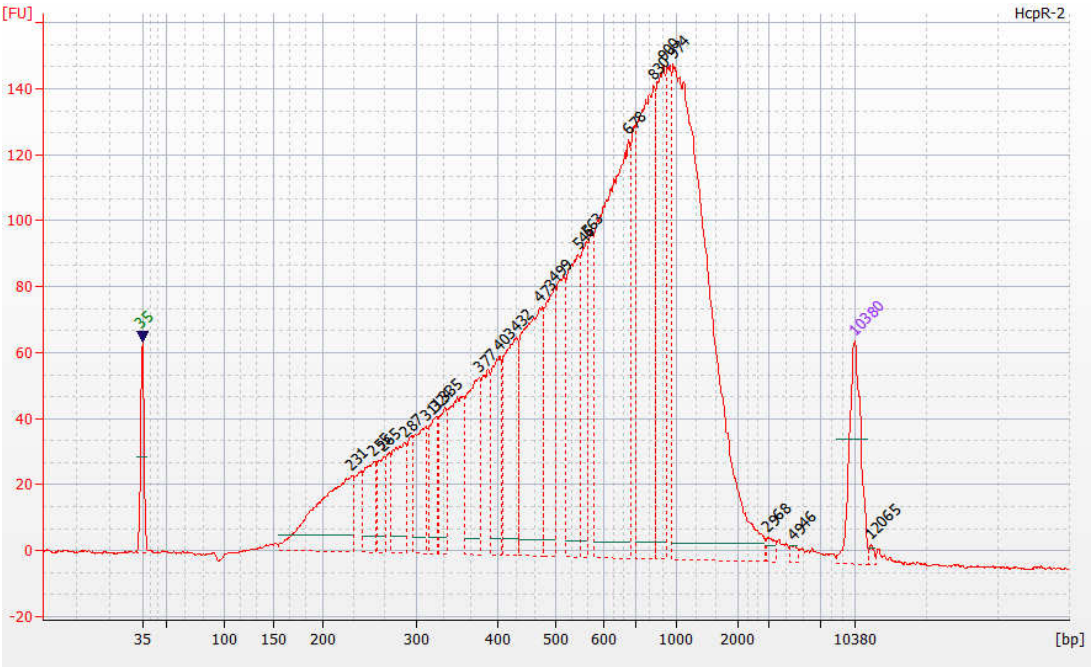

Figure S12: Bio-analyzer Result for *P. gingivalis* HcpR Library: HcpR 2

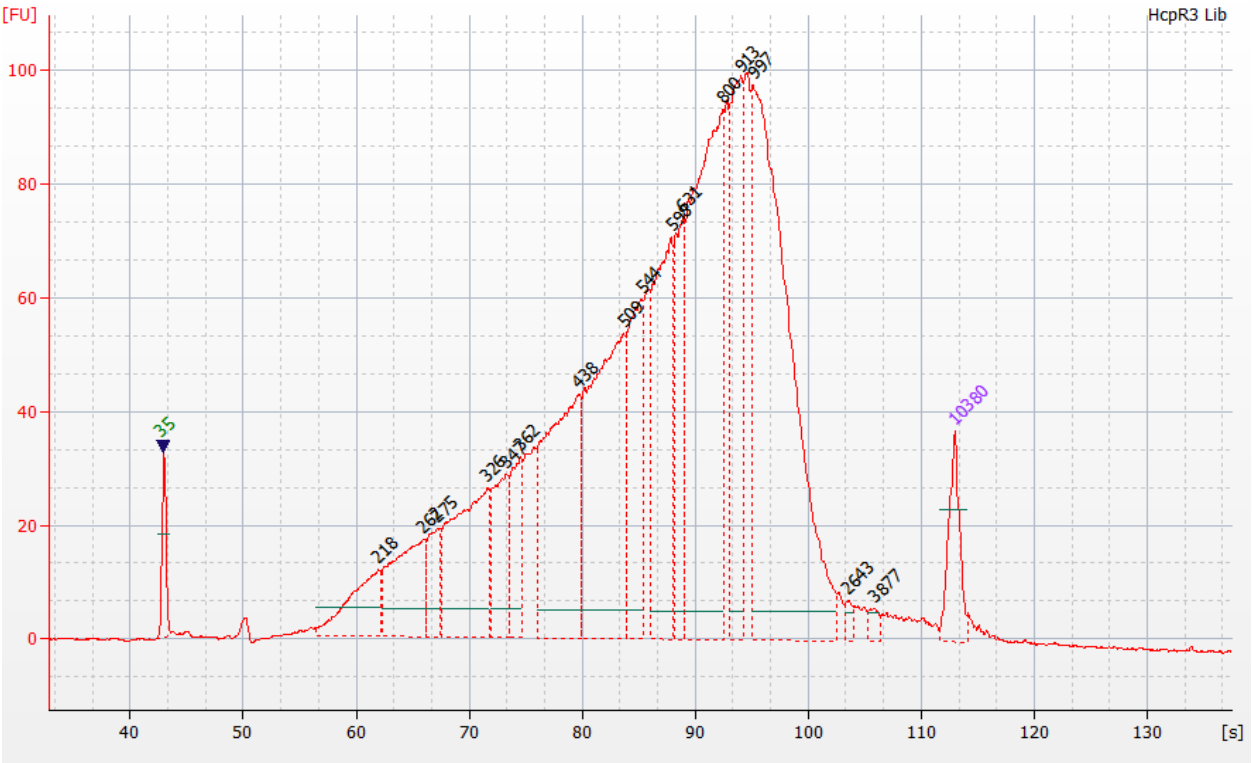

Figure S13: Bio-analyzer Result for *P. gingivalis* HcpR Library: HcpR 3

Mapping	Region	Length	FDR (%)	# Reads	# Forward reads	# Reverse reads	Normalized difference	Wilcoxon filter p-value	5' gene	5' distance	3' gene	3' distance	Overlapping annotations
lpxA	+(402..454	52	1.6E-68	2713	1430	1283	0.05418	5.3E-08	lpxA	0		0	lpxA, lpxA
ribD	+(382..422	40	4.2E-75	3529	1641	1888	0.06999	1E-05	ribD	0		0	ribD, ribD
radA	+(645..694	49	1.4E-70	5245	2545	2700	0.02955	6.3E-08	radA	0		0	radA, radA
PG0469	+(103..117	14	5.1E-34	535	220	315	0.17757	3.5E-05	PG0469	0		0	PG0469, PG0469
PG0694	+(497..551	54	2.8E-85	4553	2087	2466	0.08324	7.3E-10	PG0694	0		0	PG0694, PG0694
PG0879	+(257..293	36	6E-180	3928	1998	1930	0.01731	9.3E-05	PG0879	0		0	PG0879, PG0879
dut	+(201..228	27	2E-76	1524	746	778	0.021	6.3E-05	dut	0		0	dut, dut
PG1372	+(699..731	32	1.2E-80	5697	2775	2922	0.0258	1.7E-05	PG1372	0		0	PG1372, PG1372
mmdC	+(198..225	27	4.2E-74	1585	808	777	0.01956	3.4E-05	mmdC	0		0	mmdC, mmdC
galK	+(597..635	38	7.6E-71	4102	2041	2061	0.00488	5.6E-05	galK	0		0	galK, galK
PG1964	+(656..737	81	2E-76	5209	2640	2569	0.01363	5.6E-08	PG1965	0		0	PG1964, PG1964

Table S1 – Seq Data for PG 218 Library

Mapping	Region	Length	FDR (%)	# Reads	# Forward reads	# Reverse reads	Normalized difference	Wilcoxon filter p-value	5' gene	5' distance	3' gene	3' distance	Overlapping annotations
glyA	+(629..689	60	2.5E-88	4968	2382	2586	0.04106	2.5E-08	glyA	0		0	glyA, glyA
cdsA	+(403..456	47	4.7E-85	3196	1591	1605	0.00438	8.9E-05	cdsA	0		0	cdsA, cdsA
lpxA	+(405..456	45	1.4E-83	3006	1608	1398	0.06986	6.1E-05	lpxA	0		0	lpxA, lpxA
PG0115	+(180..211	31	3E-115	1956	1003	953	0.02556	1.7E-06	PG0116	0		0	PG0115, PG0115
PG0146	+(351..402	51	2.4E-90	2610	1308	1302	0.0023	1.4E-06	PG0145	0		0	PG0146, PG0146
radA	+(654..722	68	5.7E-93	5838	2722	3116	0.06749	3.9E-08	radA	0		0	radA, radA
PG0274	+(199..204	5	1E-160	2429	1198	1231	0.01359	8.4E-08	PG0274	0		0	PG0274, PG0274
PG0361	+(624..661	37	1.5E-88	5394	2654	2740	0.01594	3.1E-05	PG0362	0		0	PG0361, PG0361
PG0413	+(153..176	23	8.7E-85	1268	622	646	0.01893	2E-05	mutL	0		0	PG0413, PG0413
PG0694	+(492..561	69	2E-109	5400	2516	2884	0.06815	2.3E-09	PG0694	0		0	PG0694, PG0694
PG0695	+(567..604	37	3E-100	5596	2720	2876	0.02788	2E-05	PG0695	0		0	PG0695, PG0695
PG0834	+(582..634	52	1E-136	7602	3722	3880	0.02078	5.8E-06	PG0834	0		0	PG0834, PG0834
PG1038	+(1030..11	122	2E-109	10484	4985	5499	0.04903	2.8E-07	PG1038	0		0	PG1038, PG1038
PG1069	+(485..543	58	6E-106	5153	2587	2566	0.00408	7.2E-06	PG1069	0		0	PG1069, PG1069
kamD	+(815..855	40	7E-115	7383	3815	3568	0.03346	8.6E-05	kamE	0		0	kamD, kamD
pgm	+(658..712	54	2.8E-83	5160	2564	2596	0.0062	3.3E-05	pgm	0		0	pgm, pgm
PG1367	+(289..326	31	8E-109	2864	1439	1425	0.00489	7E-05	PG1367	0		0	PG1367, PG1367
PG1372	+(695..729	34	1E-110	6593	3186	3407	0.03352	6.4E-07	PG1372	0		0	PG1372, PG1372
PG1480	+(308..340	32	8E-87	2559	1302	1257	0.01758	6.1E-05	PG1480	0		0	PG1480, PG1480
PG1481	+(1217..12	60	1E-102	11329	5829	5500	0.02904	2.6E-05	PG1481	0		0	PG1481, PG1481
PG1483	+(134..159	25	3.7E-50	737	404	333	0.09634	1.1E-08	PG1483	0		0	PG1483, PG1483
PG1487	+(117..139	22	6.3E-67	745	342	403	0.08188	9.9E-06	PG1487	0		0	PG1487, PG1487
galK	+(599..652	53	4E-98	4622	2366	2256	0.0238	2.2E-05	galK	0		0	galK, galK
PG1634	+(199..228	29	2.6E-95	1616	813	803	0.00619	8.4E-05	PG1634	0		0	PG1634, PG1634
PG1644	+(442..467	25	3E-240	8873	4440	4433	0.00079	1.5E-05	PG1644	0		0	PG1644, PG1644, mobile_element
PG1660	+(244..286	42	3E-99	2152	1079	1073	0.00279	3.4E-07	PG1659	0		0	PG1660, PG1660
PG1692	+(337..368	31	1.1E-85	2255	1142	1113	0.01286	3.6E-05	PG1692	0		0	PG1692, PG1692
PG1779	+(220..243	23	5.6E-61	1368	645	723	0.05702	4.2E-05	PG1779	0		0	PG1779, PG1779

Table S2 – Seq Data for PG 219

Mapping	Region	Length	FDR (%)	# Reads	# Forward reads	# Reverse reads	Normalized difference	Wilcoxon filter p-value	5' gene	5' distance	3' gene	3' distance	Overlapping annotations
rplS	+(151..186	37	5.78E-45	763	388	375	0.017038	7.63E-06	rplS	0		0	rplS, rplS
glyA	+(620..676	50	2E-48	3604	1720	1884	0.045505	3.97E-05	glyA	0		0	glyA, glyA
PG0065	+(449..516	61	1.8E-51	2901	1378	1523	0.049983	5.77E-06	PG0065	0		0	PG0065, PG0065
lpxA	+(402..451	49	2.44E-49	2101	1144	957	0.089005	1.91E-08	lpxA	0		0	lpxA, lpxA
radA	+(620..682	62	1.75E-55	4115	1927	2188	0.063426	2.01E-08	radA	0		0	radA, radA
PG0338	+(1674..18	153	4.92E-59	11722	5961	5761	0.017062	3.13E-05	PG0338	0		0	PG0338, PG0338
PG0469	+(105..124	19	2.99E-24	421	177	244	0.159145	3.06E-05	PG0469	0		0	PG0469, PG0469
PG0647	+(456..501	45	2.26E-61	3022	1455	1567	0.037062	2.32E-05	PG0647	0		0	PG0647, PG0647
PG0676	+(368..398	30	6.49E-55	2249	1101	1148	0.020898	5.78E-05	PG0676	0		0	PG0676, PG0676
PG0694	+(496..567	71	4.06E-60	3570	1680	1890	0.058824	2.71E-09	PG0694	0		0	PG0694, PG0694
kamA	+(551..640	89	1.21E-57	3979	1968	2011	0.010807	1.46E-05	kamA	0		0	kamA, kamA
PG1481	+(1235..13	73	2.76E-58	7874	4075	3799	0.035052	1.74E-05	PG1481	0		0	PG1481, PG1481
mmdC	+(199..234	35	1.01E-53	1263	631	632	0.000792	6.02E-05	mmdC	0		0	mmdC, mmdC

Table S3 – Seq Data for PG 226

Mapping	Region	Length	FDR(%)	#Readr	# Forward readr	# Reverse readr	Normalized differences	Wilcoxon filter p-value	5' gene	5' distance	3' gene	3' distance	Overlapping annotations
relS	+(150..17	22	2.8E-50	1394	611	783	0.12339	5.5E-06	relS	0		0	relS,relS
glyA	+(622..63	51	3.4E-69	6847	3245	3602	0.05214	1.3E-13	glyA	0		0	glyA,glyA
lexA	+(393..45	65	1.2E-69	4085	2288	1797	0.1202	5.3E-12	lexA	0		0	lexA,lexA
kraA	+(365..39	29	8.5E-68	3725	1768	1957	0.05074	2.1E-05	kraA	0		0	kraA,kraA
PG0145	+(293..31	24	2.4E-65	2597	1302	1295	0.0027	3.4E-06	PG0146	0		0	PG0145,PG0145
ribD	+(396..41	23	2.7E-76	5211	2466	2745	0.05354	1.8E-06	ribD	0		0	ribD,ribD
recR	+(236..24	13	3E-65	2420	1210	1210	0	2.2E-05	PG0158	0		0	recR,recR
radA	+(636..65	57	1.3E-73	7814	3618	4196	0.07397	5.6E-14	radA	0		0	radA,radA
PG0272	+(552..60	51	1.1E-76	7267	3615	3652	0.00509	3.3E-05	PG0272	0		0	PG0272,PG0272
PG0322	+(596..62	28	1.4E-76	7219	3556	3663	0.01482	6.6E-05	PG0322	0		0	PG0322,PG0322
hutI	+(611..62	13	3.3E-71	6702	3467	3235	0.03462	3.9E-06	hutI	0		0	hutI,hutI
PG0338	+(1694..1	98	9.9E-78	21719	10933	10786	0.00677	6.2E-06	PG0338	0		0	PG0338,PG0338
mcaL	+(505..57	71	8.5E-68	6293	3113	3180	0.01065	6.2E-09	mcaL	0		0	mcaL,mcaL
PG0345	+(305..33	33	7.8E-75	3205	1636	1569	0.0209	5E-05	PG0345	0		0	PG0345,PG0345
PG0366	+(261..29	36	1.4E-85	2864	1410	1454	0.01536	1.9E-05	PG0366	0		0	PG0366,PG0366
casD	+(209..23	21	4.1E-65	2174	1135	1039	0.04416	6.6E-05	casD	0		0	casD,casD
rplK	+(211..23	22	1.6E-75	2347	1154	1193	0.01662	1.3E-05	rplK	0		0	rplK,rplK
PG0426	+(541..57	32	8E-139	8503	4176	4327	0.01776	2.6E-08	PG0426	0		0	PG0426,PG0426,mobile_elemer
PG0458	+(492..50	16	9E-243	11487	5779	5708	0.00618	1.1E-07	PG0458	0		0	PG0458,PG0458,mobile_elemer
PG0469	+(101..115	14	4.6E-34	677	247	430	0.27031	6.4E-06	PG0469	0		0	PG0469,PG0469
yajC	+(162..18	18	5.4E-55	1769	849	920	0.04014	3.8E-05	yajC	0		0	yajC,yajC
PG0487	+(738..77	32	4.2E-70	3371	1723	1648	0.02225	5.2E-06	PG0487	0		0	PG0487,PG0487,mobile_elemer
PG0535	+(300..32	28	1.4E-84	3976	1984	1992	0.00201	1E-07	PG0535	0		0	PG0535,PG0535
PG0539	+(509..55	45	1.3E-71	5870	2859	3011	0.02589	8.1E-05	PG0540	0		0	PG0539,PG0539
PG0647	+(454..50	47	1.1E-76	5511	2651	2860	0.03792	2.6E-06	PG0647	0		0	PG0647,PG0647
PG0679	+(640..71	71	1.6E-68	7373	3621	3752	0.01777	6.1E-09	PG0679	0		0	PG0679,PG0679
PG0694	+(483..55	63	1.6E-75	6701	3077	3624	0.08163	0	PG0694	0		0	PG0694,PG0694
PG0695	+(555..59	38	2.2E-83	7271	3369	3902	0.0733	8.1E-10	PG0695	0		0	PG0695,PG0695
PG0708	+(416..44	26	6.6E-75	4822	2528	2294	0.04853	6.1E-06	PG0708	0		0	PG0708,PG0708
PG0789	+(367..39	13	6.8E-68	3680	1882	1798	0.02283	9.7E-05	PG0789	0		0	PG0789,PG0789
PG0834	+(575..62	46	1.2E-85	8388	4251	4137	0.01359	2.2E-07	PG0834	0		0	PG0834,PG0834
bcp	+(237..23	40	3.2E-70	2396	1197	1199	0.00083	3.9E-06	bcp	0		0	bcp,bcp
PG0882	+(417..47	58	2.2E-81	5290	2642	2648	0.00113	8E-06	PG0883	0		0	PG0882,PG0882
dut	+(192..22	31	6.8E-76	2180	1101	1079	0.01009	6.8E-07	dut	0		0	dut,dut
PG0956	+(581..65	70	2.5E-73	8093	3982	4111	0.01594	4.8E-06	ribF	0		0	PG0956,PG0956
PG0986	+(254..28	34	1.6E-68	2773	1338	1435	0.03498	3.3E-08	PG0986	0		0	PG0986,PG0986
kamD	+(822..82	1	1.2E-77	9687	4947	4740	0.02137	6.9E-05	kamE	0		0	kamD,kamD
PG1261	+(501..51	17	0	46508	23257	23251	0.00013	8.8E-06	PG1261	0		0	PG1261,mobile_element,PG1261
qmd	+(522..57	52	4.5E-84	6499	3229	3270	0.00631	9.8E-08	fcl	0		0	qmd,qmd
ilvE	+(416..47	62	2.2E-62	4996	2308	2688	0.07606	9.1E-08	ilvE	0		0	ilvE,ilvE
PG1302	+(333..36	36	5.7E-71	3806	1909	1897	0.00315	5.5E-05	PG1302	0		0	PG1302,PG1302
PG1311	+(280..32	43	2E-69	2793	1447	1346	0.03616	3.2E-07	PG1311	0		0	PG1311,PG1311
PG1335	+(234..25	17	2.2E-63	2014	991	1023	0.01589	3.4E-05	PG1335	0		0	PG1335,PG1335
PG1372	+(692..70	17	3E-74	8471	4001	4470	0.05537	4.6E-05	PG1372	0		0	PG1372,PG1372
PG1481	+(1139..1	139	2E-78	15013	7792	7221	0.03803	0	PG1481	0		0	PG1481,PG1481
PG1483	+(140..16	27	4.6E-34	995	546	449	0.09749	9.4E-09	PG1483	0		0	PG1483,PG1483
PG1487	+(109..13	26	2.5E-44	866	371	495	0.14319	1.4E-08	PG1487	0		0	PG1487,PG1487
tapB-2	+(856..92	70	1.1E-76	10518	5378	5140	0.02263	3.7E-07	tapB-2	0		0	tapB-2,tapB-2
PG1501	+(262..30	41	2E-81	3342	1645	1697	0.01556	6.2E-08	PG1501	0		0	PG1501,PG1501
PG1594	+(744..80	58	1.1E-73	8890	4395	4495	0.01125	3.5E-05	araK	0		0	PG1594,PG1594
galK	+(595..64	53	5.5E-70	6119	2980	3139	0.02598	5.5E-08	galK	0		0	galK,galK
PG1644	+(446..48	24	3E-189	11880	6107	5773	0.02811	1.1E-10	PG1644	0		0	PG1644,PG1644,mobile_elemen
PG1654	+(281..32	42	2.5E-73	3431	1735	1696	0.01137	2.7E-10	PG1654	0		0	PG1654,PG1654
PG1660	+(243..28	37	1.5E-74	2873	1504	1369	0.04699	4.2E-06	PG1659	0		0	PG1660,PG1660
PG1694	+(547..57	28	1.1E-63	5546	2935	2611	0.05842	1.2E-05	PG1693	0		0	PG1694,PG1694
PG2038	+(187..21	31	2.2E-83	2145	1084	1061	0.01072	1.5E-10	PG2037	0		0	PG2038,PG2038
PG2057	+(383..41	33	8E-178	11848	6014	5834	0.01519	2.5E-05	PG2057	0		0	PG2057,PG2057,mobile_elemer
PG2072	+(1593..1	80	5.5E-82	20387	10071	10316	0.01202	2.7E-05	PG2072	0		0	PG2072,PG2072
thiG	+(382..44	65	2E-70	3615	1611	2004	0.10871	5E-12	thiG	0		0	thiG,thiG
arvA	+(546..60	54	3.9E-75	6025	3034	2991	0.00714	8.6E-06	arvA	0		0	arvA,arvA
PG2199	+(892..96	68	6E-79	11352	5715	5637	0.00687	1.9E-05	PG2199	0		0	PG2199,PG2199

Table S4 – Seq Data for PG 229

Mapping	Region	Length	FDR (%)	# Reads	# Forward reads	# Reverse reads	Normalized difference	Wilcoxon filter p-value	5' gene	5' distance	3' gene	3' distance	Overlapping annotations
rplS	+(151..18(	37	6E-45	763	388	375	0.017	8E-06	rplS	0		0	rplS, rplS, ChIP peak
glyA	+(620..6(	50	2E-48	3604	1720	1884	0.0455	4E-05	glyA	0		0	glyA, glyA, ChIP peak
PG0065	+(449..5(	61	2E-51	2901	1378	1523	0.05	6E-06	PG0065	0		0	PG0065, PG0065, ChIP peak
lpxA	+(402..4(	49	2E-49	2101	1144	957	0.089	2E-08	lpxA	0		0	lpxA, lpxA, ChIP peak
radA	+(620..6(	62	2E-55	4115	1927	2188	0.0634	2E-08	radA	0		0	radA, radA, ChIP peak
PG0338	+(1674..1	153	5E-59	11722	5961	5761	0.0171	3E-05	PG0338	0		0	PG0338, PG0338, ChIP peak
PG0469	+(105..12	19	3E-24	421	177	244	0.1591	3E-05	PG0469	0		0	PG0469, PG0469, ChIP peak
PG0647	+(456..5(	45	2E-61	3022	1455	1567	0.0371	2E-05	PG0647	0		0	PG0647, PG0647, ChIP peak
PG0676	+(368..3(	30	6E-55	2249	1101	1148	0.0209	6E-05	PG0676	0		0	PG0676, PG0676, ChIP peak
PG0694	+(496..5(	71	4E-60	3570	1680	1890	0.0588	3E-09	PG0694	0		0	PG0694, PG0694, ChIP peak
kamA	+(551..64	89	1E-57	3979	1968	2011	0.0108	1E-05	kamA	0		0	kamA, kamA, ChIP peak
PG1481	+(1235..1	73	3E-58	7874	4075	3799	0.0351	2E-05	PG1481	0		0	PG1481, PG1481, ChIP peak
mmdC	+(199..23	35	1E-53	1263	631	632	0.0008	6E-05	mmdC	0		0	mmdC, mmdC, ChIP peak

Table S5 – Seq Data for HcpR 1

Mapping	Region	Length	FDR (%)	# Reads	# Forward reads	# Reverse reads	Normalized difference	Wilcoxon filter p-value	5' gene	5' distance	3' gene	3' distance	Overlapping annotations
PG0032	+(1314..1418)	104	2E-18	6906	3525	3381	0.0209	1E-05	PG0032	0		0	PG0032, PG0032
cdsA	+(408..458)	50	4E-17	2098	1023	1075	0.0248	3E-05	cdsA	0		0	cdsA, cdsA
lpxA	+(402..461)	59	2E-17	1943	1047	896	0.0777	1E-07	lpxA	0		0	lpxA, lpxA
ribD	+(384..445)	61	2E-18	2523	1179	1344	0.0654	1E-05	ribD	0		0	ribD, ribD
radA	+(670..721)	51	5E-20	3697	1718	1979	0.0706	4E-05	radA	0		0	radA, radA
PG0647	+(443..517)	74	1E-20	2717	1303	1414	0.0409	7E-10	PG0647	0		0	PG0647, PG0647
PG0694	+(489..558)	69	2E-18	3150	1503	1647	0.0457	4E-10	PG0694	0		0	PG0694, PG0694
PG1038	+(1039..1115)	76	2E-20	6524	3081	3443	0.0555	5E-05	PG1038	0		0	PG1038, PG1038
pgm	+(649..730)	81	2E-17	3408	1713	1695	0.0053	1E-06	pgm	0		0	pgm, pgm
PG1306	+(294..368)	74	6E-18	1477	769	708	0.0413	8E-07	PG1306	0		0	PG1306, PG1306
PG1372	+(680..722)	42	2E-18	4032	1908	2124	0.0536	4E-05	PG1372	0		0	PG1372, PG1372
PG1481	+(1212..1277)	65	6E-19	7100	3647	3453	0.0273	5E-05	PG1481	0		0	PG1481, PG1481
PG1483	+(137..176)	39	5E-11	471	247	224	0.0488	2E-05	PG1483	0		0	PG1483, PG1483
PG1660	+(250..288)	38	3E-18	1390	716	674	0.0302	6E-05	PG1659	0		0	PG1660, PG1660
PG1980	+(72..81)	9	2E-13	363	172	191	0.0523	3E-05	PG1980	0		0	PG1980, PG1980
tagD	+(198..229)	31	2E-17	1069	534	535	0.0009	4E-05	tagD	0		0	tagD, tagD
thiG	+(365..439)	74	2E-18	1745	783	962	0.1026	5E-07	thiG	0		0	thiG, thiG

Table S6 – Seq Data for HcpR 2

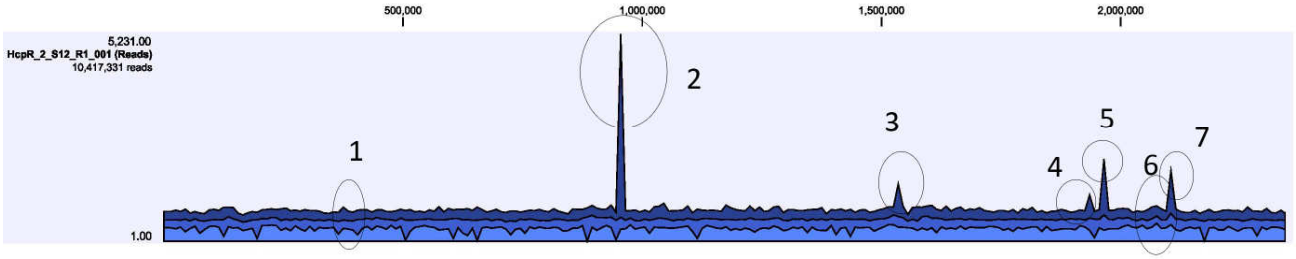

Table S7 - HcpR Genomic Libraries

Peak	Genome Location	Description
1	378827	PG0344 interior; "Purple acid phosphatase"
2	955987	PG 0893; Promoter region for Hydroxylamine Reductase
3	1535172	PG1451 interior
4	1938129	PG1841 interior; nearest gene is PG1842 (acetyl transferase); 200bp away
5	1966480	PG1870 interior; nearest gene is PG1871, but going opposite direction
6	2073807	PG1984 interior
7	2106207	cas3 interior; CRISPR-associated Cas3

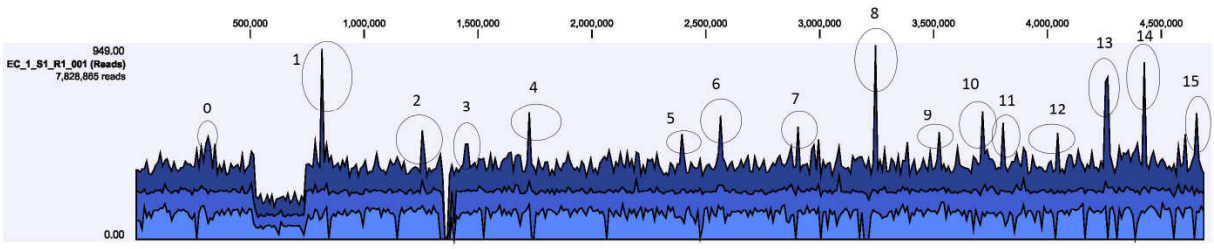

Table S8 – Ec OxyR Genomic Libraries

	Region		
0	315067	insF	inside region of gene
1	817046	moaA	inside region of gene
2	1251297	dhaR	inside region of gene
3	1454479	paaE	inside region of gene
4	1725388	nemA	inside region of gene
5	2390709	nuoM	inside region of gene
6	2566003	eutH	inside region of gene
7	2908624	mazG	inside region of gene
8	3247260	yqjC	inside region of gene
9	3522153	mrcA	inside region of gene
10	3709399	yhjX	inside region of gene
11	3808998	mutM	inside region of gene
12	4048036	spf	inside region of gene
13	**4267153**	**yjbS**	promoter region; blank region near possible promoter for yjbS which starts at 4267035; so it is about 118 bp away; no known function
14	4426512	ytfB	inside region of gene

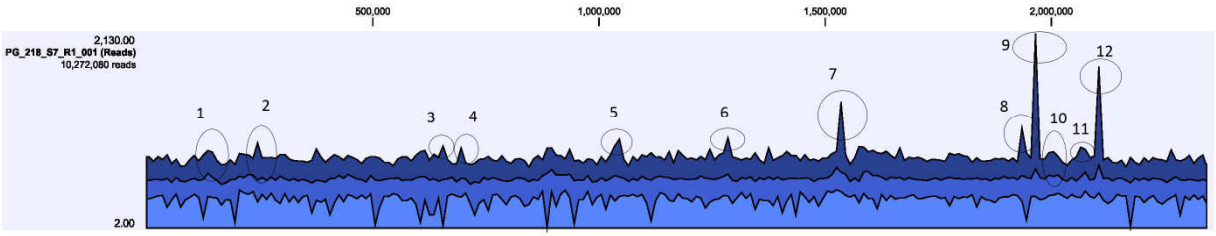

Table S9 - Pg OxyR Genomic Libraries

Peak	Gene Location	Description
1	139488	PG 0116 interior
2	243490	PG 0209 interior; which is a formate/nitrate transporter
3	657534	ribBA interior; riboflvin biosynthesis protein
4	698743	PG0 646 interior; it is an iron abc transporter
5	1046069	PG 0982 interior; encodes for hypothetical protein
6	1287432	PG1209 promoter region; NAD metabolism ATPase/kinase
7	1534681	PG 1450 interior; encodes for integrase
8	1934989	PG 1837 interior; encodes for hemagglutin A
6	1966386	PG 1870 interior; methyltransferase UbiE
10	2003670	PG 1903 interior; encodes for hypothetical protein
11	2068426	Blank region; nearest is PG 1980 but approximately 400bp away
12	2107670	cas3 interior; CRISP-associated protein Cas3